Discussion Paper

Using Satellite Technology to Measure Methane Emissions in MENA Countries

Anwar Gasim,[a] Abdelrahman Muhsen,[a] Srivatsan Anand,[b] Maxence Nevoret,[b] Apolline Pignato,[b] and Julian Akani-Guéry[b]

[a] KAPSARC

[b] Kayrros

February 2026
Doi: 10.30573/KS--2026-DP02



About KAPSARC

KAPSARC is an advisory think tank within global energy economics and sustainability providing advisory services to entities and authorities in the Saudi energy sector to advance Saudi Arabia's energy sector and inform global policies through evidence-based advice and applied research.

This publication is also available in Arabic.



Legal Notice

© Copyright 2026 King Abdullah Petroleum Studies and Research Center (“KAPSARC”). This Document (and any information, data or materials contained therein) (the “Document”) shall not be used without the proper attribution to KAPSARC. The Document shall not be reproduced, in whole or in part, without the written permission of KAPSARC. KAPSARC makes no warranty, representation or undertaking whether expressed or implied, nor does it assume any legal liability, whether direct or indirect, or responsibility for the accuracy, completeness, or usefulness of any information that is contained in the Document. Nothing in the Document constitutes or shall be implied to constitute advice, recommendation or opinion. The views and opinions expressed in this publication are those of the authors and do not necessarily reflect the official views or position of KAPSARC.

Key Points

Decision-makers need high-quality information on greenhouse gas (GHG) emissions to take effective climate action. Among the GHGs, methane is particularly difficult to measure, which has led to massive discrepancies in methane emission measurements for countries around the world. In recent years, satellites have emerged as a powerful tool for providing accurate, transparent, and timely measurements of methane emissions. This marks the third paper published by KAPSARC in collaboration with Kayrros to provide high-quality measurements of country-level methane emissions using satellite technology, specifically the TROPOMI sensor aboard the Sentinel-5 Precursor (Sentinel-5P) satellite. This third report introduces refinements to our satellite-based method and expands our satellite measurements to nine countries in the Middle East and North Africa (MENA): Algeria, Egypt, Iran, Iraq, Kuwait, Libya, Oman, Saudi Arabia, and the United Arab Emirates. It also covers two key sectors: 1) oil and gas; and 2) waste from urban areas.

Through our analysis, we find that:

- There are massive discrepancies in methane emissions data for MENA countries. In the case of their oil and gas sectors, methane emission estimates from different sources can differ by over 100-fold for some countries.
- For most MENA countries, our satellite estimates were consistently higher than the estimates from their official national GHG inventories that were submitted by MENA governments to the UNFCCC.
- However, for most MENA countries, our satellite estimates were also consistently lower than the estimates provided by organizations like the IEA.
- Using our satellite measurements for the oil and gas sector, Saudi Arabia and the UAE emerge as the top-performing countries with the lowest methane intensities (methane emissions per barrel of oil and gas equivalent).
- Countries and organizations that use activity-based methods to measure methane emissions need to move away from assuming emission factors and instead start measuring them to improve the accuracy of activity-based estimates.
- While activity-based methods will remain prevalent, satellite measurements of methane emissions can enhance transparency and provide necessary information for reconciling methane emissions data and improving the underlying assumptions that are made to generate those estimates.

Abstract

Accurate methane emission measurement is needed for meeting Paris Agreement goals, yet methane emission datasets diverge substantially. Activity-based datasets rely heavily on assumed emission factors and often produce inconsistent results, while satellite-based estimates remain underutilized. This study develops a novel, transparent, and reproducible satellite-based framework to estimate national-level methane emissions across nine Middle East and North Africa (MENA) countries: Algeria, Egypt, Iran, Iraq, Kuwait, Libya, Oman, Saudi Arabia, and the United Arab Emirates (UAE). We focus on two key sectors: 1) oil and gas and 2) urban waste. Our approach combines two complementary satellite methods: a wind-rotated model for zone-level quantification and a basin-inversion model for larger regions with densely clustered assets. Where direct satellite observation is not possible (e.g., offshore facilities or mountainous urban areas), we apply extrapolations to generate complete national-level estimates. Our results show that the methane emissions reported by MENA governments to the UNFCCC are generally lower than our satellite-based estimates. In contrast, global datasets such as the IEA and EDGAR generally overestimate methane emissions, particularly in the oil and gas sector. We also find that urban waste is typically a larger methane source than oil and gas across the region. Saudi Arabia and the UAE emerge as top performers, exhibiting the lowest methane intensities, while other producers show substantial abatement potential. Our findings highlight the value of satellite data for strengthening national and corporate MRV systems and improving emission factors within activity-based methodologies. As satellite capabilities advance, integrating satellite, ground-based, and activity data will enable more accurate, timely, and transparent methane emissions tracking.

Key words: Methane, Emissions, Satellites, MRV, Oil & Gas, Waste, Greenhouse Gas Inventories

Introduction

01

The measurement of greenhouse gas (GHG) emissions is one component of the widely used term measurement, reporting and verification (MRV), which originated under the United Nations Framework Convention on Climate Change (UNFCCC) and is a fundamental part of the Paris Agreement (UNFCCC 2022). This paper contributes to improving emission measurement by providing transparent satellite-based estimates of methane emissions for countries in the Middle East and North Africa (MENA).

As noted in the Intergovernmental Panel on Climate Change's (IPCC's) Sixth Assessment Report (AR6), carbon dioxide and methane are the main GHGs contributing to global warming, with methane the second-largest contributor after carbon dioxide (IPCC 2023a). Of the two, methane is much more potent at trapping heat. In fact, a tonne of methane traps almost 30 times as much heat as a tonne of carbon dioxide when they are compared over 100 years (IPCC 2023b). This value of 30 is known as methane's 100-year global warming potential (GWP), a metric that shows how well different GHGs trap heat relative to carbon dioxide, which always has a GWP equal to 1.[1]

Compared to carbon dioxide, where the divergences between emission estimates are relatively small, there are massive discrepancies between methane emission estimates (Luomi, Al Shehri, and Howarth 2021; Gasim, Matar, and Muhsen 2023). These discrepancies stem in part from the complexity of methane emissions sources, which include oil and gas systems, livestock, manure, rice cultivation, landfills, and wastewater, among others. Compared to carbon dioxide, which is generated primarily from fuel combustion, methane emissions result from a variety of processes, such as methane leaks from gas pipelines, the digestive processes of livestock, and the decomposition of organic waste in landfills, and some of these processes can be particularly difficult to track and measure.

To help meet the goals of the Paris Agreement and reduce methane emissions, the Global Methane Pledge (GMP) was launched at the 2021 United Nations Climate Change Conference (COP26). Around 160 countries pledged to "take voluntary actions to contribute to a collective effort to reduce global methane emissions at least 30 percent from 2020 levels by 2030" (GMP, 2025). Methane's short atmospheric lifetime, high global-warming potential, and recoverable commercial value make its abatement a strategic and cost-effective lever for meeting the goals of the Paris Agreement and minimizing the near-term global temperature increase.

To effectively reduce methane emissions, it is necessary to have high-quality methane emission measurements. The National Academies of Sciences, Engineering, and Medicine (2022) categorize GHG measurement approaches into two categories: activity-based and atmospheric-based. Activity-based methods are arguably the most widely used, and parties to the Paris Agreement must use them when reporting their national GHG inventories to the UNFCCC. The specific activity-based methods

that they must use were developed by the IPCC and are known as the IPCC (2006) guidelines. Under these methods, activity data is first collected for activities that generate GHG emissions, such as gasoline consumption or oil and gas production. The activity data is subsequently multiplied by the appropriate emission factor (e.g., the carbon dioxide emitted per unit of gasoline or the methane generated per unit of oil and gas) to calculate emissions.

Emission factors lie at the heart of activity-based methods. These emission factors are generally calculated based on a sample of measurements. The IPCC (2006) guidelines provide users with several tiers that differ mainly in the application of emission factors. Under Tier 1, global default emission factors are used in the calculations. Most developing countries use Tier 1 equations, and Tier 1 use is even common in developed nations (Banja et al. 2025). Under Tier 3, which is the most complex to apply, country-specific, technology-specific, or facility-specific emission factors must be used – emission factors that most countries do not have, hence the prevalent use of Tier 1 equations.

Using default emission factors can work well in some cases, but not in others. For example, for carbon dioxide emissions from gasoline combustion, the actual emission factor (the carbon dioxide generated per unit of gasoline burned) is relatively stable across countries and over time, so using a default or average emission factor should yield accurate estimates. In contrast, applying a default emission factor to fugitive methane emissions from oil and gas production does not work well because of the massive temporal and spatial variations in methane leakage rates across facilities and countries. Alvarez et al. (2018) highlighted this "large spatial and temporal variability" in methane emissions between similar facilities across the United States (U.S.), and even larger variations are expected to exist between different countries. Studies show that assumed emission factors, which may not reflect actual methane emissions, are a key reason behind the discrepancies in methane emission estimates (Brandt et al. 2016; Alvarez et al. 2018; Rutherford et al. 2021).

While the activity-based approach is arguably the most widely used, atmospheric-based approaches are gaining traction. Atmospheric-based approaches measure GHG emissions by observing their atmospheric concentrations, which can be done using technologies such as ground-based sensors, drones, aircraft, and satellites (National Academies of Sciences, Engineering, and Medicine 2022). Some of these technologies, such as sensors and drones, are more effective for measuring facility-level emissions but are very difficult to deploy at a national scale. In contrast, satellites are more feasible for producing national-level methane emission measurements; hence our focus on satellite methods in this paper.

Satellites generally measure methane concentrations using instruments that detect solar radiation backscattered from the Earth's surface in shortwave infrared wavelengths (Jacob, Turner et al. 2016; Jacob, Varon et al. 2022; Schneising et al. 2020). At least 33 satellites have been launched to monitor GHG emissions, ranging from those focused on point-source emission measurement to those that provide daily global observations (Jacob, Varon et al. 2022; Committee on Earth Observation Satellites 2025). These satellite observations of methane concentrations then require robust methods to infer actual methane emission rates and volumes. Two primary approaches have gained prominence for inferring these emission rates: 1) atmospheric inversion models; and 2) direct plume quantification techniques.

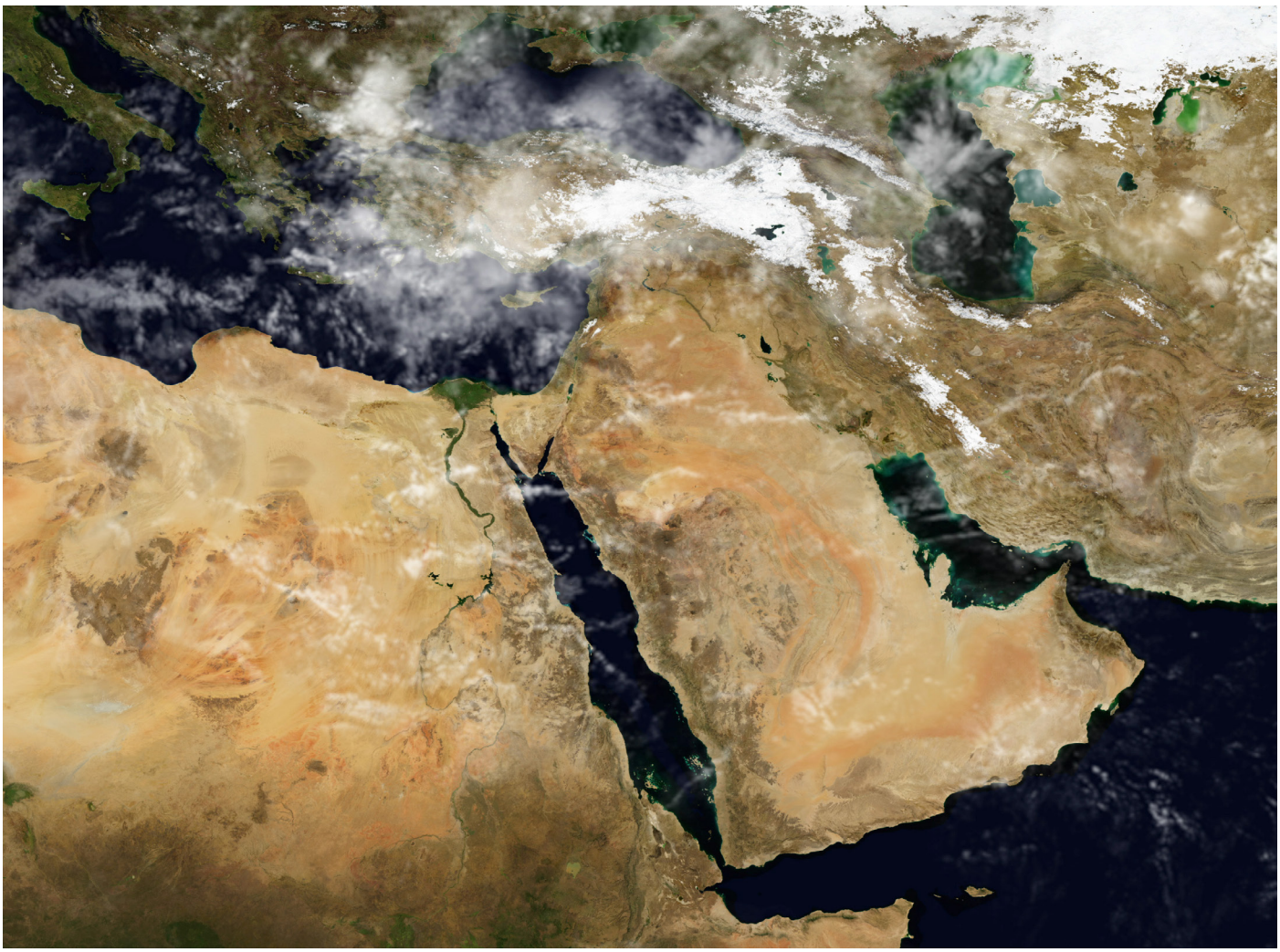
Atmospheric (or basin) inversion models utilize sophisticated atmospheric transport models to simulate how gases are emitted and move in the atmosphere, integrating satellite methane concentration data to infer emission fluxes over a given area. Studies by Chen et al. (2023), Shen et al. (2023), and Yu et al. (2023), for example, have successfully used atmospheric inversion models to estimate national and regional methane emissions, including for the MENA region. While such basin inversion models represent a powerful method for inferring methane emissions for a region, country, or basin, they generate a single estimate of methane emissions for the region, country, or basin. Subsequent sectoral disaggregation of that single estimate relies on prior inventories of methane emissions (like those estimated using the activity-based method) or on proxy spatial data. Furthermore, this method does not allow for direct, asset-level attribution.

In parallel, direct plume quantification methods, such as the wind-rotation approach (also known as the wind-rotated model), have been developed to pinpoint and quantify methane emissions from specific point sources or facility clusters. This method involves aligning multiple satellite observations of methane concentrations over a point source according to wind direction, enhancing the signal-to-noise ratio to delineate methane plumes, and then quantifying methane emission rates and volumes (Maasakkers et al. 2022; Schneising et al. 2020).

Unlike the atmospheric inversion model, the wind-rotated model allows direct attribution of emissions from an isolated point source within a zone or from a group of point sources within a zone. This approach has typically been applied to measure emissions from specific assets, including landfills (Maasakkers et al. 2022; Balasus et al. 2025) and oil and gas infrastructure (Schneising et al. 2020). However, to the best of our knowledge, applying the wind-rotation approach to assets across an entire country or region and aggregating the measurements to the national level has not been done previously, except in our two previous studies (Gasim, Matar, and Muhsen 2023; Gasim et al. 2024).

This paper builds on our previous work, where we highlighted the existence of massive methane discrepancies and produced satellite-based emission estimates for Saudi Arabia and selected Gulf countries (Gasim, Matar, and Muhsen 2023; Gasim et al. 2024). Relative to our previous satellite-based estimates, the International Energy Agency (IEA) and the European Commission's EDGAR database generally overstate oil and gas methane emissions in the region, whereas national inventories generally understate them. In this paper, we expand our analysis to cover nine MENA countries: Algeria, Egypt, Iran, Iraq, Kuwait, Libya, Oman, Saudi Arabia, and the United Arab Emirates (UAE). Moreover, we introduce refinements to our previously used satellite-based methods and a comprehensive benchmarking analysis for the region. In line with our previous work, our satellite-based measurements cover two sectors: 1) oil and gas; and 2) waste.[2]

The remainder of this paper is organized as follows: Section 2 compares existing estimates from the literature and highlights the discrepancies. Section 3 introduces our satellite-based methods, while also discussing limitations. Section 4 examines our satellite-based measurements and presents a benchmarking analysis. Section 5 discusses the policy implications and concludes.



Comparing Existing Methane Emissions Estimates

02

This section compiles and compares methane emission estimates from the literature for each of the nine MENA countries (see Figure 1 to Figure 9). Each figure compares activity-based and satellite-based estimates of methane emissions across two key sectors: 1) oil and gas; and 2) waste, with all remaining emissions, if measured, allocated to: 3) other sector.

The figures show that the largest discrepancies in methane emissions occur in the oil and gas sector across most MENA countries, with noticeable but smaller discrepancies in waste methane emissions.[3] In the case of Saudi Arabia's oil and gas sector, the IEA's (2022) estimate for 2021 was 11 times larger than the official estimate submitted by the Saudi government's focal point to the UNFCCC (DNA 2025). Satellite-based estimates for Saudi Arabia's oil and gas sector by Chen et al. (2023) and Shen et al. (2023) were between the IEA and UNFCCC estimates. For Iraq, the differences between the Republic of Iraq's Ministry of Environment (2025) estimate for oil and gas that was submitted to the UNFCCC and external estimates by the IEA and EDGAR were approximately sixfold to ninefold.

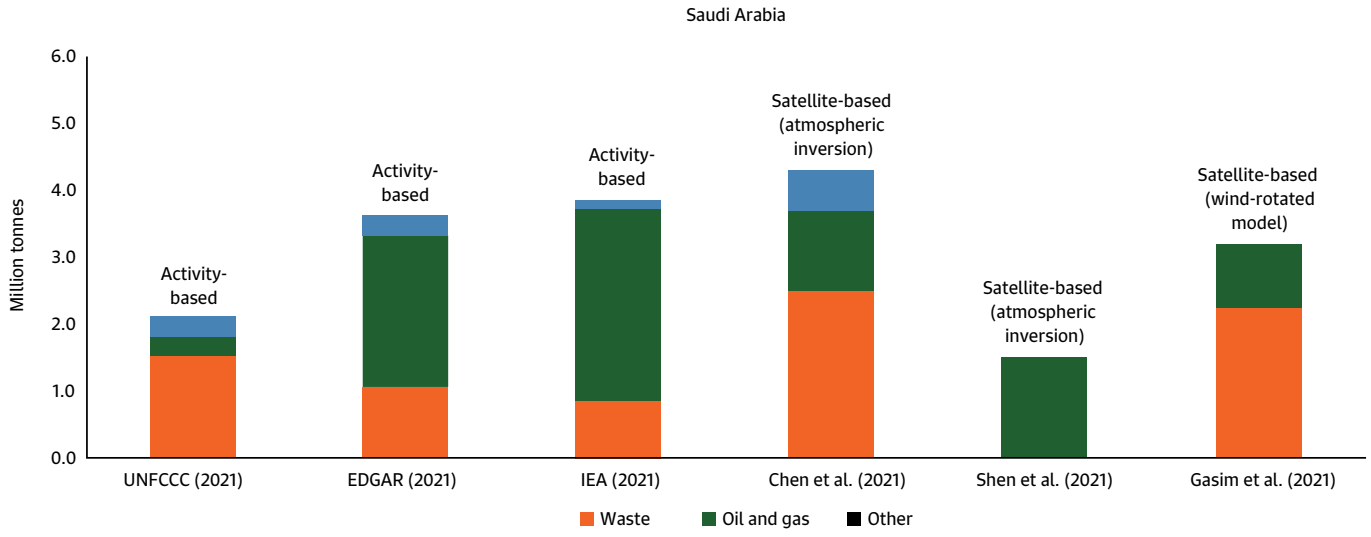
Even starker discrepancies were observed for the UAE and Kuwait in particular. In the case of the UAE's oil and gas sector, the IEA's (2022) estimate for 2021 was 47 times larger than the government estimate (UAE 2024). In Kuwait's oil and gas sector, the IEA's (2022) estimate was over 100 times larger than the government's estimate (Kuwait Environment Public Authority 2019). In contrast to other Arabian Gulf countries, the IEA (2022) and EDGAR (2024) estimates for Oman's oil and gas sector were very consistent with the government's estimate. One satellite-based estimate for Oman was also consistent with the activity-based estimates (Shen et al. 2023), while the other satellite-based estimate by Chen et al. (2023) was surprisingly higher than all other estimates.

In the case of Iran, estimates were generally consistent. Unexpectedly, greater variation was found between Iran's satellite-based estimates compared to its activity-based estimates. The satellite-based estimate for Iran's oil and gas sector by Tiberwal et al. (2024) was almost three times the satellite-based estimate of Chen et al. (2023), suggesting that even satellite-based estimates can have significant discrepancies, although they are generally smaller than the discrepancies in activity-based estimates, which can be larger than 100-fold. Looking across North African countries, 30-fold discrepancies were found in Egypt's oil and gas sector, while estimates for Libya were consistent across activity-based and satellite-based methods. Discrepancies in Algeria were also modest, with the IEA's estimate for the country's oil and gas sector consistent with satellite-based estimates but three times higher than the government's UNFCCC submission.

The figures also show methane emission estimates from our previous work for five of the nine MENA countries (Gasim et al. 2024). In general, our earlier estimates, which we refine further in this paper, lie above the UNFCCC submissions but below the IEA and EDGAR. Our satellite estimates were generally consistent with other satellite studies, except for the UAE, where our estimates were significantly smaller, and Kuwait, where our oil and gas sector estimate was considerably larger than that of Chen et al. (2023).

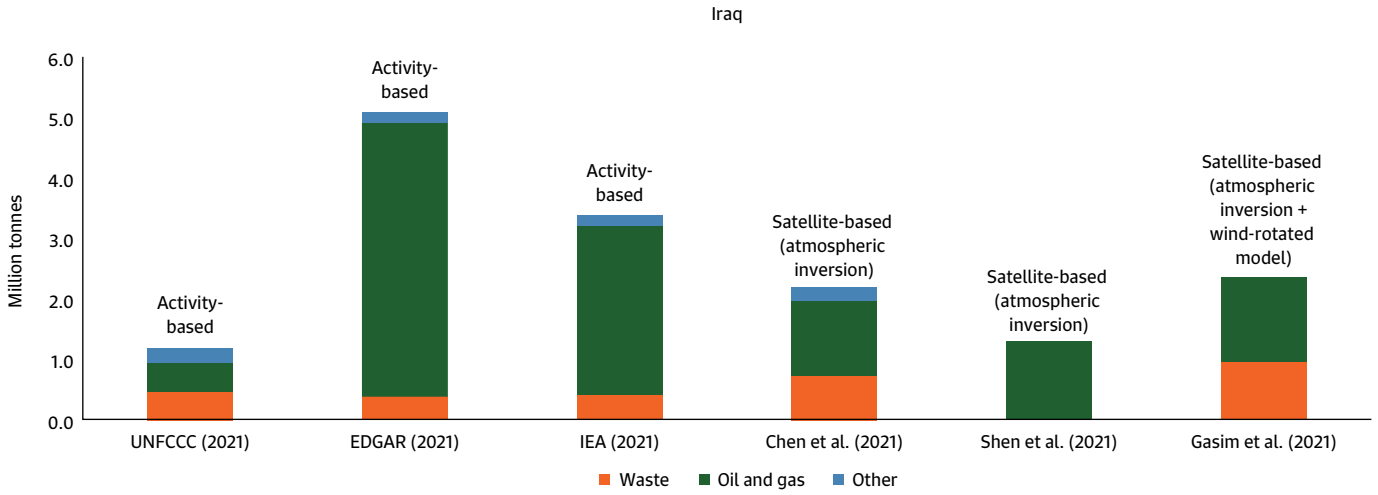
This paper introduces refinements to the satellite methods used in our previous work, resulting in updated estimates for the five Arabian Gulf countries we examined earlier. We also expand our analysis to include nine MENA countries. Additionally, we standardize assumptions across countries and develop a satellite-based framework for estimating national-level inventories in a transparent, reproducible, and progressively improvable manner.

Figure 1. Methane emissions estimates for Saudi Arabia.



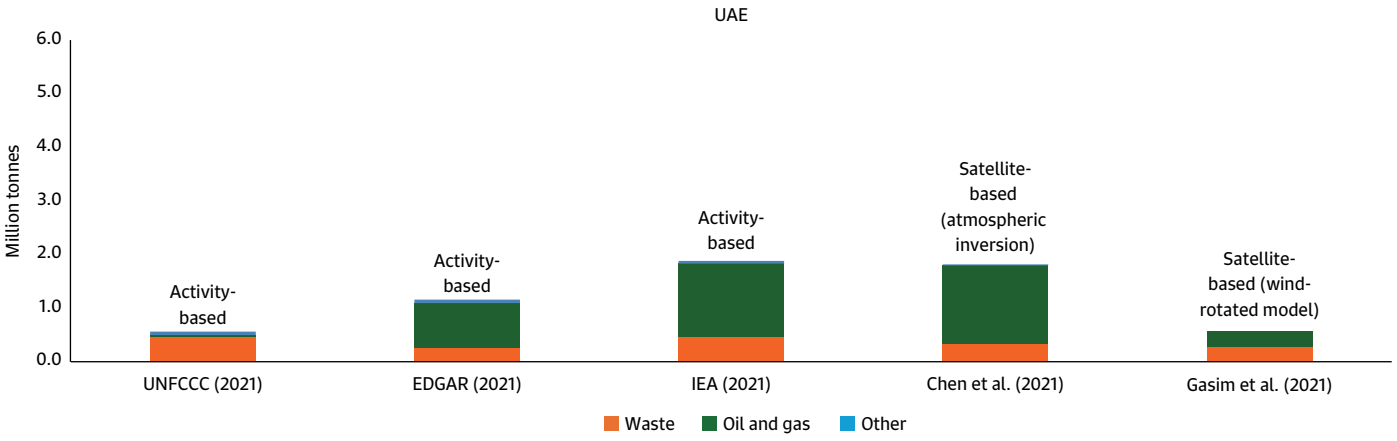
Note: Year of estimate is shown in brackets on the x-axis. Only the most recent national estimate submitted to the UNFCCC is shown in the figure. For any data source that provides multiple annual estimates, the estimate that is closest in time to the UNFCCC estimate is shown in the figure.
Sources: DNA (2025), IEA (2022), EDGAR (2024), Chen et al. (2023), Shen et al. (2023), and Gasim et al. (2024).

Figure 2. Methane emissions estimates for Iraq.



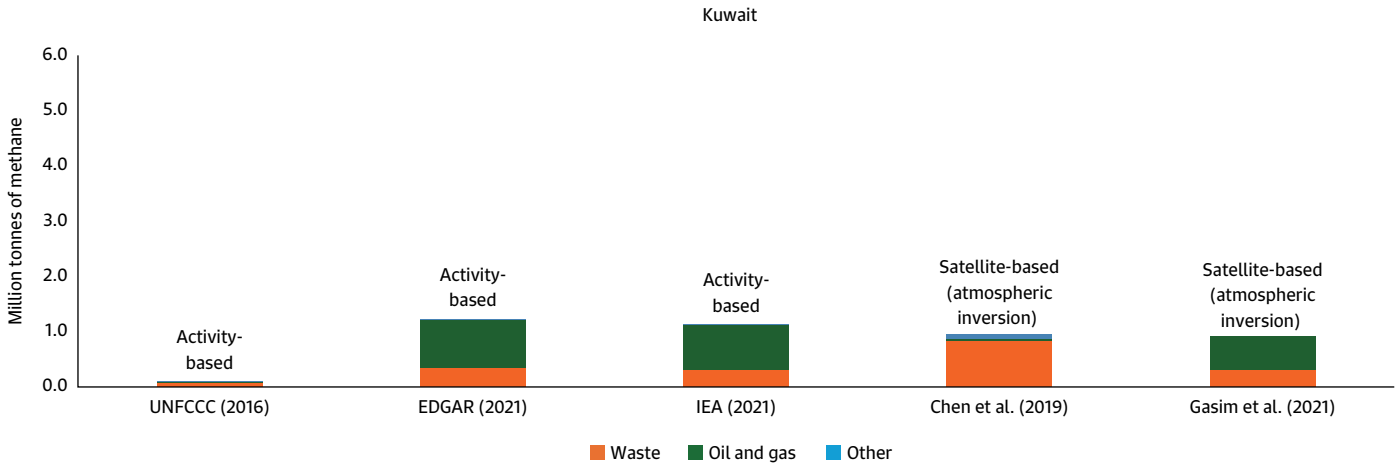
Note: Year of estimate is shown in brackets on the x-axis. Only the most recent national estimate submitted to the UNFCCC is shown in the figure. For any data source that provides multiple annual estimates, the estimate that is closest in time to the UNFCCC estimate is shown in the figure.
Sources: Republic of Iraq Ministry of Environment (2025), IEA (2022), EDGAR (2024), Chen et al. (2023), Shen et al. (2023), and Gasim et al. (2024).

Figure 3. Methane emissions estimates for the UAE.



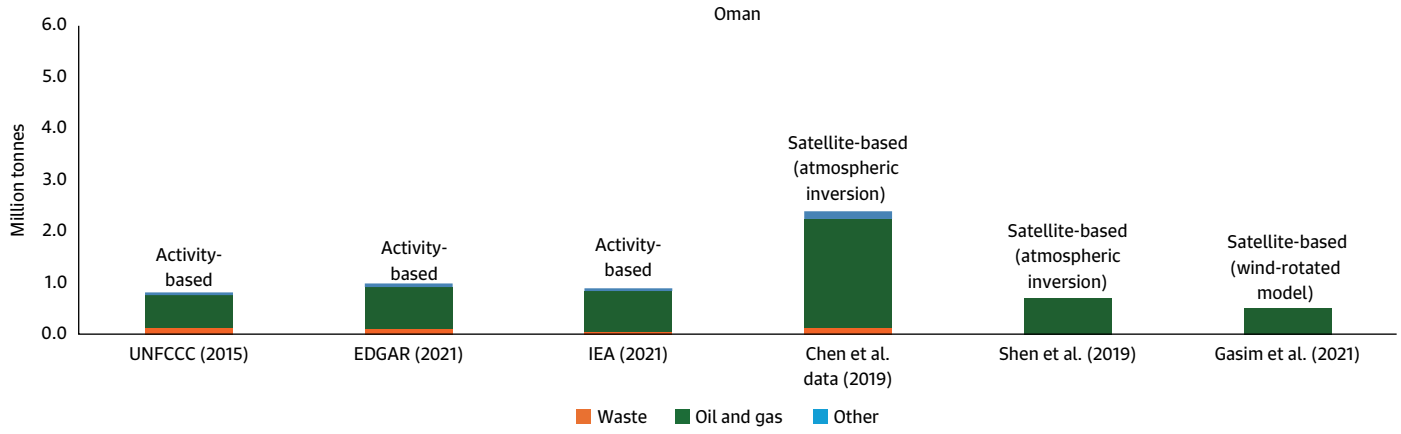
Note: Year of estimate is shown in brackets on the x-axis. Only the most recent national estimate submitted to the UNFCCC is shown in the figure. For any data source that provides multiple annual estimates, the estimate that is closest in time to the UNFCCC estimate is shown in the figure.
Sources: UAE (2024), IEA (2022), EDGAR (2024), Chen et al. (2023), and Gasim et al. (2024).

Figure 4. Methane emissions estimates for Kuwait.



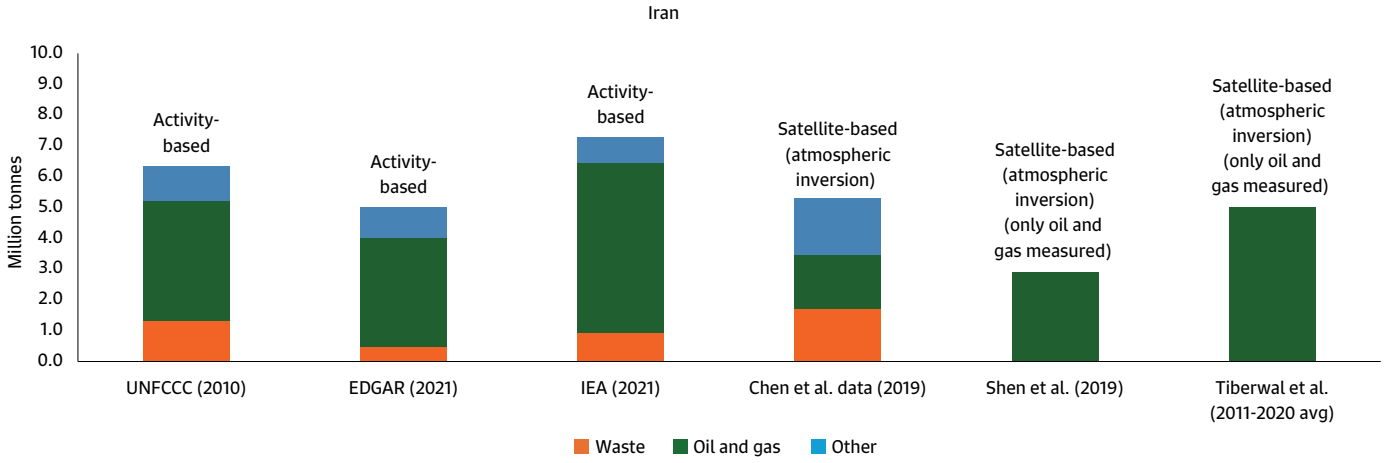
Note: Year of estimate is shown in brackets on the x-axis. Only the most recent national estimate submitted to the UNFCCC is shown in the figure. For any data source that provides multiple annual estimates, the estimate that is closest in time to the UNFCCC estimate is shown in the figure.
Sources: Kuwait Environment Public Authority (2019), IEA (2022), EDGAR (2024), Chen et al. (2023), and Gasim et al. (2024).

Figure 5. Methane emissions estimates for Oman



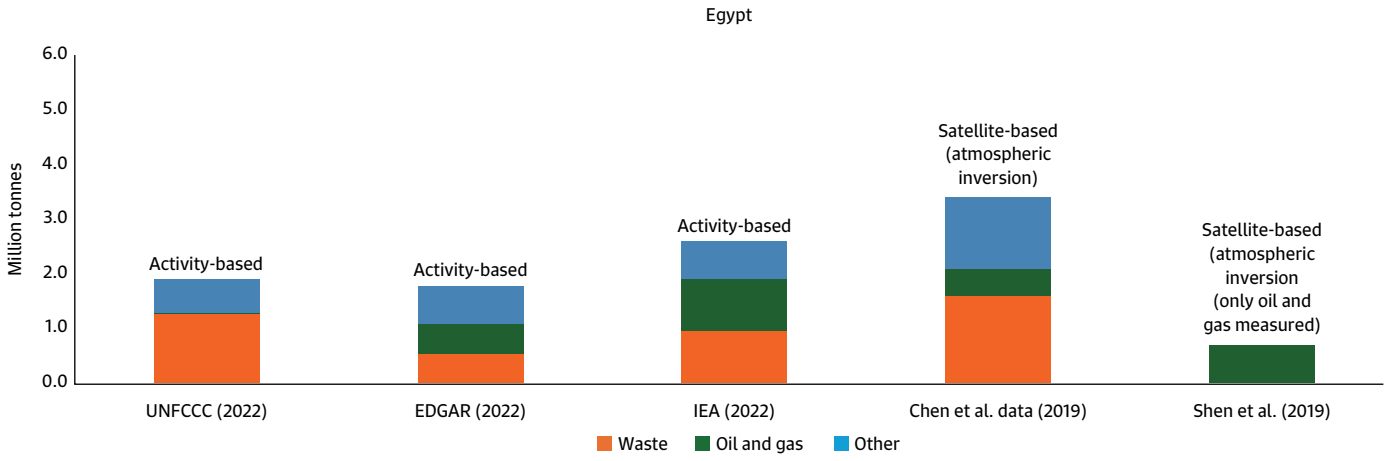
Note: Year of estimate is shown in brackets on the x-axis. Only the most recent national estimate submitted to the UNFCCC is shown in the figure. For any data source that provides multiple annual estimates, the estimate that is closest in time to the UNFCCC estimate is shown in the figure.
Sources: Ministry of Environment and Climate Affairs (2019), IEA (2022), EDGAR (2024), Chen et al. (2023), Shen et al. (2023), and Gasim et al. (2024).

Figure 6. Methane emissions estimates for Iran.



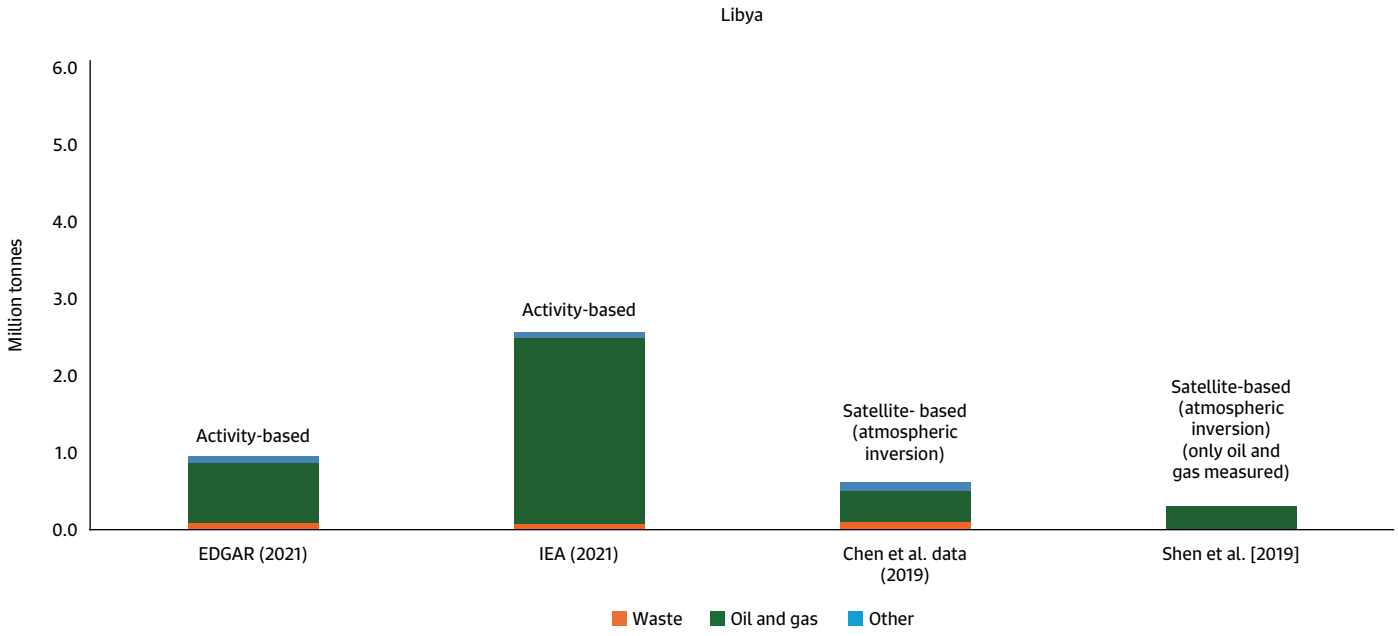
Note: Year of estimate is shown in brackets on the x-axis. Only the most recent national estimate submitted to the UNFCCC is shown in the figure. For any data source that provides multiple annual estimates, the estimate that is closest in time to the UNFCCC estimate is shown in the figure.
Sources: Islamic Republic of Iran (2017), IEA (2022), EDGAR (2024), Chen et al. (2023), Shen et al. (2023), and Tiberwal et al. (2024).

Figure 7. Methane emissions estimates for Egypt.



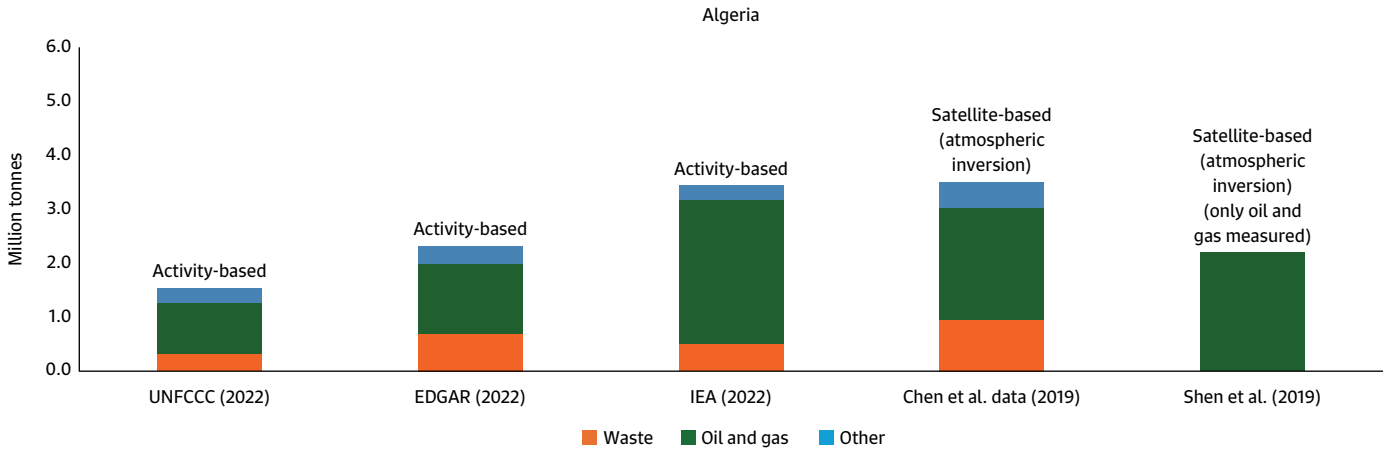
Note: Year of estimate is shown in brackets on the x-axis. Only the most recent national estimate submitted to the UNFCCC is shown in the figure. For any data source that provides multiple annual estimates, the estimate that is closest in time to the UNFCCC estimate is shown in the figure.
Sources: Arab Republic of Egypt Ministry of the Environment (2024), IEA (2023), EDGAR (2024), Chen et al. (2023), and Shen et al. (2023).

Figure 8. Methane emissions estimates for Libya.



Note: Year of estimate is shown in brackets on the x-axis. Given the absence of a UNFCCC national GHG emission inventory by the Libyan government, the datapoints are chosen to be as close as possible to 2021, a common reporting year for the region.
Sources: IEA (2022), EDGAR (2024), Chen et al. (2023), and Shen et al. (2023).

Figure 9. Methane emissions estimates for Algeria.



Note: Year of estimate is shown in brackets on the x-axis. Only the most recent national estimate submitted to the UNFCCC is shown in the figure. For any data source that provides multiple annual estimates, the estimate that is closest in time to the UNFCCC estimate is shown in the figure.
Sources: People's Democratic Republic of Algeria Ministry of the Environment and the Quality of Life (2024), IEA (2023), EDGAR (2024), Chen et al. (2023), and Shen et al. (2023).

Methods and Data

03

In this section, we present a novel satellite-based framework for measuring national-level methane emissions. Our approach uses basin inversion and/or wind-rotated models to quantify methane emissions from satellite observations of methane concentrations. We then combine and/or extrapolate these estimates to produce annual, national-level methane emission inventories with full spatial coverage.

3.1 TROPOMI Satellite Observations

We rely on satellite observations of methane concentrations from TROPOMI (2024), which provides daily global coverage of atmospheric trace gases, including methane, at a spatial resolution of 5.5 × 7 kilometers (km). TROPOMI retrieves methane column concentrations as the column-averaged dry air mole fraction (XCH_4). Its combination of relatively fine spatial resolution, global coverage, and daily revisit frequency enables the systematic detection of methane emissions at the national level.

3.2 Basin-Inversion Model

The basin-inversion model simulates methane emissions using an atmospheric transport model by matching satellite methane concentrations to TROPOMI images. The transport model employed is HYSPLIT (2019), the Hybrid Single-Particle Lagrangian Integrated Trajectory. Our basin-inversion model utilizes input data that includes the locations of potential methane sources within the basin (more details on this input data can be found in Appendix A). Based on these inputs, referred to as the "prior," model simulations are performed using ERA5 meteorological data (Hersbach et al. 2024).[4] The simulations are then fitted to the TROPOMI images, providing a comprehensive understanding of methane emissions in the basin. These observed emissions are subsequently converted into an estimate of annual emissions, assuming stable output. The basin-inversion model is well documented in the scientific community (Peng et al. 2022; Chen et al. 2023; Shen et al. 2023; Tiberwal et al. 2024).

While previous studies have applied the basin-inversion model to estimate national-level methane emissions, our study differs in its approach to "priors," which refer to the prior emission information used as input for solving the basin-inversion equations. For example, both Chen et al. (2023) and Shen et al. (2023) used basin-inversion models to estimate national-level methane emissions for MENA countries based on TROPOMI images. However, a key distinction between our basin-inversion model and those of Chen et al. (2023) and Shen et al. (2023) lies in our use of "priors." In this study, our "prior" consists solely of

the locations of potential methane-emitting sources, making our approach entirely independent of previously estimated methane emissions. In contrast, Chen et al. (2023) and Shen et al. (2023) rely on public inventories not only to identify locations but also to use the emissions as initial values in their basin-inversion models. Consequently, we anticipate that their estimates will be sensitive to the magnitudes of methane emissions from the public inventories they use as priors, whereas our approach does not depend on these magnitudes.

3.3 Wind-Rotated Model

We use the wind-rotated model to infer methane emissions from satellite-based methane concentration data. This method has been applied in the literature to various gases measured by TROPOMI, including sulfur dioxide (Fioletov et al. 2015) and methane (Schneising et al. 2020). The wind-rotated method consists of five main steps. First, TROPOMI images are preprocessed to retain only high-quality observations. Second, the images are rotated and aligned to orient methane plumes relative to the wind direction, improving plume signal detection. Third, background methane concentrations are subtracted to isolate the excess methane signal attributable to the emission source. Fourth, plume detection and masking are performed to delineate the methane plume within the image. Finally, methane fluxes are estimated by integrating the plume signal with wind data to calculate emission rates.

Before applying the first step, methane-emitting assets (e.g., oil and gas fields, urban areas) were identified in each country, and an area of interest (AOI) was defined to cover each asset or group of assets. AOI sizes were based on the spatial extent of the assets, typically ranging from 90 to 120 km, and up to 150 km for grouped assets.

3.3.1 Preprocessing of Satellite Observations

A key preprocessing step involves locating the methane source within each AOI. We conducted an 8 km grid search over candidate locations and selected the one that produced the strongest and most coherent plume (characterized by high intensity and a smooth shape). TROPOMI images surrounding each selected source were then extracted and resampled to a consistent 1 km resolution. Pixels with quality assurance values below recommended thresholds were discarded, following Landgraf et al. (2023).[5]

Following Schneising et al. (2020), we also removed images with unsuitable winds – below 2 m/s or above 12 m/s. In areas with nearby methane sources that lie outside our AOI but are relatively close to our source, images were discarded if winds transported emissions from those neighboring sources into our AOI to prevent double-counting. Finally, we masked surfaces prone to retrieval artifacts (e.g., coastlines, water, steep terrain, and dense vegetation) to reduce these artifacts in the images.

3.3.2 Satellite Image Rotation and Alignment

After preprocessing, images were rotated so that the wind blows southwards and the methane plume extends south from the center of the image. The angle of rotation is determined by fitting a simulated Gaussian plume, using wind speed and the plume's center coordinates as parameters. Specifically, an exponentially modified gaussian (EMG) plume model was applied to the rotated images. The EMG model effectively captures both methane dispersion around the source and its exponential decay downwind, following the formulation of Fioletov et al. (2015). Finally, to mitigate artifacts introduced by sparse valid pixels at the edges of the image, the edges were clipped as necessary.

3.3.3 Background Methane Subtraction

After rotating the images, background atmospheric methane concentrations were removed to isolate the excess methane emitted by the source. Two methods were applied, depending on the asset type. For non-coastal assets (the majority), the rotated images were first averaged. The background methane concentration was estimated as the minimum value in the aggregated pixels north of the source. Additionally, background areas were restricted to homogeneous regions (with no mountains, water, or dense vegetation) to enhance precision. Finally, the background methane concentration was subtracted from the averaged image, with any resulting negative values clipped to zero. This approach differs from Gasim et al. (2024), who conducted background subtraction before image aggregation.

However, for coastal assets, offshore winds often resulted in background areas containing invalid offshore pixels after rotation, preventing accurate estimation of the background methane concentration. In these cases, a methane-free area near the source was selected, and the background methane concentration was then taken from that area. Care was taken

to ensure that the background area was not downwind of the source. The background methane concentration was then subtracted from each image individually before aggregation, in order to reduce the effect of anomalous TROPOMI measurements across both the source and the nearby methane-free area.

3.3.4 Plume Delineation and Masking

After background subtraction, we obtain a methane plume image that is ready for quantification. A mask is then applied to delineate the methane plume within the image. This was done by identifying the pixels in the image that form the plume using a statistical outlier detection approach inspired by de Jong et al. (2024). In their method, plume detection relies on the median absolute deviation (MAD), in which the image's pixel values are normalized by the MAD, smoothed, and compared against thresholds to delineate which of the image pixels are part of the methane plume and which are not.[6] In some cases, the algorithm can fail to delineate a methane plume clearly. This can occur when the methane signal is too weak or when noise interferes with plume identification. In such instances, we do not generate a plume mask and do not proceed with methane quantification. Instead of satellite measurement, we extrapolate emissions following the approach discussed in Section 3.5.

3.3.5 Quantification of Methane

After successfully delineating the methane plume, methane emission rates were estimated using the cross-section flux method (White 1976; Krings et al. 2011) applied to the plumes within the plume mask. This method defines a series of vertical cross-sections that are perpendicular to the plume direction. For each cross-section, the excess methane is integrated across the plume width and combined with the wind component perpendicular to the cross-section to derive a methane flux. The overall plume flux is calculated as the mean of all individual cross-section fluxes. Assuming constant emissions over time, the overall plume flux is integrated over an entire year to obtain annual methane emission estimates for each AOI.[7]

3.4 Application of Models

For each country, either the wind-rotated model or the basin-inversion model was chosen, depending on whether assets were isolated or closely clustered within a country (or within a specific part of a country). For isolated assets, the wind-rotated model was applied. For clustered assets, the basin-inversion model was used. In some cases, both methods were applied to the same country, but in a way that ensures no overlap so that each model was implemented in a different part of the country. Table 1 summarizes the model(s) applied to each of the nine MENA countries examined in this paper.

Table 1. Satellite approaches used for each MENA country.

	Wind-rotated model only	Basin-inversion model only	Both models used (with no overlap)
Saudi Arabia	Yes		
Kuwait		Yes	
Iraq			Yes
Oman	Yes		
UAE	Yes		
Algeria	Yes		
Iran			Yes
Libya	Yes		
Egypt	Yes		

Source: Authors.

3.5 Extrapolation and Disaggregation

Several factors limit satellite-based estimation of methane emissions. Coastal or mountainous areas make wind-rotation measurements more challenging, as do water surfaces, preventing the measurement of methane emissions from offshore oil and gas assets, for instance. Since we cannot directly measure methane emissions from every emitting source in a country using satellites, we extrapolate methane emissions for such challenging assets.

The extrapolation is carried out separately for each sector. In the oil and gas sector, each asset (or group of assets) is assigned a share of national-level oil and gas production. After directly measuring methane emissions for all oil and gas assets in a country where satellite measurements were possible, these satellite methane emission estimates were converted into methane emission intensities. Subsequently, an average methane intensity was then calculated across all the oil and gas assets that were measured directly by satellite.[8] This average methane intensity was then multiplied by the level of oil and gas production for each onshore asset that was not directly measured by satellite, thereby producing an extrapolated estimate for that asset. However, for offshore assets, studies have shown that offshore methane emissions can diverge significantly from onshore emissions (Gorchov Negron et al. 2020). Instead of directly applying the onshore satellite-measured methane intensity to offshore assets, we first multiplied it by a country-specific scaling factor equal to the ratio of the emission intensity of offshore assets to the emission intensity of onshore assets. This scaling ratio was calculated for each country using EDGAR's (2024) gridded inventory.

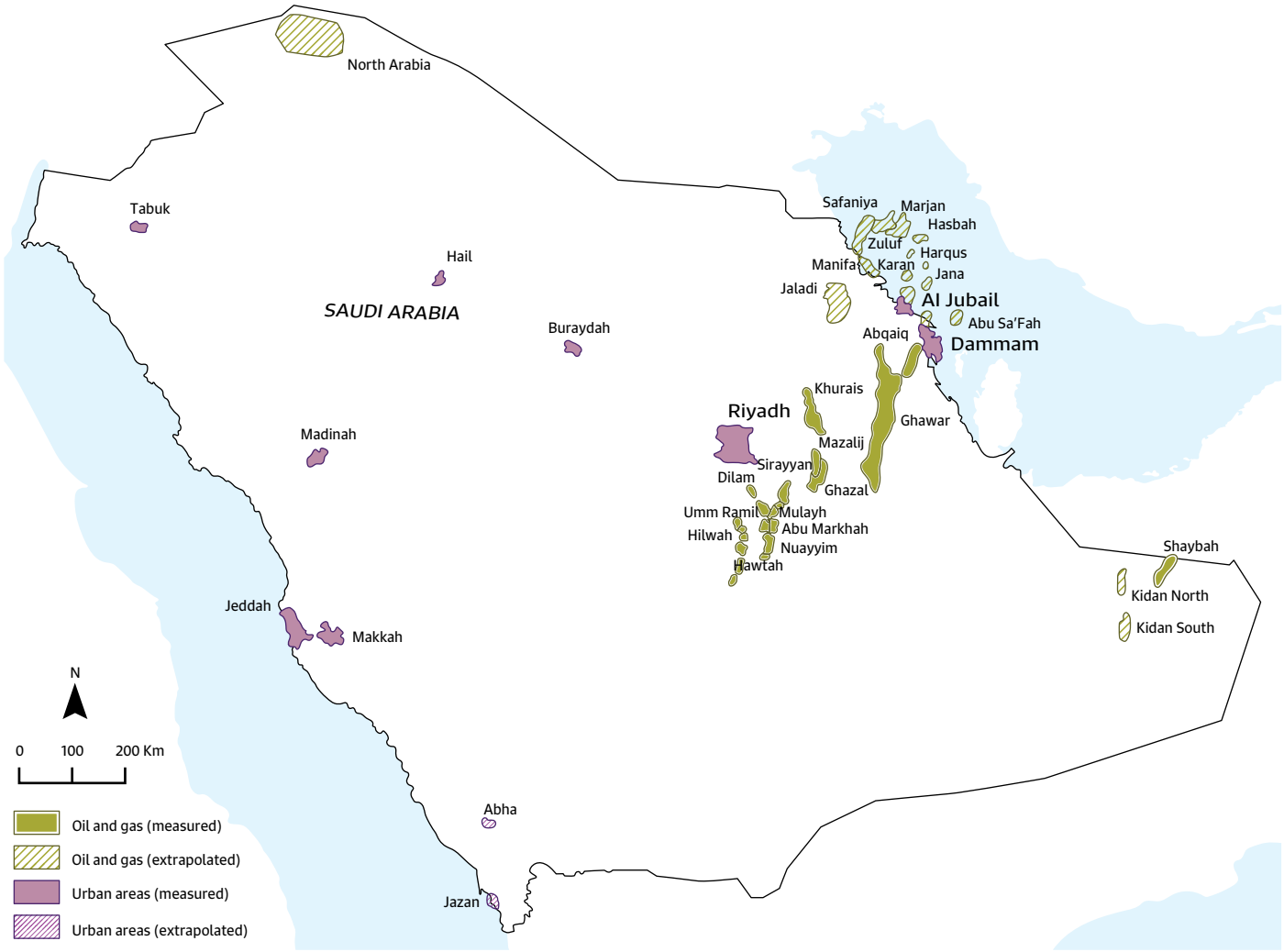
For urban area emissions, each urban area was assigned a share of national-level population and waste generation. After directly measuring methane emissions for all urban areas in a country where satellite measurements were possible, an average urban area intensity was calculated, which was then used to extrapolate methane emissions from urban areas not directly measured by satellite.

After extrapolating methane emissions for all assets not directly measured by satellite, the methane emissions from satellite-measured assets and extrapolated assets were summed to produce annual sectoral national-level methane emission estimates with full spatial coverage.

In countries where the basin-inversion model was applied, a single estimate was produced that encompasses all assets across all sectors within the basin's boundaries. To disaggregate this basin-level estimate into sectoral estimates, we split our basin-level estimate by sector using average sectoral methane emissions shares from publicly available inventories.[9]

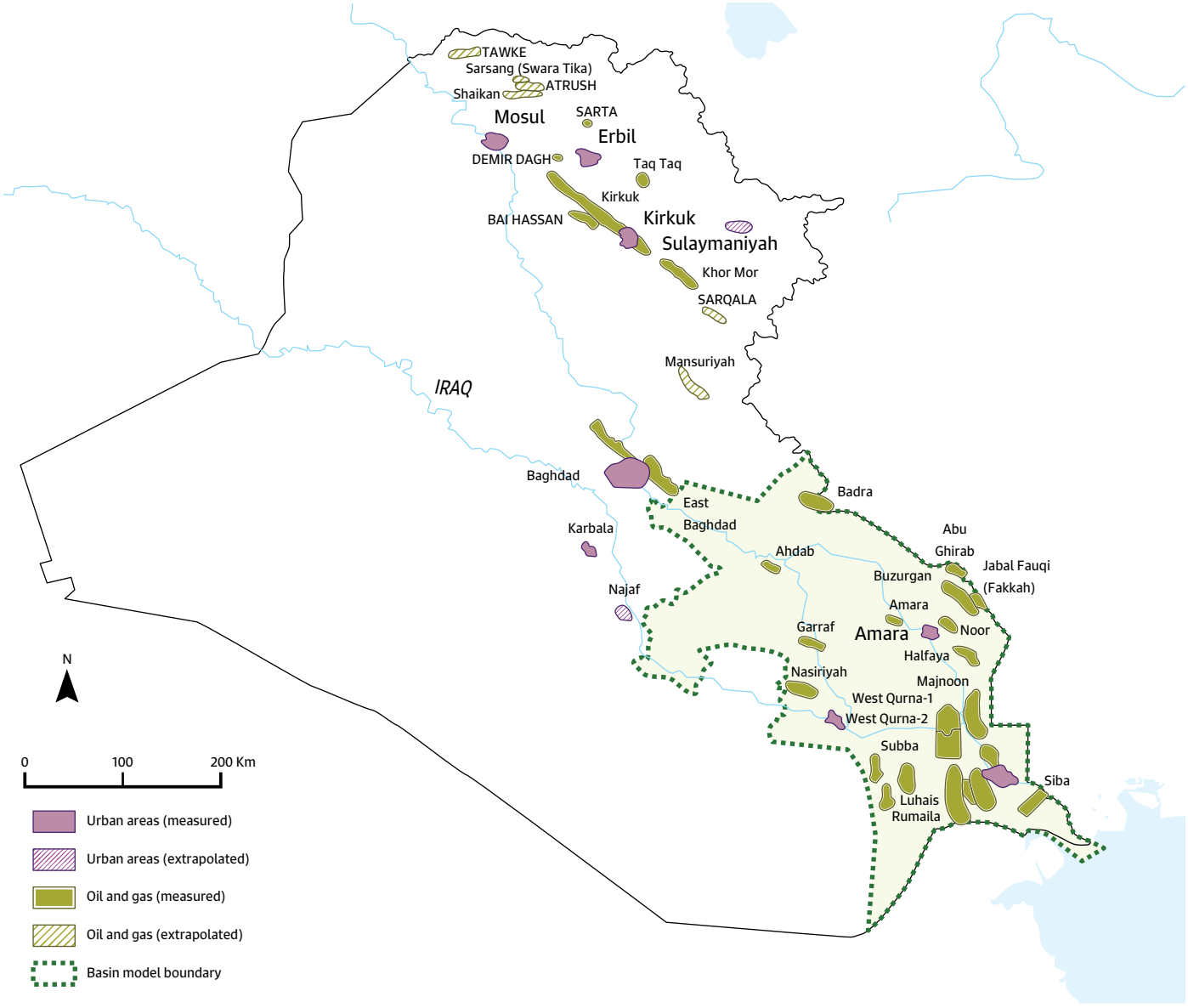
Figures 10 to 18 illustrate all the oil and gas fields and urban areas in each of the nine MENA countries, highlighting which method was applied and where extrapolations were needed. Whenever the basin-inversion model was applied, the basin model's boundary was plotted in the figures. Additional country-specific notes regarding the extrapolation and disaggregation of methane emissions estimates can be found in Appendix B, while a detailed list of assumptions used for extrapolation is presented in Appendix C.

Figure 10. Geospatial visualization of methane sources and methods applied to Saudi Arabia.



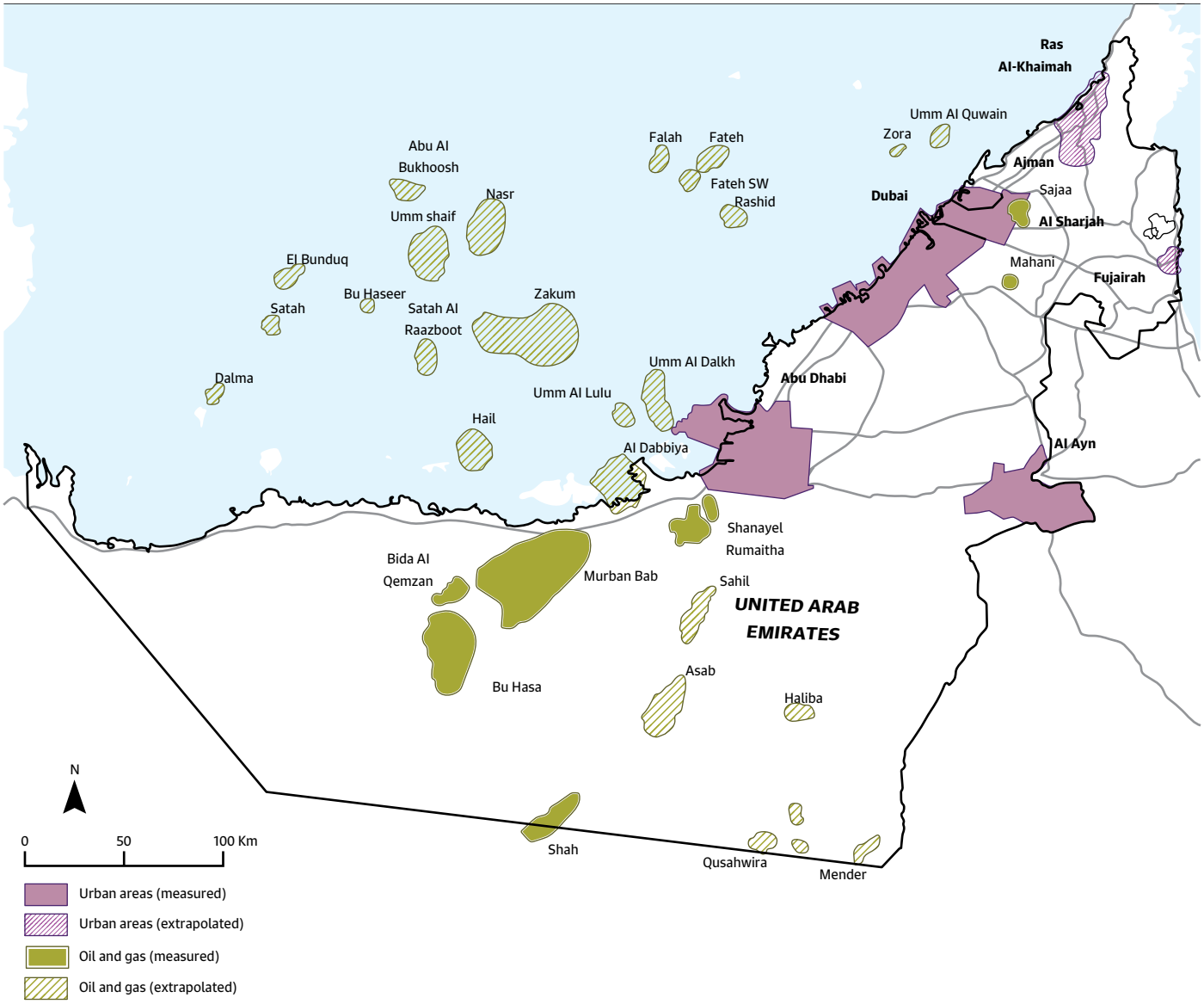
Source: Authors.

Figure 11. Geospatial visualization of methane sources and methods applied to Iraq.



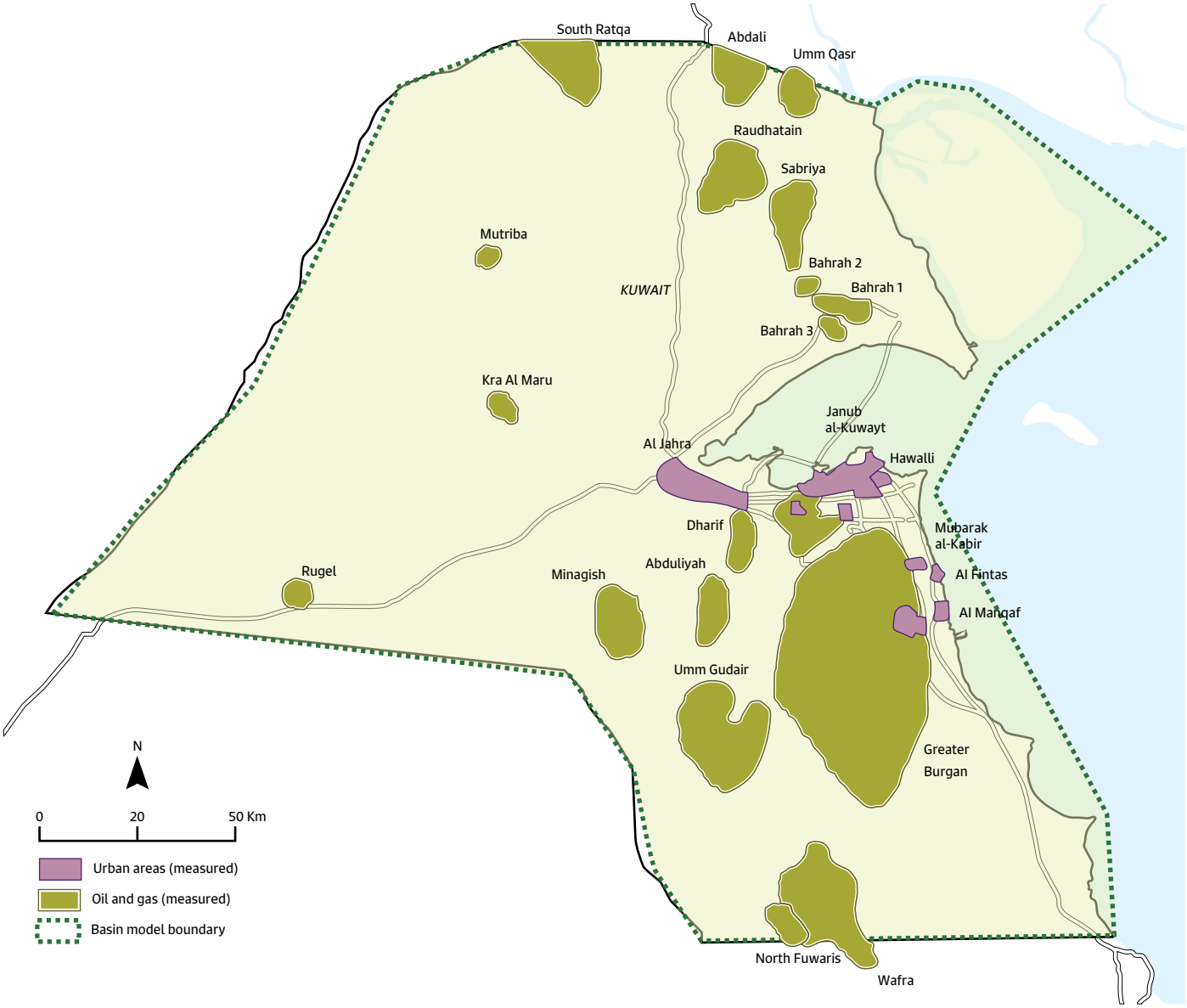
Source: Authors.

Figure 12. Geospatial visualization of methane sources and methods applied to the UAE.



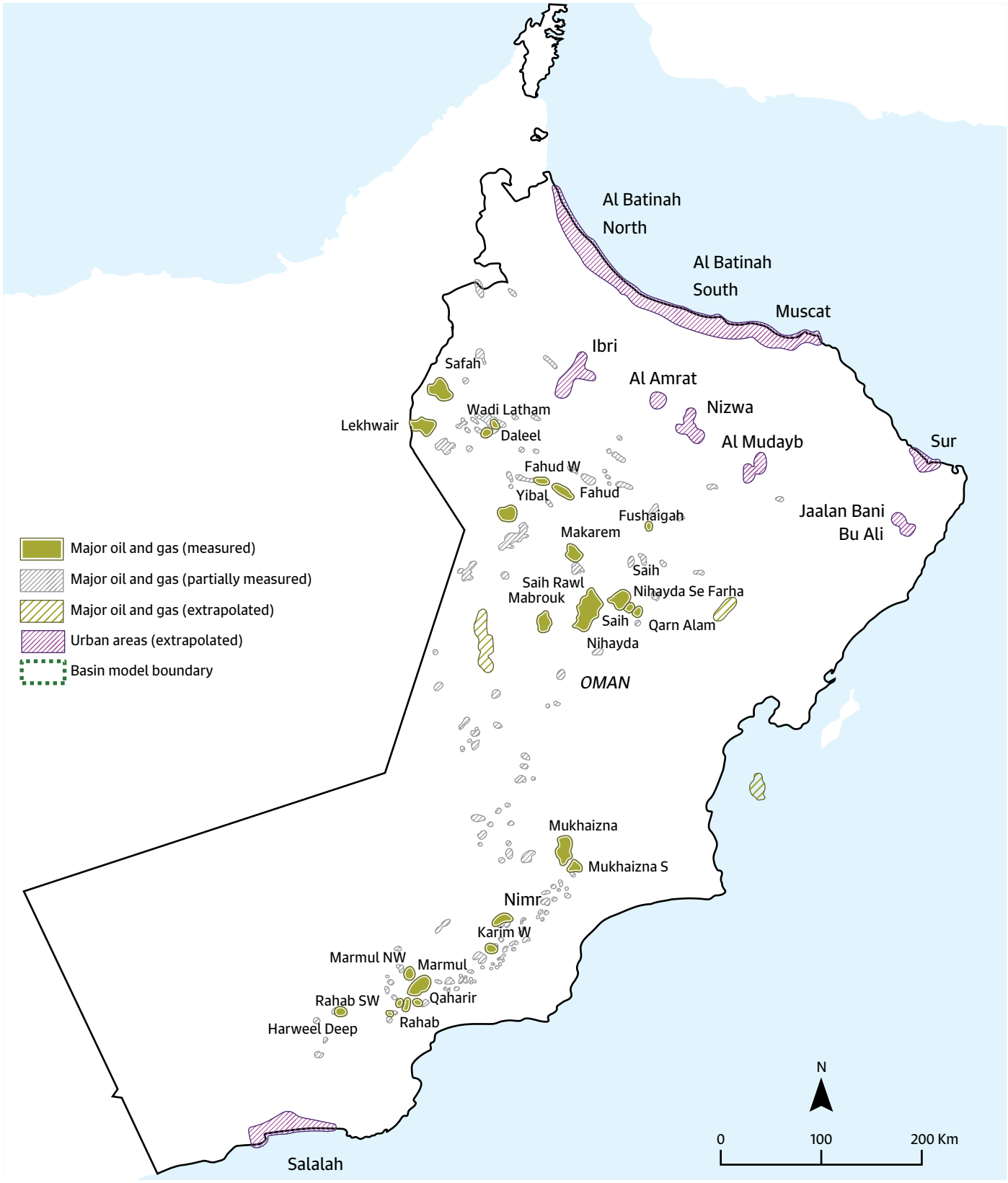
Source: Authors.

Figure 13. Geospatial visualization of methane sources and methods applied to Kuwait.



Source: Authors.

Figure 14. Geospatial visualization of methane sources and methods applied to Oman.



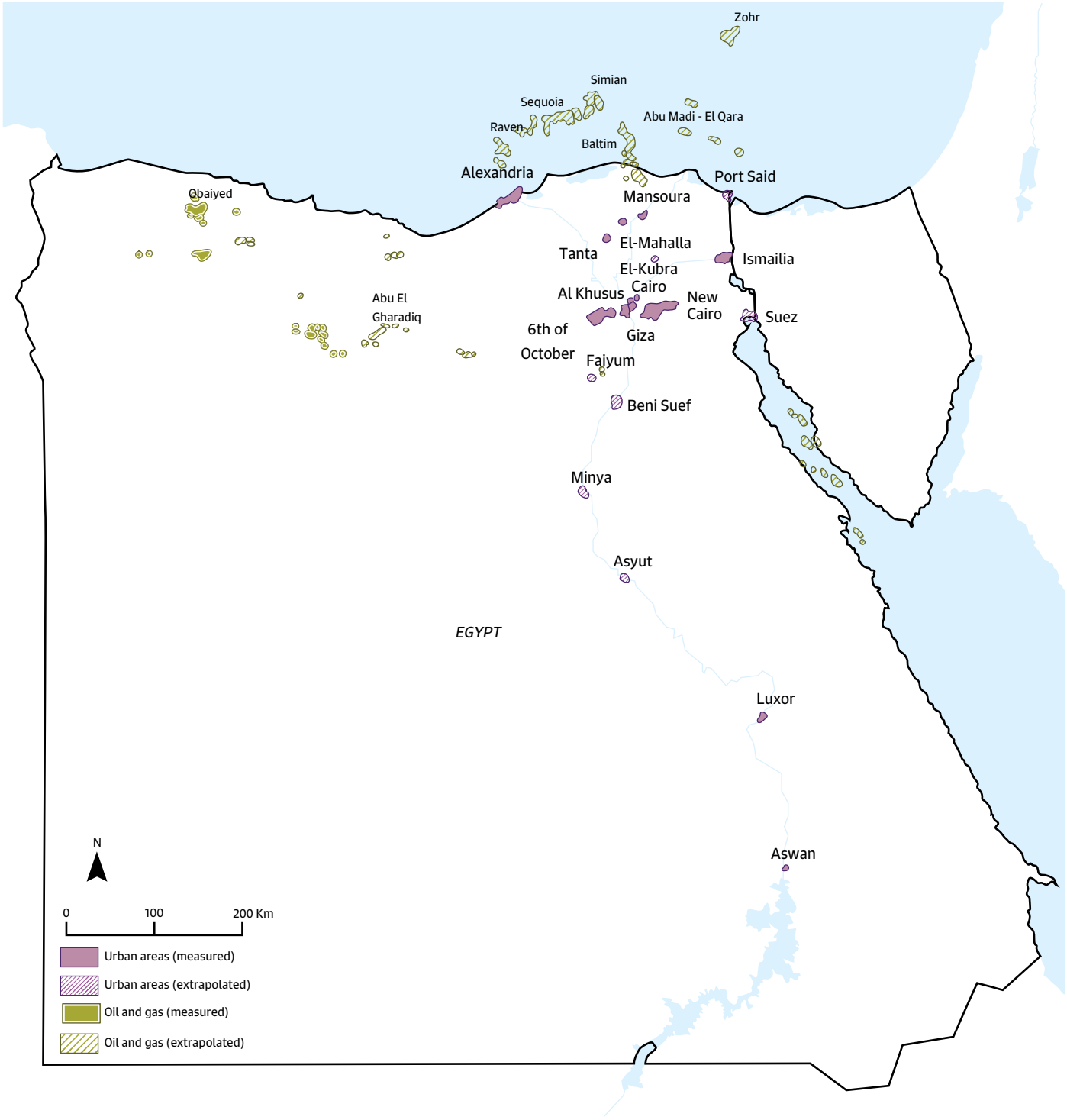
Source: Authors.

Figure 15. Geospatial visualization of methane sources and methods applied to Iran.



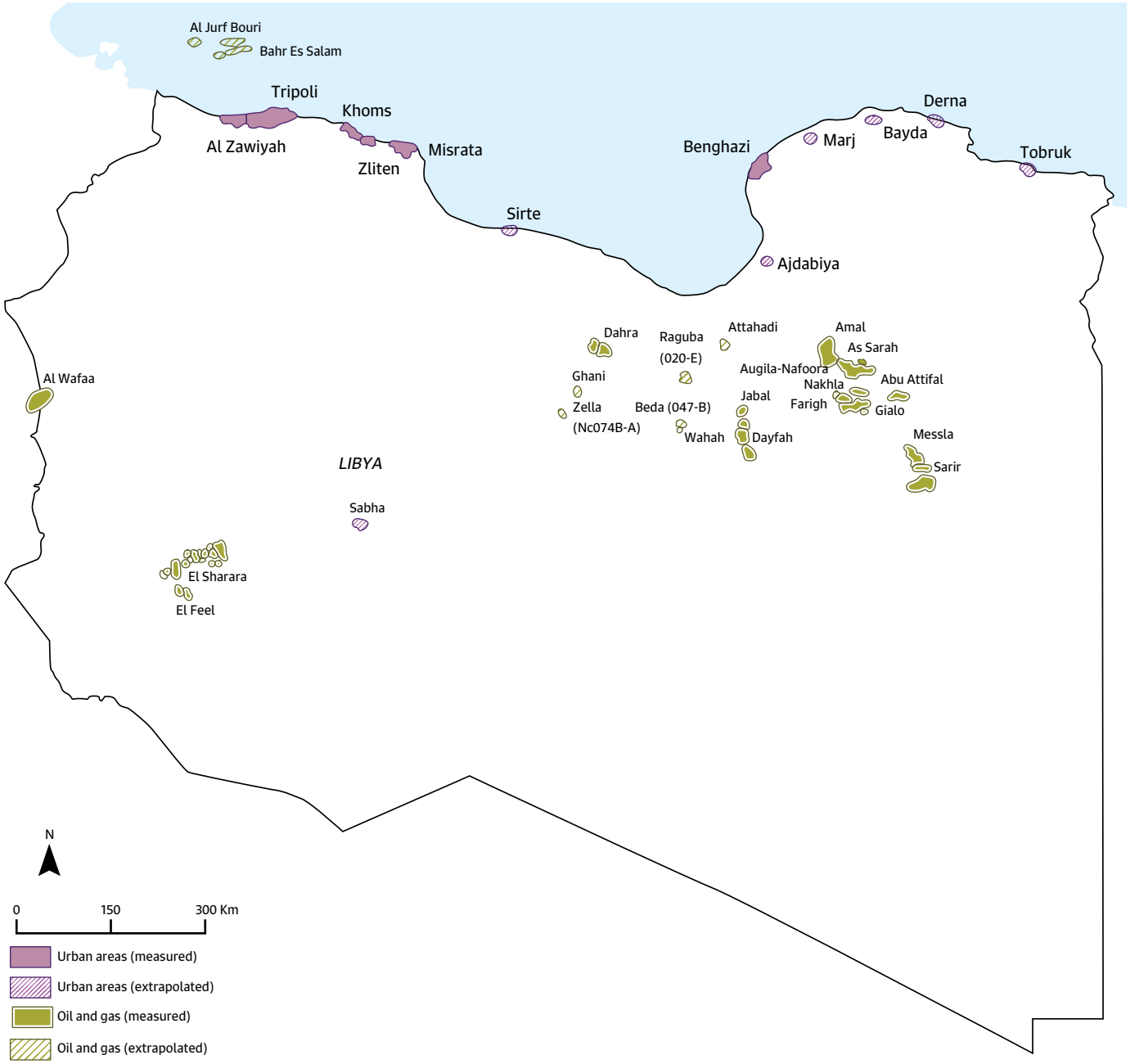
Source: Authors.

Figure 16. Geospatial visualization of methane sources and methods applied to Egypt.



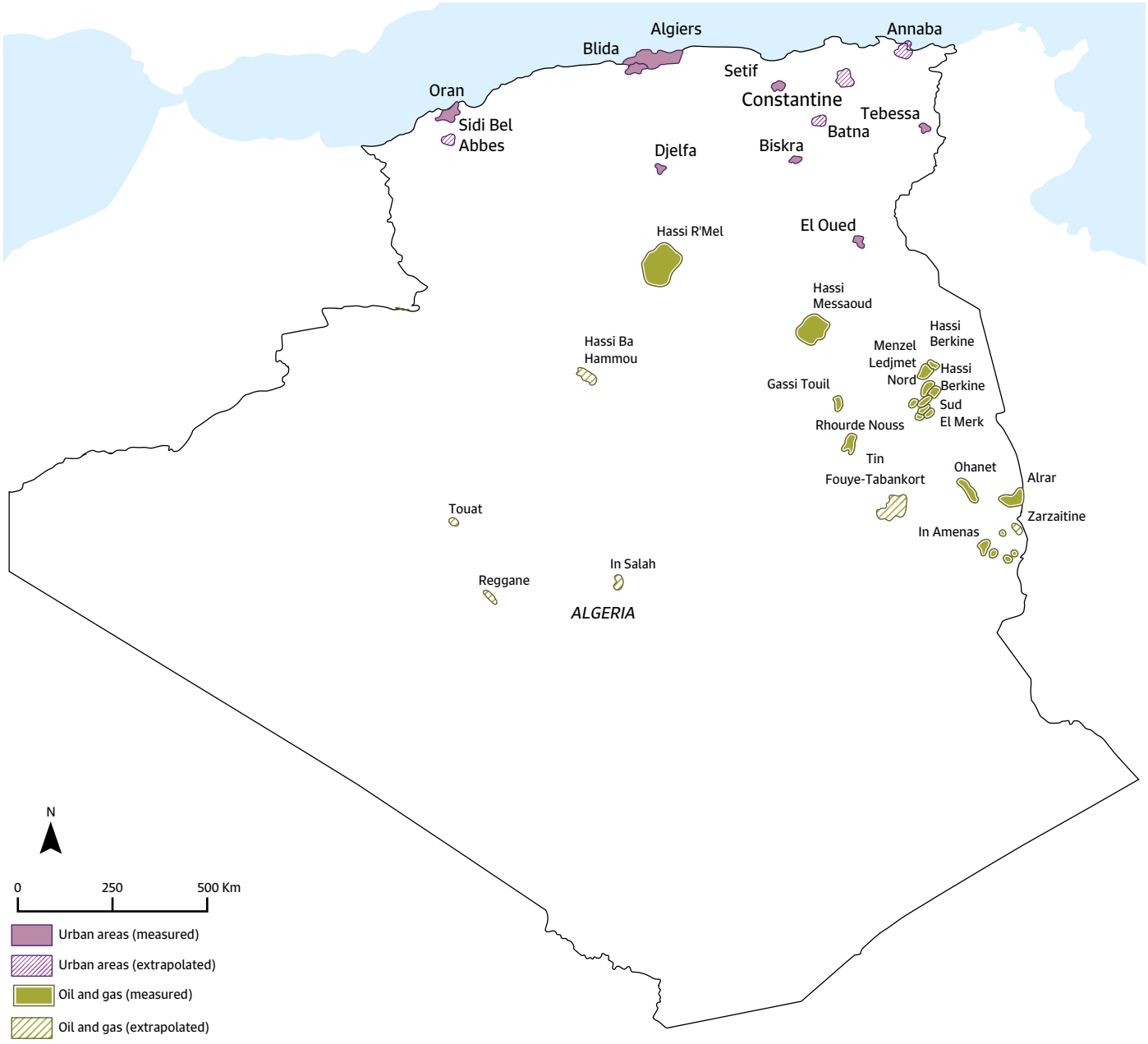
Source: Authors.

Figure 17. Geospatial visualization of methane sources and methods applied to Libya.



Source: Authors.

Figure 18. Geospatial visualization of methane sources and methods applied to Algeria.



Source: Authors.

3.6 Calculating Uncertainties

Uncertainties were calculated for all our satellite-based emission estimates generated using the basin-inversion and wind-rotated models.

For our basin-inversion measurements, we derived the associated uncertainties by following the sensitivity analysis approach described in Peng et al. (2023) that they used to calculate uncertainties.

For the wind-rotated model, we introduced a new approach for calculating uncertainties that is also based on a sensitivity analysis. The reliability of the wind-rotated estimates is influenced by uncertainties in both the input data and parameter calibration. To compute confidence intervals for each wind-rotated estimate, we derived uncertainty bounds using a sensitivity analysis framework like that used by Lauvaux et al. (2022). In this approach, we propagate variations in input data and parameters to assess their impact on the emission estimates, which produces a range of potential estimates that make up our uncertainty range. Further details on the parameters and data inputs and how they were perturbed to derive the uncertainty ranges can be found in Appendix D.

3.7 Data and Assumptions

Since our methods do not provide full coverage of all methane-emitting assets in a country, additional data were collected to support the extrapolation and disaggregation of our satellite-based estimates. The additional data sources are listed below, with further details available in Appendix E.

Population data were obtained from a variety of sources. The United Nations (UN) World Urbanization Prospects (UN 2018) dataset, produced by the UN Department of Economic and Social Affairs' Population Division, provides estimates for the annual urban population of each country's largest cities from 1950 to 2035 using census data and/or UN estimates. We used data from the 2016-2023 period.

The World Pop Dataset (Bondarenko et al. 2025) provides consistent 100-meter resolution gridded population count data, adjusted to align with official UN estimates at the national level and developed using unconstrained top-down methods. This dataset is produced for each year and country worldwide from 2000 to 2020. For our study, we utilized the dataset from 2016 to 2020.

The Global Human Settlement Layer (GHSL) (European Commission: Joint Research Centre 2023) is a 100-meter resolution gridded population count dataset created by the European Commission's Joint Research Centre. It combines satellite imagery with census data and UN estimates, providing data in five-year intervals from 1975 to 2030, and was used on a supplementary basis.

- **Census data:** The most recent census data at the city level were used, obtained from national statistical agencies.
- **Oil and gas data:** The Global Energy Monitor's *Global Oil and Gas Extraction Tracker* (2025) is a comprehensive dataset that documents oil and gas resources worldwide. It provides field-level information, including production data, typically offering one or two recorded data points since each field's inception.

  Rystad Energy's (2024) oil and gas production dataset covers total national-level production of both liquids and gas, and is available for all countries for the entire study period.
- **Waste data:** We used regional or city-level waste generation factors coming from a variety of sources, including Golhosseini and Ghazizade (2024), Okkacha et al. (2014), EDGAR (2024), Kuwait Environment Public Authority (2019), Ministry of Construction and Housing and Municipalities and Public Works (2022), and the Statistics Centre (2018).
- **Agriculture data:** The "FAOSTAT Emissions from Livestock" (FAO 2024) dataset reports national-level greenhouse gas emissions from four key livestock processes: enteric fermentation, manure left on pastures, manure management, and manure applied to soils. Estimates are calculated using the Tier 1 methodology outlined in the IPCC (2006) guidelines.

  "Gridded Livestock Density" is a gridded dataset from FAO (2024) for 2020 at a 10 km resolution, with a breakdown by livestock species. The dataset also contains the density of livestock per square km estimated with a Random Forest model.

3.8 Caveats and Limitations

3.8.1 Limitations in TROPOMI Data

TROPOMI retrievals degrade over coasts and mountains. Over water, absorption in the shortwave infrared bands, sharp land-water reflectance contrasts (known as "adjacency effects"), and higher humidity and aerosol loads reduce TROPOMI's sensitivity to methane. Over complex terrain, varying slopes and surface types create albedo artifacts that can be misread as methane. Additionally, vegetation and rocks with low albedo introduce further bias, while the instrument's "striping" can diminish image quality and weaken the methane signal in the wind-rotated method. Our image aggregation and background-removal steps alleviate some of these issues, but issues related to surface albedo remain.

3.8.2 Limitations in Wind Data

Both the basin-inversion and wind-rotation models rely on ERA5 wind fields. Inaccurate or insufficient meteorological data can affect the robustness of our models and the accuracy of our emission estimates.

3.8.3 Limitations in the Wind-Rotated Model

This method depends on numerous parameters, so calibration can have a strong influence on measurements. We sample ERA5 winds at the source; however, plumes can extend beyond 20 km in size, meaning the sampled wind at the center may not accurately represent conditions along the plume, which introduces uncertainty. TROPOMI artifacts (e.g., stripes and positive biases over bright surfaces) can be reinforced when images are rotated and aggregated, potentially overstating the methane plume signal. For high methane intensity assets, we ran a stripe-removal algorithm and discarded cases where corrected (with the algorithm) and uncorrected (without the algorithm) results diverged too much, or where striping was simply too excessive.

Annual totals are derived by aggregating only images that pass cloud and wind filters, so they rely on a subset of days in the year. As a preventive measure, we verify that the dates of the images used for wind-rotated measurements are evenly distributed throughout the year to avoid temporal bias, but an additional bias may arise due to Sentinel-5P consistently acquiring images at 1:30 pm local time.

3.8.4 Limitations in the Basin-Inversion Model

Inversions remain sensitive to the prior. Even though we restrict the prior to source locations only and apply conditioning tests, inaccurate or incomplete priors can bias the posterior estimate that is obtained from the basin inversion model and cause it to miss methane emission hotspots. Correct background selection is also particularly important. Peng et al. (2023) demonstrated that background selection can account for 38% of the variance in inversion-based estimates. Additionally, the atmospheric transport model (HYSPLIT, in our case) used in the inversion process can also introduce uncertainties (e.g., 12% in Peng et al. 2023) due to imperfect lateral boundary conditions and emission errors outside the basin's boundaries.[10]

The accuracy of the basin-inversion model is also heavily reliant on TROPOMI data quality, which requires cloud-free conditions and adherence to specific quality assurance thresholds. Only high-quality pixels can be utilized, significantly limiting data availability. However, because of our focus on annual measurement, we mitigated such issues. Finally, while TROPOMI offers improved resolution compared to older satellites, its resolution may still be insufficient to distinguish between closely located emission sources within the basin's boundaries.

Results and Discussion

04

4.1 Country-by-Country Results and Comparisons

Figure 19 presents our satellite-based methane emission estimates for Saudi Arabia's two principal emitting sectors (oil and gas, and waste) over the 2019-2023 period, along with the corresponding satellite coverage rates.

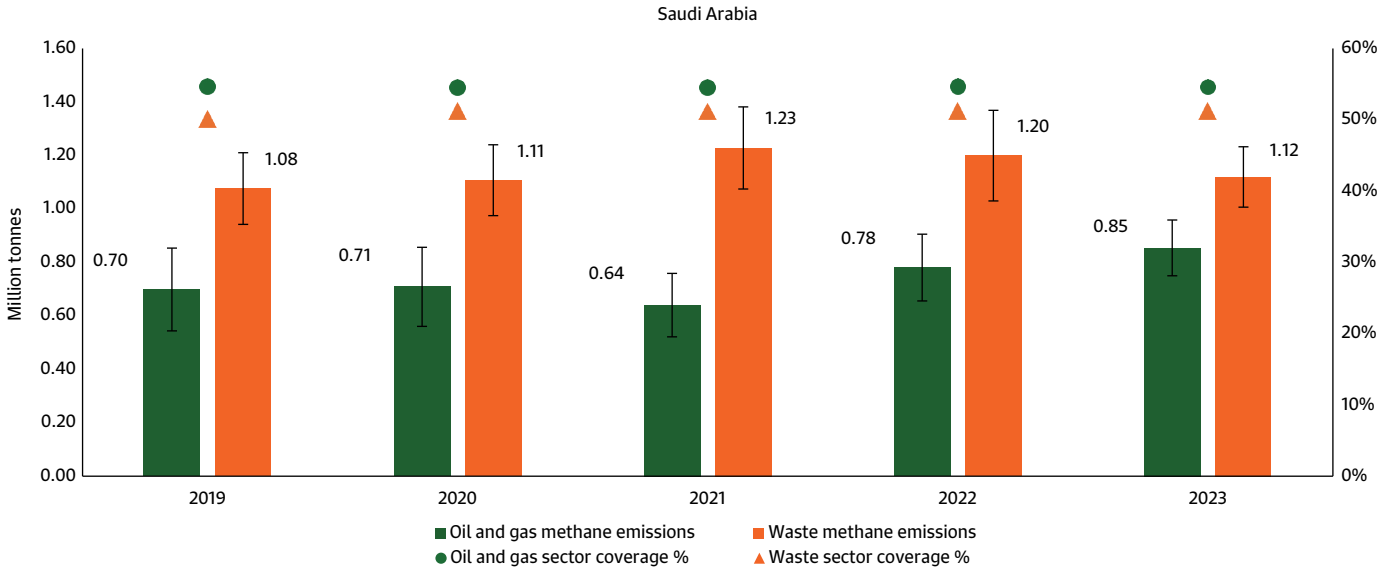
Saudi oil and gas emissions remain relatively stable throughout this period, slightly increasing from 0.70 to 0.85 million tonnes between 2019 and 2023, while waste-related emissions in Saudi Arabia fluctuate between 1.08 and 1.12 million tonnes over the same period. The uncertainty bars indicate that year-to-year changes should be interpreted cautiously. However, the overall ranking of the two sectors is clear: waste consistently represents the larger source of methane emissions in Saudi Arabia throughout the period.

The markers on the secondary (right-hand) axis indicate that satellite coverage for both sectors is broadly similar and hovers at around one-half of the activity. For oil and gas, coverage from direct satellite measurement is slightly above 50%, while for waste, it is slightly below 50%. This implies that the remaining shares were derived from extrapolation based on the satellite-observed assets. This level of coverage is relatively high for a satellite-based approach, providing us with confidence in the results. However, it also highlights that improvements in observing offshore or topographically complex onshore assets would further enhance our confidence in the satellite-based measurements.

Figure 20 compares our 2021 satellite-based estimate for Saudi Arabia (1.87 million tonnes across oil and gas, and waste) with activity-based inventories and other satellite studies. Our total is generally consistent with the country's official UNFCCC submission (1.79 million tonnes) but significantly lower than the IEA (3.72 million tonnes) and EDGAR (3.32 million tonnes) activity-based figures. This gap is primarily driven by the oil and gas sector: IEA and EDGAR report values roughly three times our satellite estimate, while our estimate is about three times the Saudi UNFCCC figure. This suggests that the appropriate oil and gas emission factor for Saudi Arabia likely lies between these two extremes. The two atmospheric inversion studies by Chen et al. (2023) and Shen et al. (2023) are higher than our oil and gas estimate but remain closer to it than to the higher IEA/EDGAR figures, indicating more consistency in the satellite measurements despite differing inference methods. For the waste sector, our estimate (1.23 million tonnes) aligns most closely with the government's estimate (1.53 million tonnes), suggesting that the other atmospheric inversion-based estimates overstate the sector's emissions, while the IEA and EDGAR underestimate them.

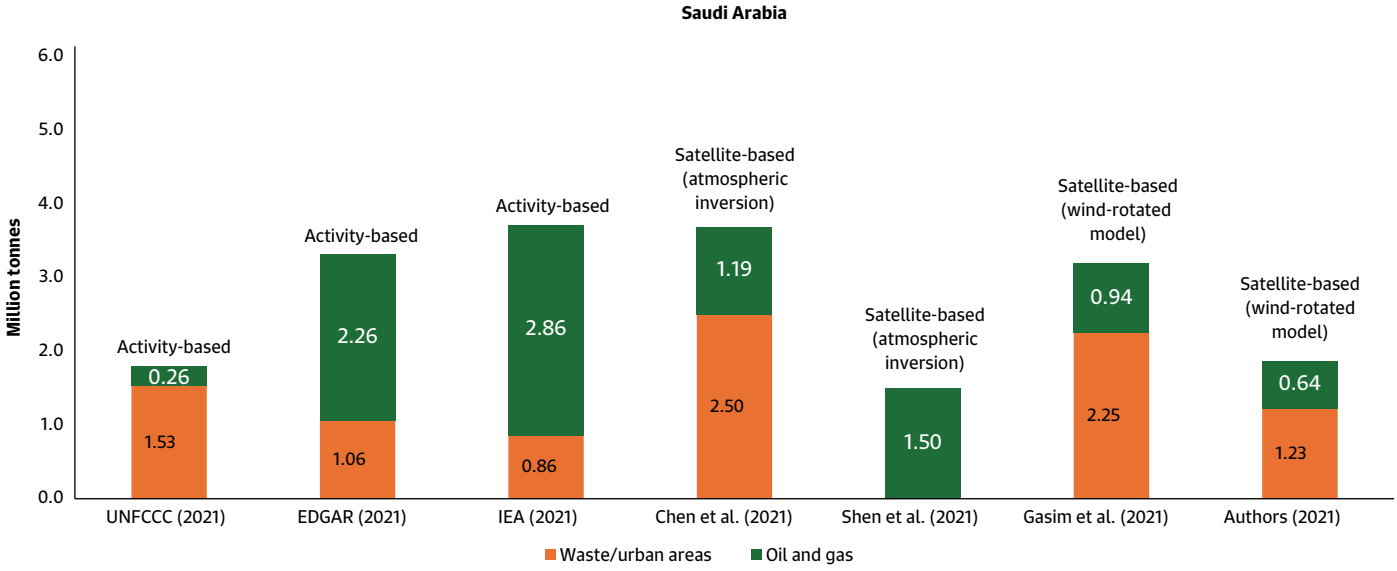
Figure 20 also compares our latest satellite estimate with our earlier work (Gasim et al. 2024). For 2021, our revised oil and gas estimate is 0.64 million tonnes versus 0.94 million tonnes previously, and the revised waste estimate is 1.39 million tonnes versus 2.25 million tonnes previously. These changes mainly reflect methodological refinements, specifically 1) replacing the rectangular box mask used previously with a plume-conforming "precise" mask, 2) adjusting the background-removal step to occur after, rather than before, image aggregation, and 3) extrapolating emissions from offshore assets by assuming that the ratio of their methane intensity to our satellite-measured methane intensity follows the ratio observed between both asset types in each country's gridded emissions inventory from EDGAR (2024). In our previous estimate in Gasim et al. (2024), we assumed that offshore and onshore oil fields in the same country share exactly the same methane intensity. [11]

Figure 19. Authors' satellite-based estimates of methane emissions in Saudi Arabia for the 2019-2023 period, utilizing the wind-rotated model. The uncertainty bars are also shown, along with the percentages of assets covered by direct satellite measurement.



Note: All author estimates presented include both methane emissions from assets directly measured by satellite and assets whose emissions were extrapolated. In other words, these estimates represent the total methane emissions across the entire country. The uncertainty bars are calculated based on the satellite-measured assets and are then extrapolated to the total estimates using coverage shares. However, the additional uncertainty introduced by extrapolating emissions from offshore and complex topography assets is not included in the uncertainty bars.
Sources: Authors.

Figure 20. Methane emissions estimates for Saudi Arabia from the literature compared to our satellite-based estimates.

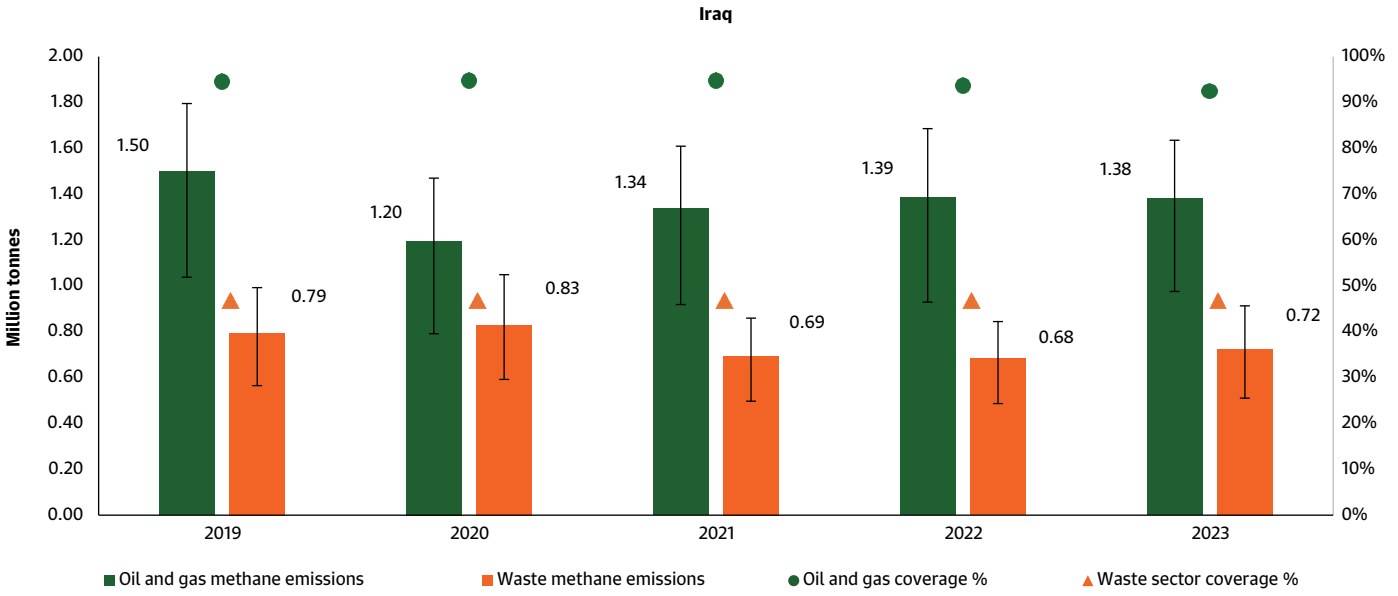


Note: Year of estimate is shown in brackets on the x-axis. Only the most recent national estimate submitted to the UNFCCC is shown in the figure. For any data source that provides multiple annual estimates, the estimate that is closest in time to the UNFCCC estimate is shown in the figure, and the other estimates are aligned in terms of reporting year as much as possible.
Sources: DNA (2025), IEA (2022), EDGAR (2024), Chen et al. (2023), Shen et al. (2023), Gasim et al. (2024), and authors.

Figure 21 presents our satellite-based methane estimates for Iraq for the 2019-2023 period, disaggregated into oil and gas emissions and waste emissions. Oil and gas emissions dominate, falling from 1.50 to 1.38 million tonnes over the study period. There is a sharper dip in the sector's emissions in 2020 that may be partially explained by the reduction in oil and gas production during that year. Waste emissions in Iraq are relatively smaller, decreasing from 0.79 to 0.72 million tonnes throughout the study period. Although measurements for both sectors indicate a slight reduction in methane emissions after 2019, the uncertainty bars for both sectors overlap across years, preventing us from inferring a statistically robust trend. Nevertheless, a key strength of our results for Iraq is the coverage: direct satellite coverage of oil and gas fields exceeds 90% each year, meaning only limited extrapolation was required. In contrast, waste coverage is around 40%-50%, so the waste totals rely equally on the extrapolation approach described in Section 3.5.

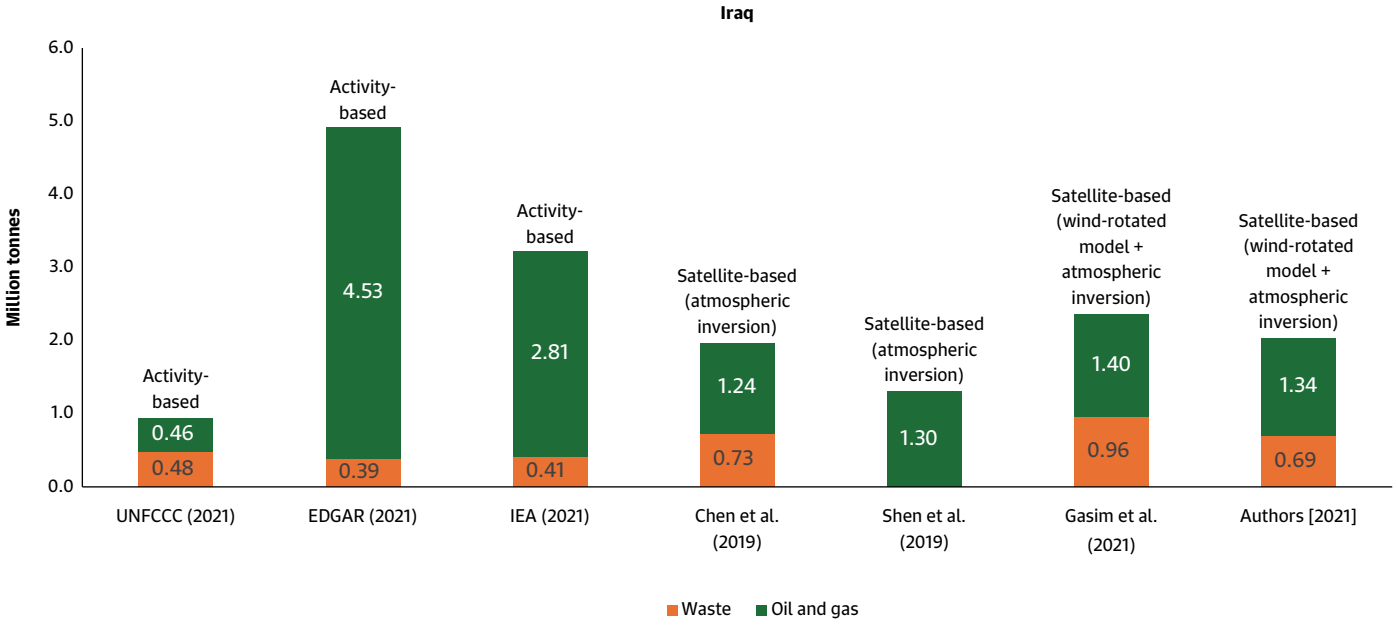
Figure 22 compares our 2021 estimate (2.03 million tonnes in total: 1.34 million tonnes from oil and gas and 0.69 million tonnes from waste) with activity-based inventories and prior satellite studies. Our estimate is significantly higher than Iraq's UNFCCC submission (0.94 million tonnes), which appears to understate oil and gas emissions in particular, but is far below the EDGAR estimate (4.92 million tonnes) and the IEA estimate (3.22 million tonnes), both of which have activity-based oil and gas numbers that exceed our full national total. Two earlier atmospheric-inversion studies by Chen et al. (2023) and Shen et al. (2023) cluster closely around 1.2 to 1.3 million tonnes for oil and gas, making their satellite-based estimates consistent with ours and highlighting the advantages of satellite-based measurements over activity-based datasets that rely on assumed emission factors. Compared to our earlier work (Gasim et al. 2024), our latest estimate is slightly lower, primarily because we refined the plume mask to more precisely match the shape of the plume and adjusted the background removal step in our application of the wind-rotated method. In summary, the comparison in Figure 22 suggests that Iraqi oil and gas emissions are being understated in official reporting and overstated in some global activity-based inventories, and that satellite-based methods can help anchor the estimates within a more realistic range.

Figure 21. Authors' satellite-based estimates for methane emissions in Iraq for the 2019-2023 period using both the wind-rotated and basin-inversion models. The uncertainty bars are also shown, along with the percentages of assets covered by direct satellite measurement.



Note: All author estimates presented include both methane emissions from assets directly measured by satellite and assets whose emissions were extrapolated. In other words, these estimates represent the total methane emissions across the entire country. The uncertainty bars are calculated based on the satellite-measured assets and are then extrapolated to the total estimates using coverage shares. However, the additional uncertainty introduced by extrapolating emissions from offshore and complex topography assets is not included in the uncertainty bars.
Sources: Authors.

Figure 22. Methane emissions estimates for Iraq from the literature compared to our satellite-based estimates.



Note: Year of estimate is shown in brackets on the x-axis. Only the most recent national estimate submitted to the UNFCCC is shown in the figure. For any data source that provides multiple annual estimates, the estimate that is closest in time to the UNFCCC estimate is shown in the figure, and the other estimates are aligned in terms of reporting year as much as possible.
Sources: Republic of Iraq Ministry of Environment (2025), IEA (2022), EDGAR (2024), Chen et al. (2023), Shen et al. (2023), Gasim et al. (2024), Authors.

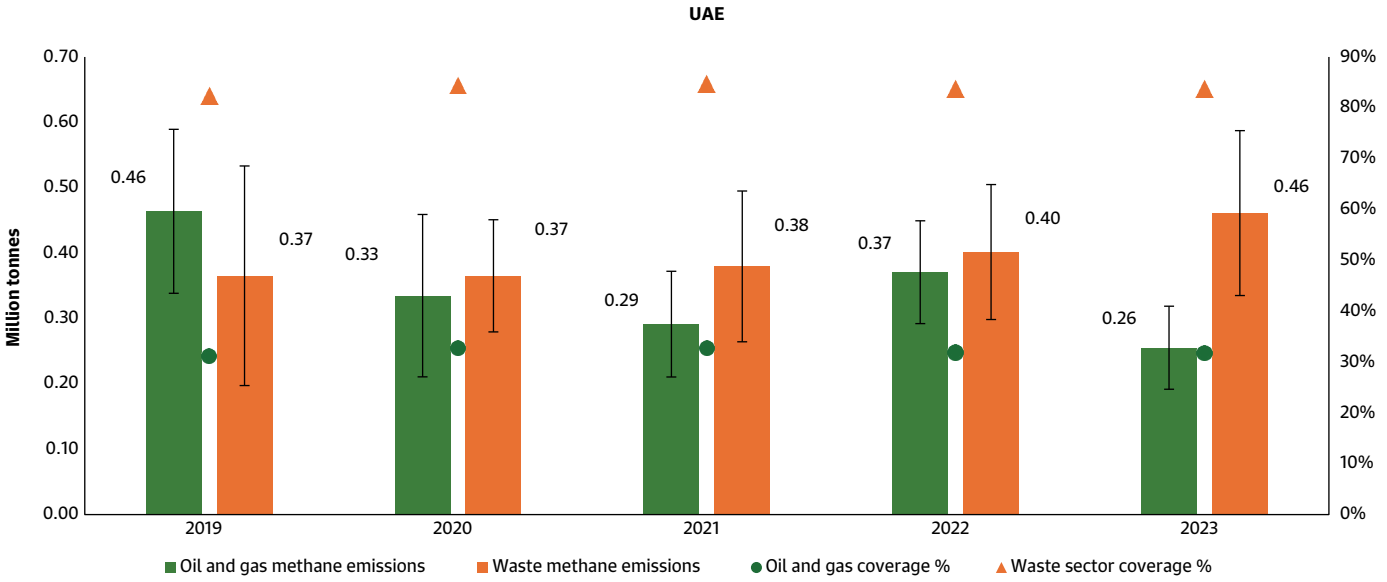
Figure 23 presents our satellite-based methane estimates for the UAE over 2019-2023. Oil and gas emissions decrease significantly from 0.46 to 0.26 million tonnes over the study period, while waste emissions gradually increase from 0.37 to 0.46 million tonnes. Our findings indicate that the waste sector becomes a relatively larger source of methane in the UAE.

Coverage varies across sectors: the waste sector benefits from very high direct satellite coverage (about 80% to 85%), requiring minimal extrapolation. In contrast, oil and gas coverage is low (around 30% to 35%) due to several onshore assets being located in challenging terrain, and a significant portion of UAE oil and gas production occurring offshore, where satellite retrievals are difficult. As discussed in Section 3.5, emissions from offshore assets were extrapolated by using the satellite-measured onshore intensities after adjusting them with the intensity ratio of both asset types from EDGAR's (2024) gridded inventories. This is done because studies have shown that offshore emission intensities can diverge significantly from onshore intensities for the same country (Gorchov Negron et al. 2020).

Figure 24 benchmarks our 2021 satellite estimate against activity-based and other satellite-based inventories for the UAE. Our total of 0.67 million tonnes (0.29 million tonnes from oil and gas, and 0.38 million tonnes from waste) is close to the country's UNFCCC submission (0.48 million tonnes) but significantly lower than the IEA (1.81 million tonnes) and EDGAR (1.08 million tonnes) figures, which tend to overstate oil and gas emissions. The notable discrepancy in oil and gas emission estimates for the UAE is striking: our 0.29 million tonnes estimate is roughly one-fifth of the IEA estimate and about one-third of the EDGAR figure, yet still much higher than the near-zero value of 0.03 million tonnes in the UNFCCC submission. This suggests that both international datasets and the national inventory are applying emission factors that do not accurately reflect the UAE's actual oil and gas methane emissions. Additionally, the atmospheric inversion estimate by Chen et al. (2023) is also much higher than our satellite-based estimate, potentially due to the prior used in their basin-inversion model, whereas our wind-rotated model does not rely on any prior. In contrast, waste-sector emission estimates from different sources cluster more closely around our estimate, indicating that the primary source of divergence for the UAE is the oil and gas sector.

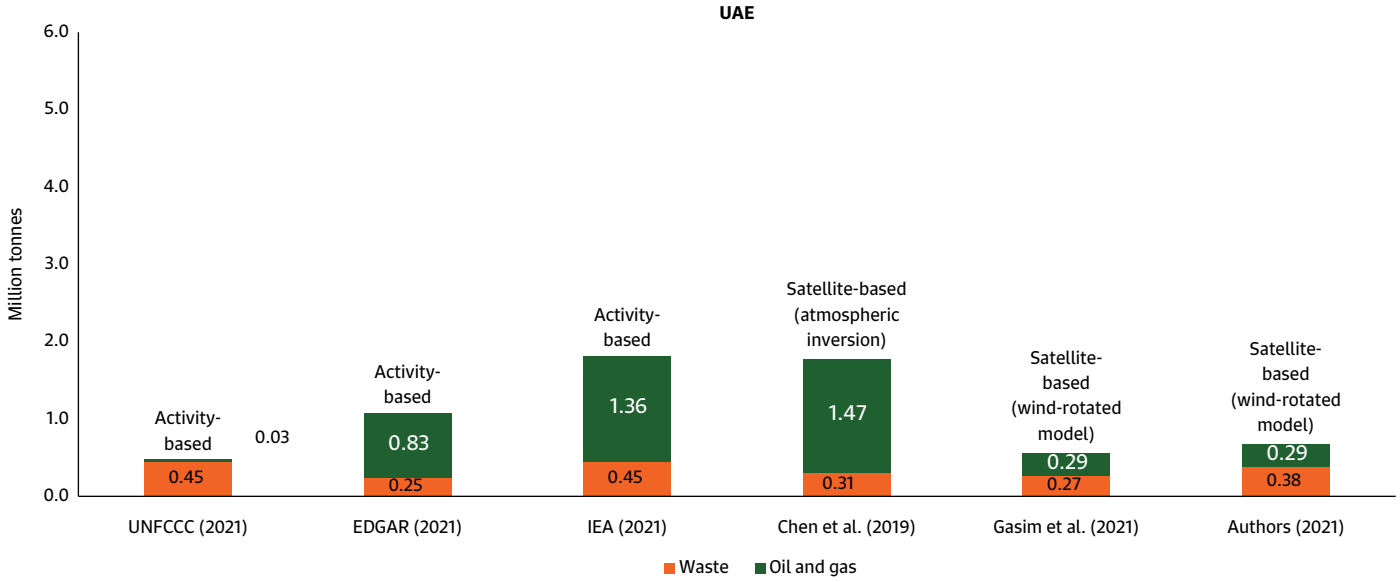
Figure 24 also compares our latest satellite-based estimates for the UAE with those from our previously published work (Gasim et al. 2024). Despite the refinements to our methodology, and especially the change to the extrapolation assumption for offshore emissions in the UAE, the methodological changes cancel out to produce very similar estimates to what we had shown previously for 2021.

Figure 23. Authors' satellite-based estimates for methane emissions in the UAE for the 2019-2023 period using the wind-rotated model. The uncertainty bars are also shown, along with the percentages of assets covered by direct satellite measurement.



Note: All author estimates presented include both methane emissions from assets directly measured by satellite and assets whose emissions were extrapolated. In other words, these estimates represent the total methane emissions across the entire country. The uncertainty bars are calculated based on the satellite-measured assets and are then extrapolated to the total estimates using coverage shares. However, the additional uncertainty introduced by extrapolating emissions from offshore and complex topography assets is not included in the uncertainty bars.
Sources: Authors.

Figure 24. Methane emissions estimates for the UAE from the literature compared to our satellite-based estimates.

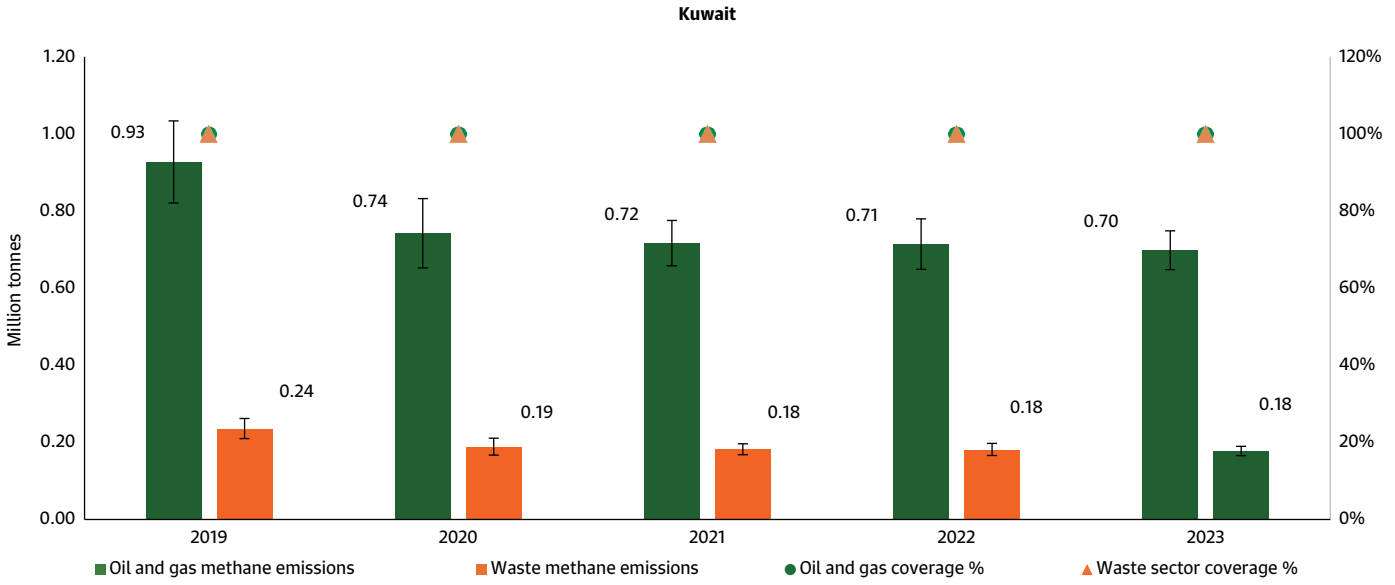


Note: Year of estimate is shown in brackets on the x-axis. Only the most recent national estimate submitted to the UNFCCC is shown in the figure. For any data source that provides multiple annual estimates, the estimate that is closest in time to the UNFCCC estimate is shown in the figure, and the other estimates are aligned in terms of reporting year as much as possible.
Sources: UAE (2024), IEA (2022), EDGAR (2024), Chen et al. (2023), Gasim et al. (2024), and authors.

Figure 25 presents our satellite-based methane estimates for Kuwait over 2019-2023 using the basin-inversion model. The initial model estimate, prior to any sectoral disaggregation, indicates a gradual decline in total national emissions over this period. After disaggregation, similar declines are observed in both sectors: oil and gas emissions fell from 0.93 million tonnes in 2019 to 0.70 million tonnes in 2023, while waste emissions decreased from 0.24 to 0.18 million tonnes. Since the basin boundary encompasses the entire country, direct satellite coverage for both sectors is effectively 100%, eliminating the need for extrapolation and resulting in narrow uncertainty bands. This complete coverage provides us with high confidence in both the level and the downward trend of Kuwait's methane emissions. However, our sectoral trends depend on sectoral shares taken from public inventories.

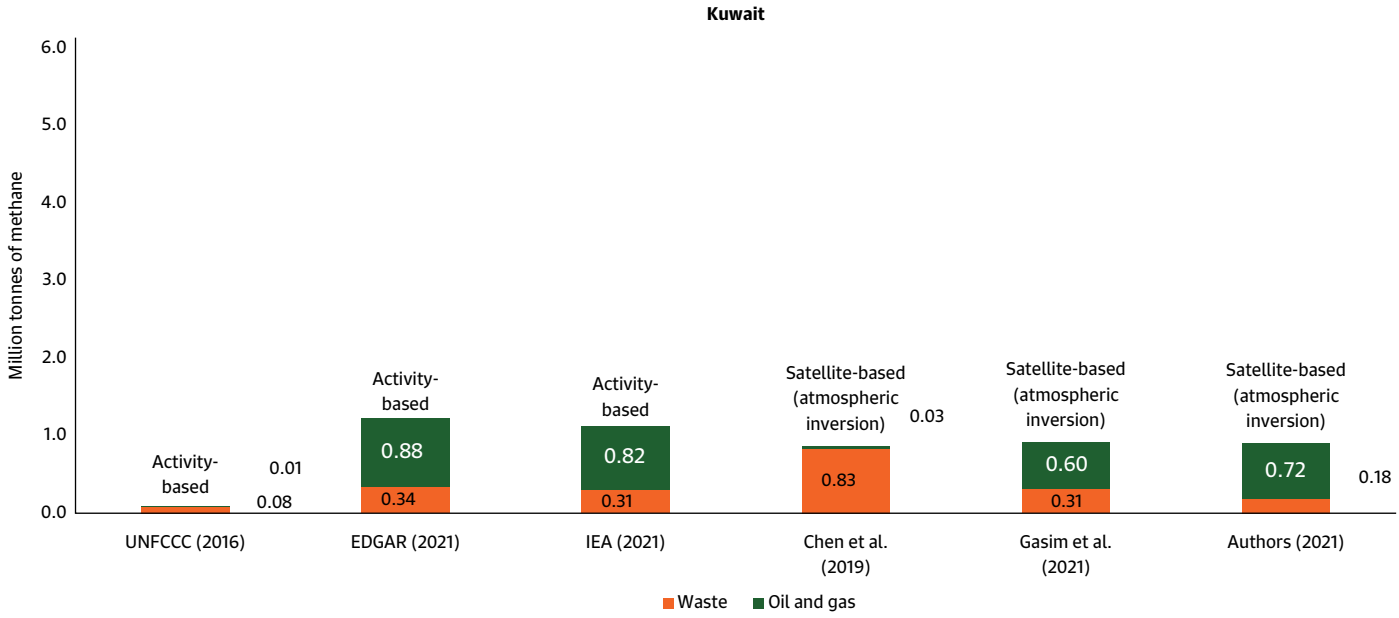
Figure 26 presents our 2021 estimate of 0.90 million tonnes in total, with 0.72 million tonnes attributed to oil and gas, alongside activity-based inventories and earlier satellite studies. Our total is an order of magnitude higher than Kuwait's latest UNFCCC submission of 0.09 million tonnes for 2016, indicating significant under-reporting in the official inventory. In contrast, our result is slightly lower than those from EDGAR (1.22 million tonnes) and the IEA (1.13 million tonnes), albeit with a different sectoral distribution. Unlike Chen et al. (2023), who allocated most of their basin-level emissions to waste (0.83 million tonnes) and only 0.03 million tonnes to oil and gas, our sectoral split, based on the assumptions discussed in Section 3.7, suggests that oil and gas is the primary source of methane. This discrepancy highlights a key limitation of inversion-based approaches: while they can accurately capture country-level totals with relatively high certainty, sectoral attribution is sensitive to the priors and auxiliary data used for disaggregation. Figure 26 also compares our latest satellite-based estimates for Kuwait with those from our previously published work (Gasim et al., 2024). There is almost no change in our basin-inversion total estimate; the only difference lies in the sectoral split, which was influenced by updates to the emissions data used for the sectoral allocations in both studies.

Figure 25. Authors' satellite-based estimates for methane emissions in Kuwait for the 2019-2023 period using the basin-inversion model. The uncertainty bars are also shown, along with the percentages of assets covered by direct satellite measurement.



Note: All author estimates presented include both methane emissions from assets directly measured by satellite and assets whose emissions were extrapolated. In other words, these estimates represent the total methane emissions across the entire country. The uncertainty bars are calculated based on the satellite-measured assets and are then extrapolated to the total estimates using coverage shares. However, the additional uncertainty introduced by extrapolating emissions from offshore and complex topography assets is not included in the uncertainty bars.
Sources: Authors.

Figure 26. Methane emissions estimates for Kuwait from the literature compared to our satellite-based estimates.



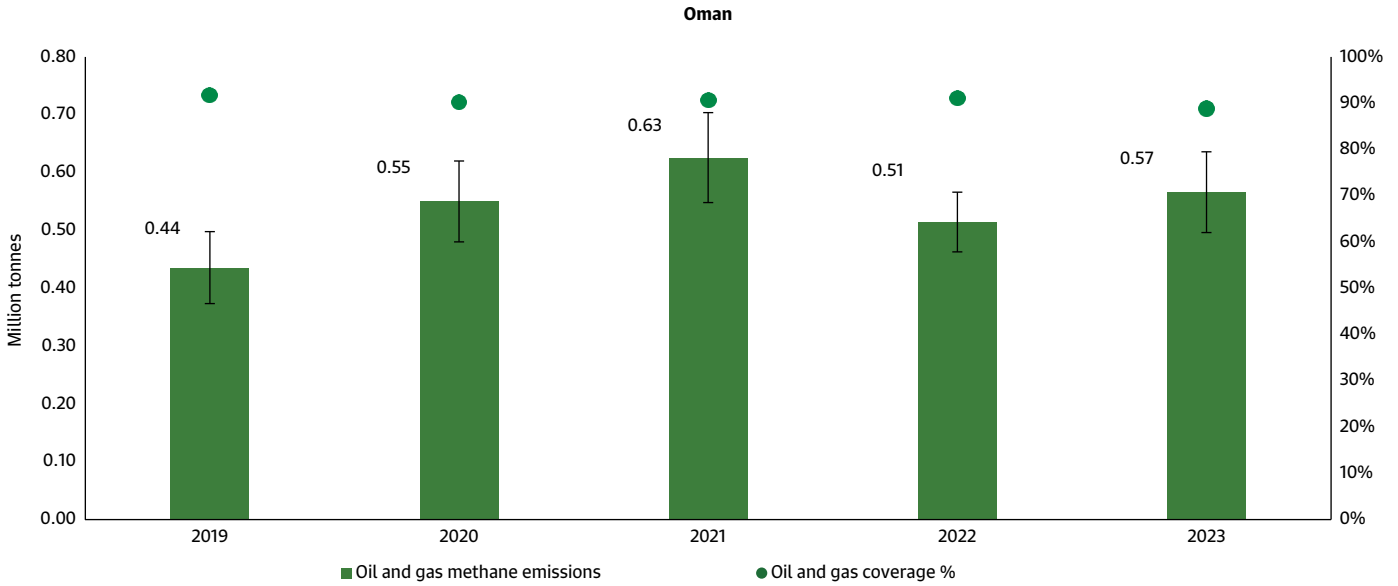
Note: Year of estimate is shown in brackets on the x-axis. Only the most recent national estimate submitted to the UNFCCC is shown in the figure. For any data source that provides multiple annual estimates, the estimate that is closest in time to the UNFCCC estimate is shown in the figure, and the other estimates are aligned in terms of reporting year as much as possible.
Sources: Kuwait Environment Public Authority (2019), IEA (2022), EDGAR (2024), Chen et al. (2023), Gasim et al. (2024), and authors.

Figure 27 presents our satellite-based oil and gas methane estimates for Oman over 2019-2023. Emissions increased from 0.44 million tonnes in 2019 to a peak of 0.63 million tonnes in 2021, dipped in 2022, and rebounded slightly to 0.57 million tonnes in 2023. This trend indicates a mild upward tendency for Oman's oil and gas emissions. Coverage of oil and gas assets is very high at approximately 90%, minimizing the need for extrapolation. We were unable to produce satellite-based waste estimates for Oman because the country's main urban areas are all located along coasts or mountains, where the wind-rotated method is unreliable.

Figure 28 benchmarks our oil and gas estimate for Oman (0.63 million tonnes in 2021) against activity-based inventories and previous satellite studies. Our estimate is almost equal to the most recent UNFCCC submission (0.63 million tonnes for 2015) and is slightly lower than the estimates from EDGAR (0.80 million tonnes in 2021) and the IEA (0.78 million tonnes in 2021). This confirms that, unlike most other MENA countries, activity-based estimates for Oman cluster around a relatively narrow range and are consistent with our satellite estimates. Surprisingly, the atmospheric inversion estimate by Chen et al. (2023) is significantly higher than all other estimates at 2.10 million tonnes, while Shen et al. (2023) is close to our estimate at 0.70 million tonnes. The divergence between these satellite-based measurements from the literature likely reflects differences in priors and sectoral attribution in their inversion models. In summary, our high-coverage, asset-level measurement supports the lower cluster of estimates and suggests that the very large value reported by Chen et al. (2023) is an overestimate for Oman.

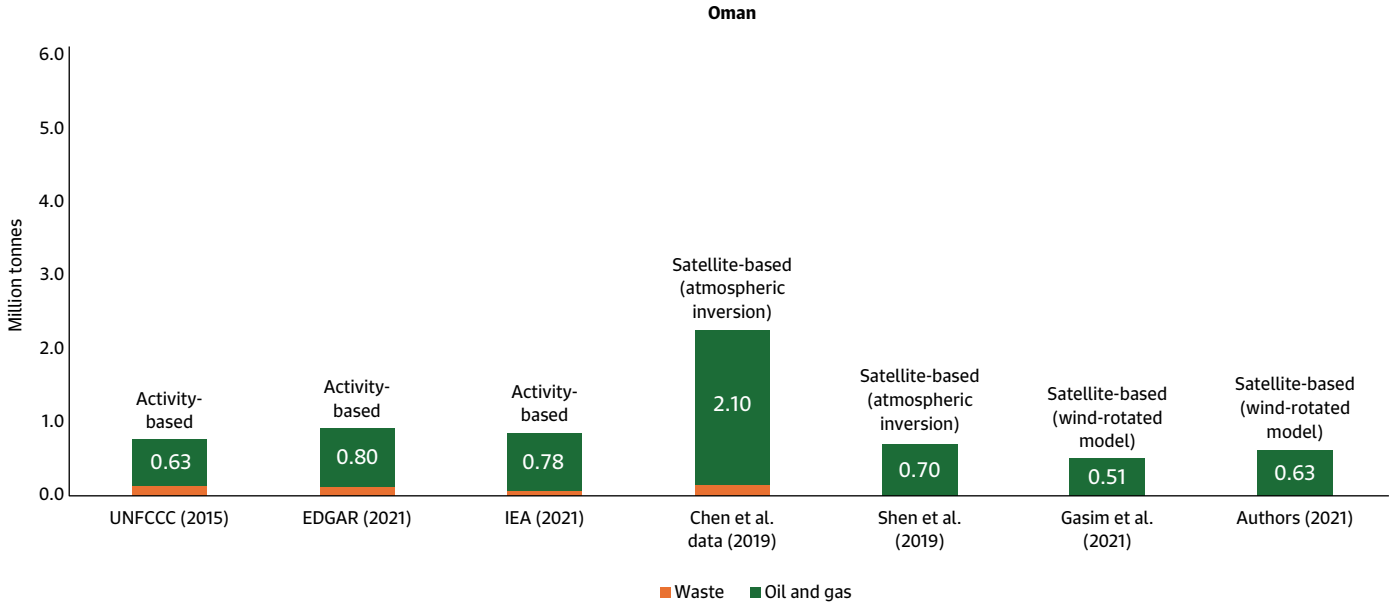
Figure 28 also compares our latest satellite-based estimates for Oman with those from our previously published work (Gasim et al. 2024). Our latest satellite-based estimates are approximately 20% higher, reflecting the refinements we have made to the wind-rotated method.

Figure 27. Authors' satellite-based estimates for methane emissions in Oman for the 2019-2023 period using the wind-rotated model. The uncertainty bars are also shown, along with the percentages of assets covered by direct satellite measurement.



Note: All author estimates presented include both methane emissions from assets directly measured by satellite and assets whose emissions were extrapolated. In other words, these estimates represent the total methane emissions across the entire country. The uncertainty bars are calculated based on the satellite-measured assets and are then extrapolated to the total estimates using coverage shares. However, the additional uncertainty introduced by extrapolating emissions from offshore and complex topography assets is not included in the uncertainty bars.
Sources: Authors.

Figure 28. Methane emissions estimates for Oman from the literature compared to our satellite-based estimates.

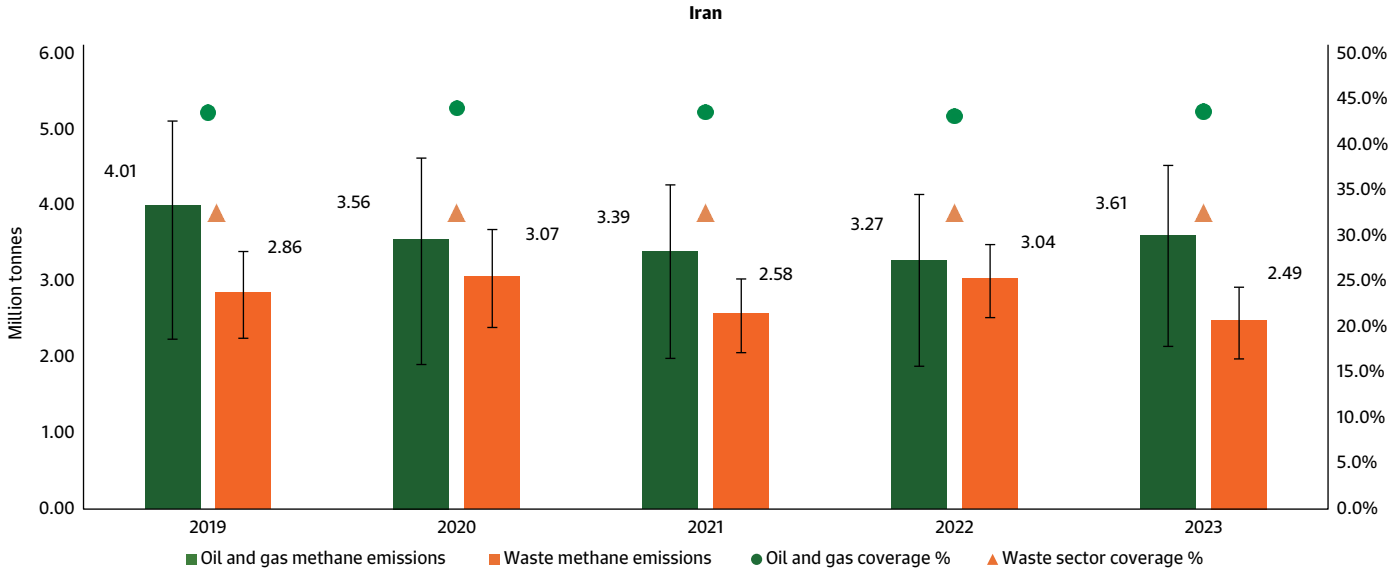


Note: Year of estimate is shown in brackets on the x-axis. Only the most recent national estimate submitted to the UNFCCC is shown in the figure. For any data source that provides multiple annual estimates, the estimate that is closest in time to the UNFCCC estimate is shown in the figure, and the other estimates are aligned in terms of reporting year as much as possible.
Sources: Ministry of Environment and Climate Affairs (2019), IEA (2022), EDGAR (2024), Chen et al. (2023), Shen et al. (2023), Gasim et al. (2024), and authors.

Figure 29 presents our combined wind-rotated and basin-inversion estimates for Iran for 2019-2023. Oil and gas emissions, which dominate the totals, declined from 4.01 million tonnes in 2019 to 3.61 million tonnes in 2023. Similarly, waste emissions also decreased from 2.86 million tonnes to 2.49 million tonnes over the study period. Given the wide uncertainty bars, these year-to-year changes should be interpreted as indicative rather than definitive. Coverage is modest for oil and gas (over 40% of producing assets were directly observed by satellite), but lower for waste (about one third of waste-generating urban areas), so a substantial portion of the national total for both sectors relies on extrapolation.

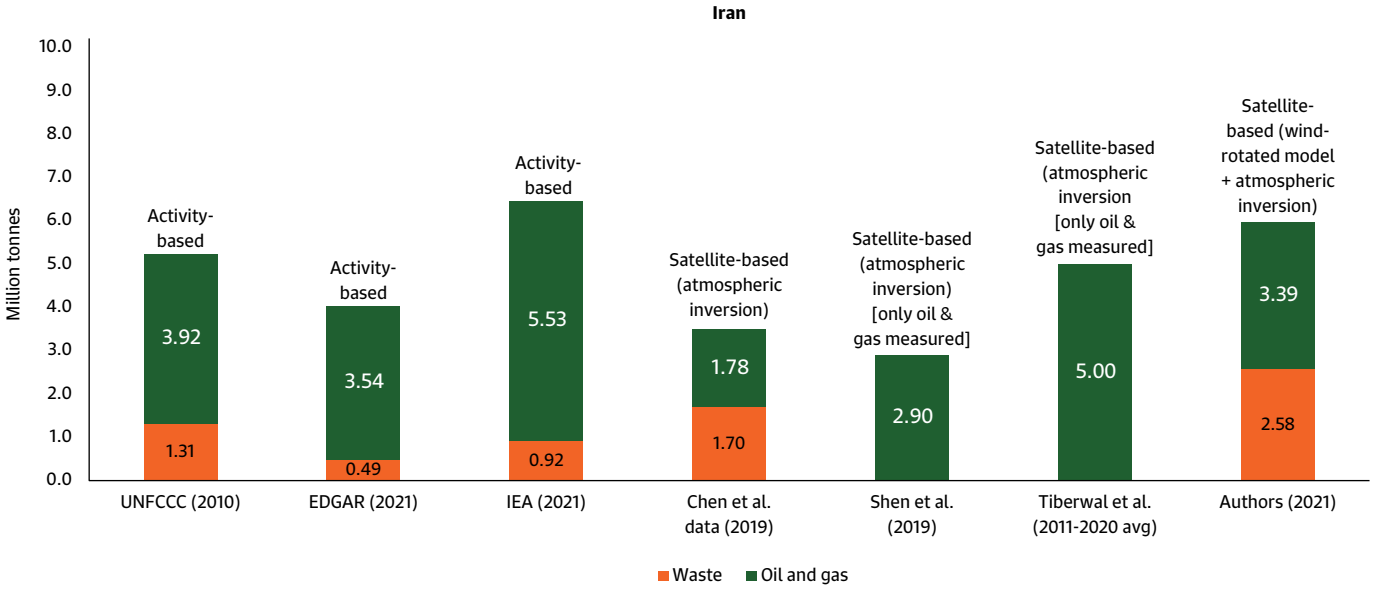
Figure 30 compares our 2021 national total of 5.97 million tonnes with activity-based inventories and other satellite studies. Our oil and gas estimate (3.39 million tonnes) is very close to EDGAR's figure (3.92 million tonnes) but significantly lower than the IEA's activity-based figure (5.53 million tonnes) and Tiberwal et al.'s (2024) satellite-based figure (5.00 million tonnes). Our satellite estimate is also closer to Iran's older UNFCCC submission (3.92 million tonnes in 2010), implying that the emission factors used by EDGAR and the Iranian government are accurate, while the emission factor used by the IEA sits too high. Surprisingly, the two inversion studies by Chen et al. (2023) and Shen et al. (2023) produced much lower oil and gas estimates (1.78 and 2.90 million tonnes, respectively), underscoring how sensitive inversion results for Iran are to different priors. The largest divergence is observed in the waste sector. Our estimate of 2.58 million tonnes is well above the 0.49 to 1.70 million tonne range reported in the literature, which may reflect systematic underreporting of waste emissions in existing inventories.

Figure 29. Authors' satellite-based estimates for methane emissions in Iran for the 2019-2023 period using the wind-rotated and basin-inversion models. The uncertainty bars are also shown, along with the percentages of assets covered by direct satellite measurement.



Note: All author estimates presented include both methane emissions from assets directly measured by satellite and assets whose emissions were extrapolated. In other words, these estimates represent the total methane emissions across the entire country. The uncertainty bars are calculated based on the satellite-measured assets and are then extrapolated to the total estimates using coverage shares. However, the additional uncertainty introduced by extrapolating emissions from offshore and complex topography assets is not included in the uncertainty bars.
Sources: Authors.

Figure 30. Methane emissions estimates for Iran from the literature compared to our satellite-based estimates.



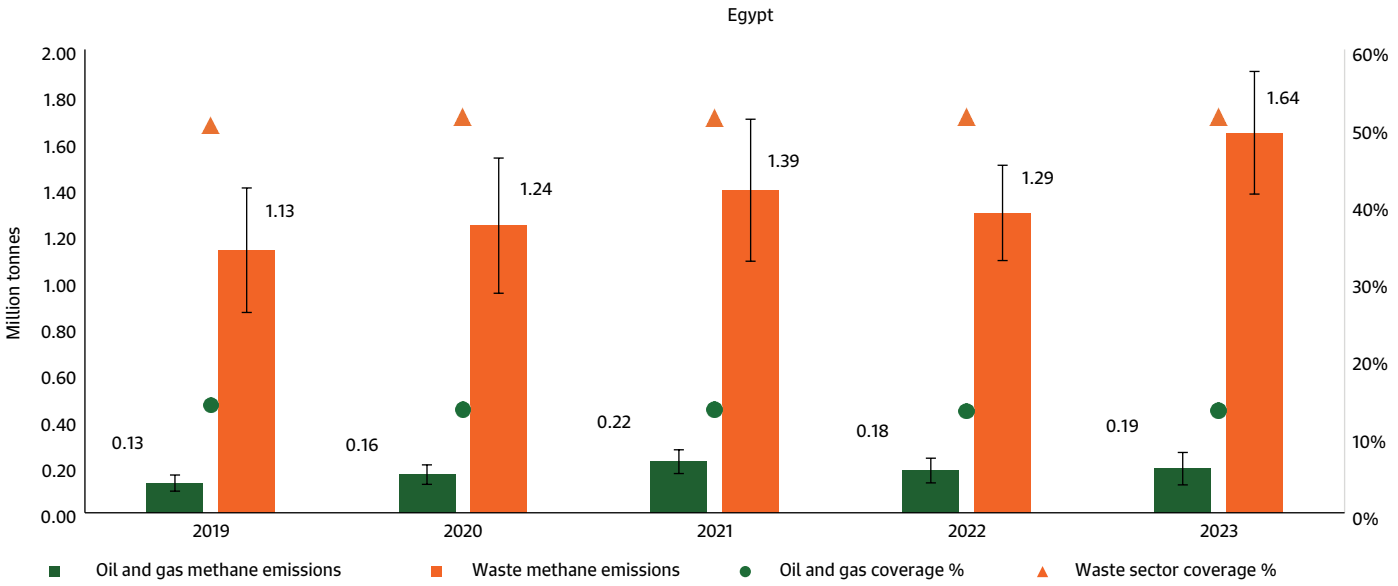
Note: Year of estimate is shown in brackets on the x-axis. Only the most recent national estimate submitted to the UNFCCC is shown in the figure. For any data source that provides multiple annual estimates, the estimate that is closest in time to the UNFCCC estimate is shown in the figure, and the other estimates are aligned in terms of reporting year as much as possible.
Sources: Islamic Republic of Iran (2017), IEA (2022), EDGAR (2024), Chen et al. (2023), Shen et al. (2023), Tiberwal et al. (2024), and authors.

Figure 31 shows our satellite-based methane estimates for Egypt over the 2019-2023 period. Emissions from oil and gas increased from 0.13 million tonnes in 2019 to 0.19 million tonnes in 2023, while waste emissions increased from 1.13 to 1.64 million tonnes over the same period. Our estimates highlight how waste is the dominant source of methane in Egypt. The trends in both sectors imply sizeable growth, although the uncertainty bands indicate that the exact magnitude of the increase should be interpreted cautiously. Coverage is a key driver of uncertainty: only about 13% to 14% of oil and gas production was directly measured by satellite in each year, so a large share of oil and gas emissions was extrapolated, including for Egypt's many offshore fields.

Figure 32 compares our 2022 estimate (totaling 1.48 million tonnes: 0.18 million tonnes from oil and gas and 1.29 million tonnes from waste) with activity-based inventories and earlier satellite studies. Our total estimate lies in the middle of the range formed by the other studies (from 1.02 to 2.1 million tonnes). However, there are major divergences in sectoral splits between the studies. Our 2022 oil and gas estimate (0.18 million tonnes) is six times larger than the UNFCCC submission (0.03 million tonnes), but five times smaller than the IEA estimate (0.96 million tonnes). For the waste sector, our 2022 estimate of 1.29 million tonnes is more than double the EDGAR estimate (0.53 million tonnes), but is relatively consistent with the other estimates by the IEA, Chen et al. (2023), and especially the UNFCCC submission (1.25 million tonnes). Our results show that, unlike oil and gas, waste sector estimates are more consistent across different methodologies.

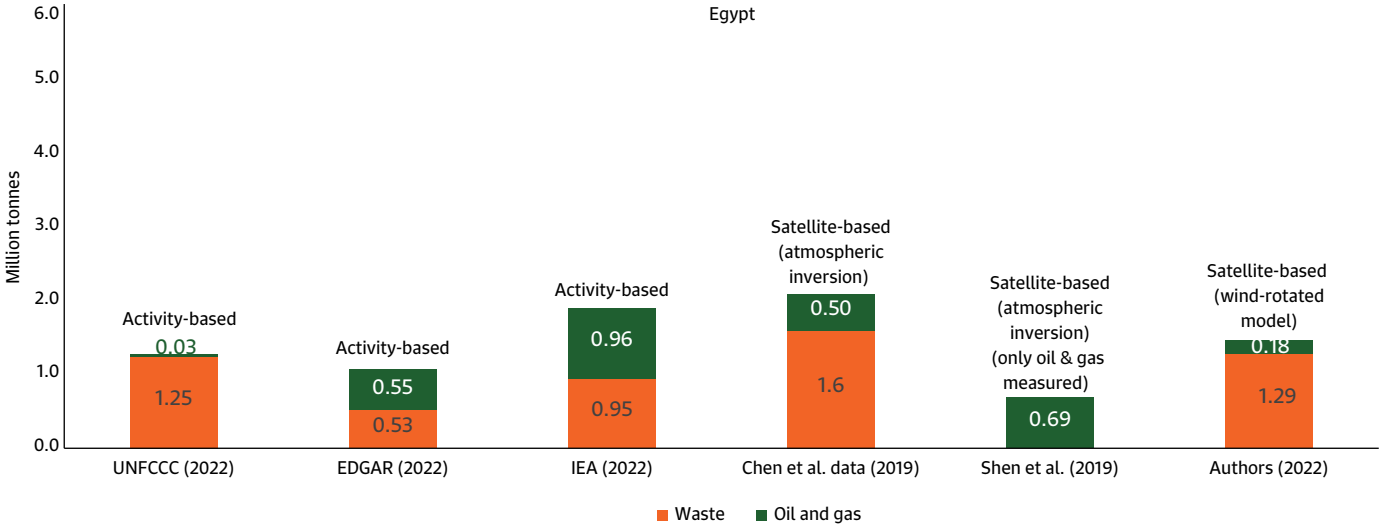
The two basin-inversion studies by Chen et al. (2023) and Shen et al. (2023) produced oil and gas estimates that were significantly higher than our estimate, which may be due to the sectoral split assumptions the authors made in their basin inversion models. Given our use of the wind-rotated model for Egypt, we did not need to make any sectoral split assumptions to estimate methane emission totals for each sector.

Figure 31. Authors' satellite-based estimates for methane emissions in Egypt for the 2019-2023 period using the wind-rotated model. The uncertainty bars are also shown, along with the percentages of assets covered by direct satellite measurement.



Note: All author estimates presented include both methane emissions from assets directly measured by satellite and assets whose emissions were extrapolated. In other words, these estimates represent the total methane emissions across the entire country. The uncertainty bars are calculated based on the satellite-measured assets and are then extrapolated to the total estimates using coverage shares. However, the additional uncertainty introduced by extrapolating emissions from offshore and complex topography assets is not included in the uncertainty bars.
Sources: Authors.

Figure 32. Methane emissions estimates for Egypt from the literature compared to our satellite-based estimates.



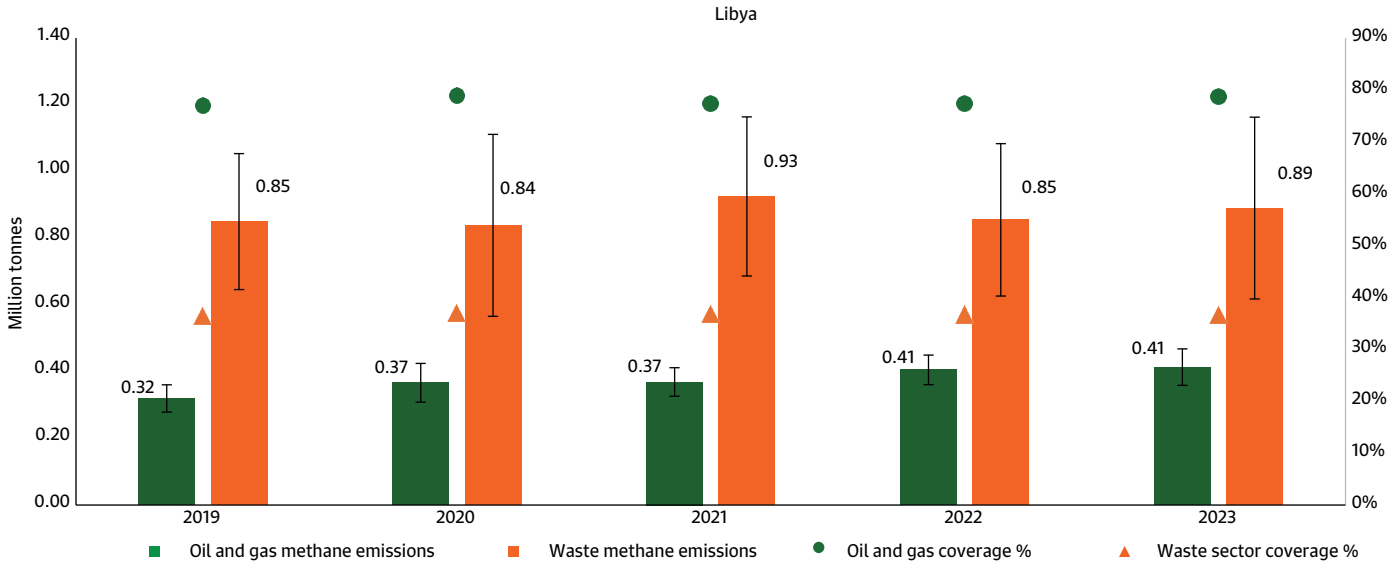
Note: Year of estimate is shown in brackets on the x-axis. Only the most recent national estimate submitted to the UNFCCC is shown in the figure. For any data source that provides multiple annual estimates, the estimate that is closest in time to the UNFCCC estimate is shown in the figure, and the other estimates are aligned in terms of reporting year as much as possible.
Sources: Arab Republic of Egypt Ministry of the Environment (2024), IEA (2023), EDGAR (2024), Chen et al. (2023), Shen et al. (2023), and authors.

Figure 33 presents our satellite-based time series for Libya. Total methane emissions rise from 1.17 to 1.30 million tonnes between 2019 and 2023, with emissions from waste consistently surpassing those from oil and gas. Emissions from oil and gas gradually increase from 0.32 million tonnes in 2019 to 0.41 million tonnes in 2023, while waste emissions fluctuate between 0.84 and 0.93 million tonnes. Coverage for oil and gas is robust, with nearly 80% of producing assets directly observed by satellite, requiring minimal extrapolation for that sector. In contrast, coverage for waste-generating urban areas is around 40%, indicating that a significant portion of the waste estimate is extrapolated from the satellite-measured cities.

Figure 34 compares our estimates with activity-based inventories and earlier satellite inversions. Our oil and gas estimate of 0.37 million tonnes for 2021 closely aligns with the findings of Chen et al. (2023) and Shen et al. (2023), but is about half of EDGAR's estimate (0.77 million tonnes) and significantly lower than the IEA's estimate of 2.41 million tonnes. This discrepancy suggests that global inventories may be using emission factors that are too high for Libyan production conditions. Unlike other MENA countries, Libya has not submitted an official national GHG inventory to the UNFCCC, making satellite observations particularly valuable for comparing differing estimates from external entities that likely assumed emission factor values. Our waste estimate of 0.93 million tonnes is a notable outlier on the high side compared to EDGAR and the IEA, both of which report waste emissions of approximately 0.1 million tonnes. Even if we disregard the roughly 60% of waste emissions calculated through extrapolation, our waste sector estimate based on only the urban areas that were directly measured with the wind-rotated method would still be higher than all the other waste estimates in the literature.

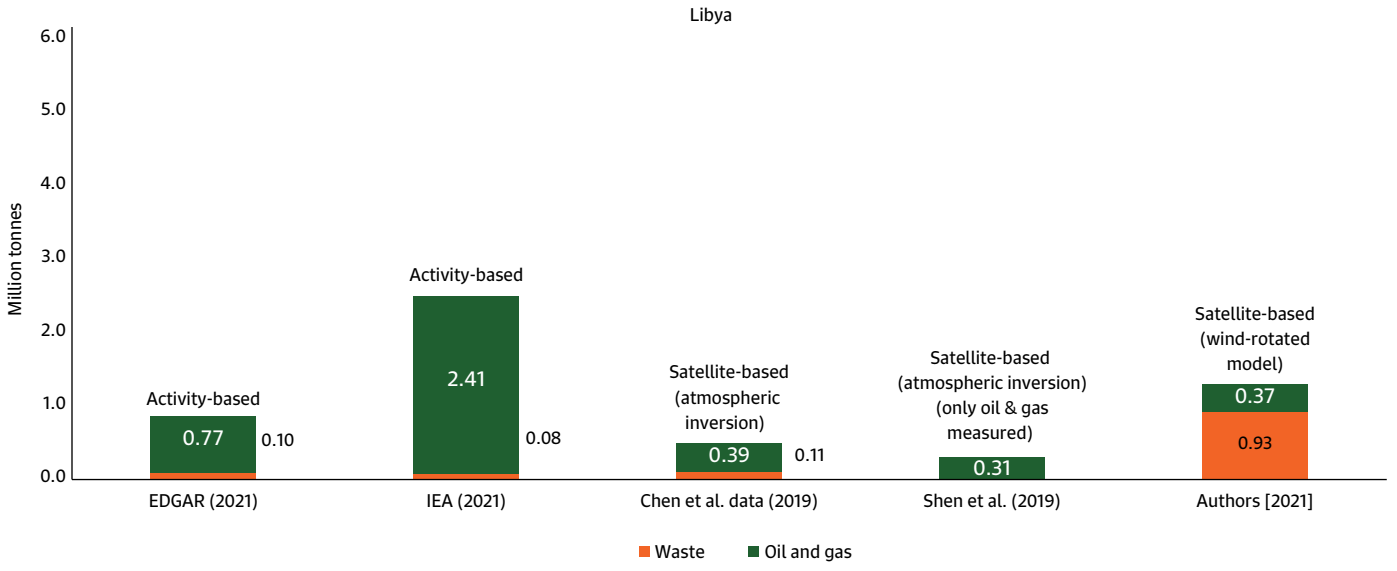
In summary, our analysis indicates that existing activity-based datasets for Libya are overreporting methane emissions from oil and gas but underreporting methane emissions from waste. Earlier satellite-based studies, which used activity-based waste sector emission estimates as priors, also appear to be under-reporting methane emissions from waste.

Figure 33. Authors' satellite-based estimates for methane emissions in Libya for the 2019-2023 period using the wind-rotated model. The uncertainty bars are also shown, along with the percentages of assets covered by direct satellite measurement.



Note: All author estimates presented include both methane emissions from assets directly measured by satellite and assets whose emissions were extrapolated. In other words, these estimates represent the total methane emissions across the entire country. The uncertainty bars are calculated based on the satellite-measured assets and are then extrapolated to the total estimates using coverage shares. However, the additional uncertainty introduced by extrapolating emissions from offshore and complex topography assets is not included in the uncertainty bars.
Sources: Authors.

Figure 34. Methane emissions estimates for Libya from the literature compared to our satellite-based estimates.

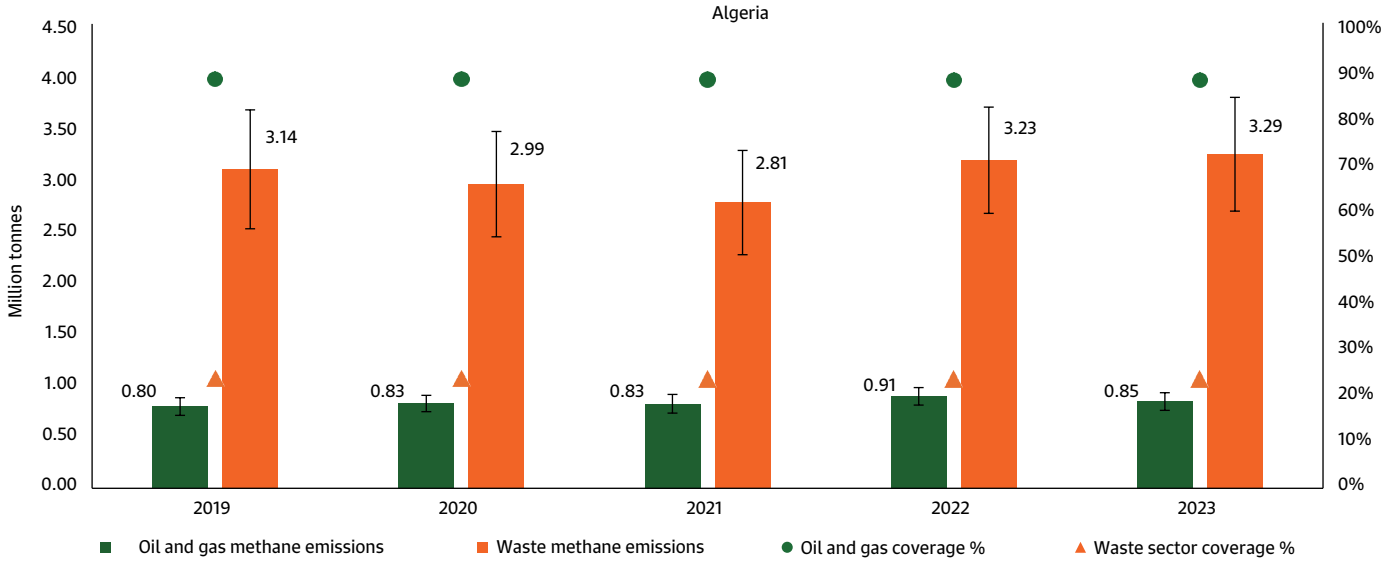


Note: Year of estimate is shown in brackets on the x-axis. Only the most recent national estimate submitted to the UNFCCC is shown in the figure. For any data source that provides multiple annual estimates, the estimate that is closest in time to the UNFCCC estimate is shown in the figure, and the other estimates are aligned in terms of reporting year as much as possible.
Sources: IEA (2022), EDGAR (2024), Chen et al. (2023), Shen et al. (2023), and authors.

Figure 35 presents our satellite-based methane estimates for Algeria for the 2019-2023 period. Total emissions remain high and relatively stable, at just over 4 million tonnes per year. In terms of sectoral contribution, waste-sector emissions dominate, rising from 3.14 million tonnes in 2019 to 3.29 million tonnes by 2023, while oil and gas emissions remain comparatively low, fluctuating between 0.80 and 0.91 million tonnes. Oil and gas coverage is strong (about 90%), necessitating only limited extrapolation for that sector. In contrast, waste coverage is low (around 25%), meaning that roughly three-quarters of the national waste emissions estimate is derived from extrapolation.

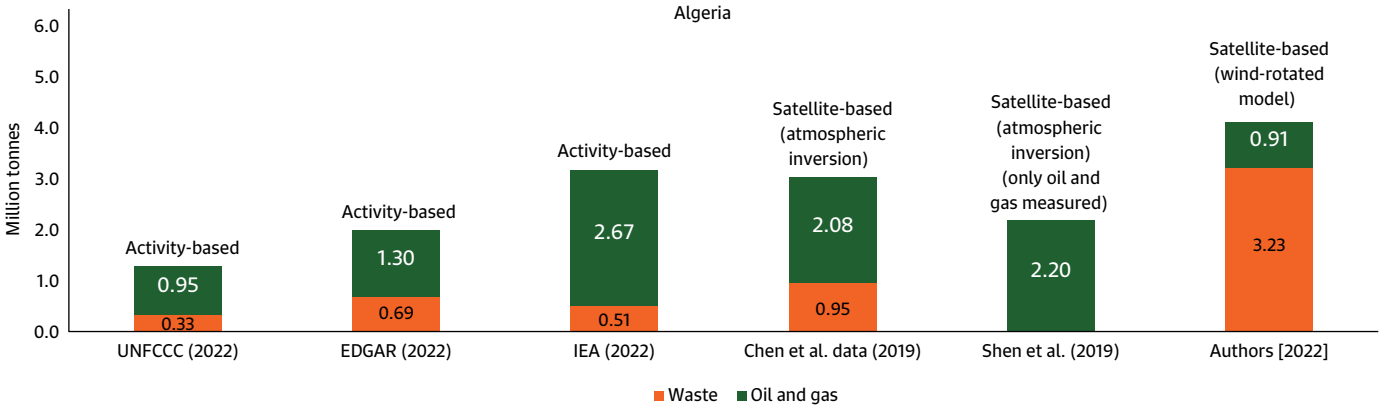
Figure 36 benchmarks our 2022 estimate (4.13 million tonnes) against activity-based inventories and earlier satellite studies. For oil and gas, our estimate of 0.91 million tonnes closely aligns with Algeria's 2022 UNFCCC submission (0.95 million tonnes) but is significantly lower than the IEA (2.67 million tonnes), as well as the inversion results from Chen et al. (2023) and Shen et al. (2023) of 2.08 and 2.20 million tonnes, respectively. In contrast to results from other MENA countries, we observe relatively larger discrepancies in waste sector emission estimates. Our estimate of 3.23 million tonnes is substantially higher than the UNFCCC submission (0.33 million tonnes), EDGAR (0.69 million tonnes), and IEA (0.51 million tonnes), and it even exceeds Chen et al.'s (2023) inversion-based value (0.95 million tonnes). Because our estimate of methane emissions from directly observed urban areas – excluding extrapolated areas – already exceeds the waste estimates of emissions from the literature, our results point to a systematic underestimation of Algerian waste methane emissions in previous studies and datasets.

Figure 35. Authors' satellite-based estimates for methane emissions in Algeria for the 2019-2023 period using the wind-rotated model. The uncertainty bars are also shown, along with the percentages of assets covered by direct satellite measurement.



Note: All author estimates presented include both methane emissions from assets directly measured by satellite and assets whose emissions were extrapolated. In other words, these estimates represent the total methane emissions across the entire country. The uncertainty bars are calculated based on the satellite-measured assets and are then extrapolated to the total estimates using coverage shares. However, the additional uncertainty introduced by extrapolating emissions from offshore and complex topography assets is not included in the uncertainty bars.
Sources: Authors.

Figure 36. Methane emissions estimates for Algeria from the literature compared to our satellite-based estimates.



Note: Year of estimate is shown in brackets on the x-axis. Only the most recent national estimate submitted to the UNFCCC is shown in the figure. For any data source that provides multiple annual estimates, the estimate that is closest in time to the UNFCCC estimate is shown in the figure, and the other estimates are aligned in terms of reporting year as much as possible.

Sources: People's Democratic Republic of Algeria Ministry of the Environment and the Quality of Life (2024), IEA (2023), EDGAR (2024), Chen et al. (2023), and Shen et al. (2023).

4.2 Cross-Country Comparisons and Benchmarking

Using our satellite measurements, we compared methane emissions among countries by employing indicators such as methane intensity, which accounts for variations in oil and gas production levels and population sizes across the nine MENA countries. Figure 37 compares the methane intensity of the oil and gas sector across these countries using our satellite-based emission estimates. Methane intensity is measured in kilograms of methane emitted per barrel of oil equivalent (boe) produced, enabling meaningful comparisons across countries with vastly different production levels. The results reveal striking cross-country differences in methane intensity – up to 15-fold – likely influenced by a combination of operational practices, infrastructure quality, regulatory regimes, and the physical characteristics of countries' oil and gas fields.

Among the nine MENA countries, Saudi Arabia and the UAE stand out as clear top performers, with the lowest methane intensities from oil and gas production. Across the 2019-2023 period, Saudi Arabia and the UAE had average satellite-based methane intensities of 0.16 and 0.19 kg of methane per boe, respectively, values that are significantly lower than the others.[12] Both countries' notably low methane intensities are consistent with their modern infrastructure, centralized production facilities (as discussed by Chen et al. 2023), and advanced operational practices.

Egypt also stands out for having the third lowest methane intensity, at an average of 0.305 kg of methane per boe. However, it should be reiterated that our satellite coverage of Egypt's oil and gas sector was the lowest among the nine countries (less than 15%), and we extrapolated satellite-measured intensities from Egypt's onshore fields (the minority) to its offshore fields (the majority) using a scaling ratio. Egypt's results and ranking are very sensitive to this scaling ratio, which is the ratio of the methane intensity of offshore fields to onshore fields. Had we assumed that this scaling ratio was equal to one for Egypt, then it would have the second-highest average methane intensity among the nine countries.

In contrast to Saudi Arabia and the UAE, Iran exhibits the highest average methane intensity at 1.301 kg of methane per boe. This high value suggests significant emissions relative to production, which likely reflect widespread flaring and venting as well as persistent leakage from aging oil and gas infrastructure. Nevertheless, Iran exhibits a clearly declining trend in its methane intensity over the 2019-2023 period, with recent values approaching 1.0 kg of methane per boe.

The remaining countries (Kuwait, Iraq, Algeria, Oman, and Libya) fall within an intermediate range. Average methane intensities for 2019-2023 in these five countries cluster between roughly 0.6 and 1.0 kg of methane per boe. The one exception is Libya in 2020, which exhibited the highest methane intensity value among all countries and years, when its oil and gas production fell drastically. During this period, its methane emissions remained flat (see Figure 33), leading to a sharp increase in its methane intensity in 2020.

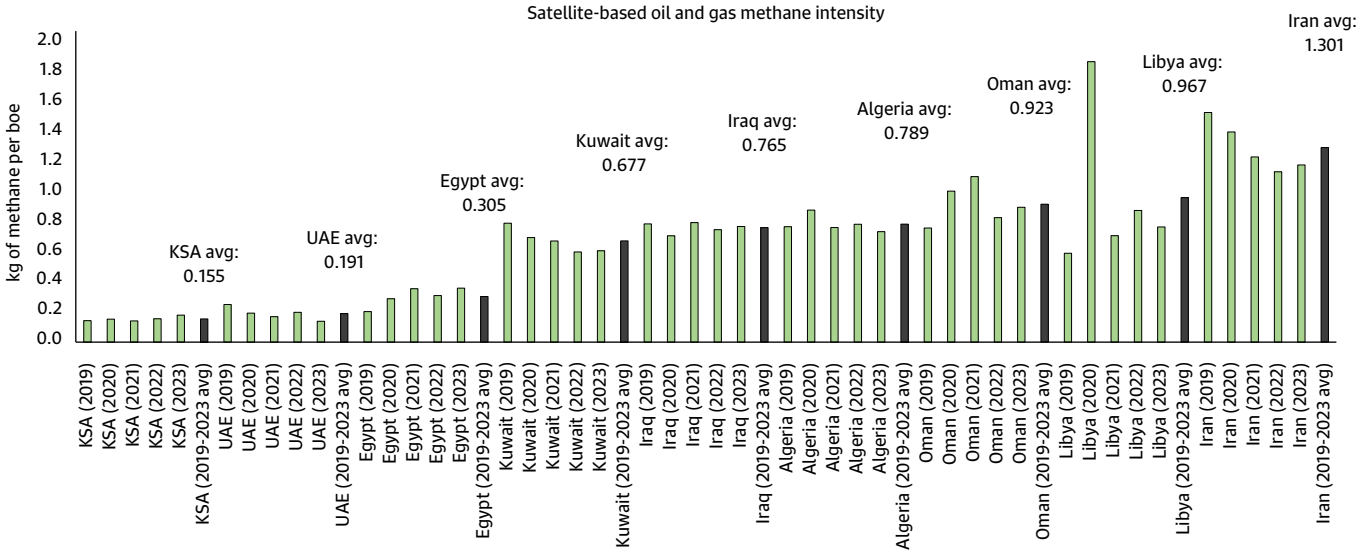
In summary, the significant disparities in methane intensity highlighted in Figure 37 underscore the potential for further emission abatement in many MENA countries by adopting best practices from low-intensity producers like Saudi Arabia and the UAE.

Figure 38 compares the methane intensity of the waste sector across the nine MENA countries using our satellite-based emission estimates. Here, methane intensity is expressed as kilograms of methane emitted per capita, facilitating more meaningful comparisons among countries with vastly different population sizes. The results reveal substantial cross-country disparities, exceeding a factor of 10 in some cases, which likely reflect differences in waste generation rates, waste management practices, landfill design, and methane capture infrastructure.

Libya stands out with by far the highest methane intensity levels, with an average intensity exceeding 120 kg of methane per capita. It is followed by Algeria, which has an average methane intensity of around 69.1 kg per capita – considerably lower than Libya's but still among the highest in the region. In contrast, Iraq and Egypt exhibited the lowest methane intensities, with respective averages of 17.3 and 12.0 kg per capita. The remaining countries (Saudi Arabia, Kuwait, the UAE, Oman, and Iran) fall within an intermediate range, with average methane intensities of roughly 30-40 kg per capita.

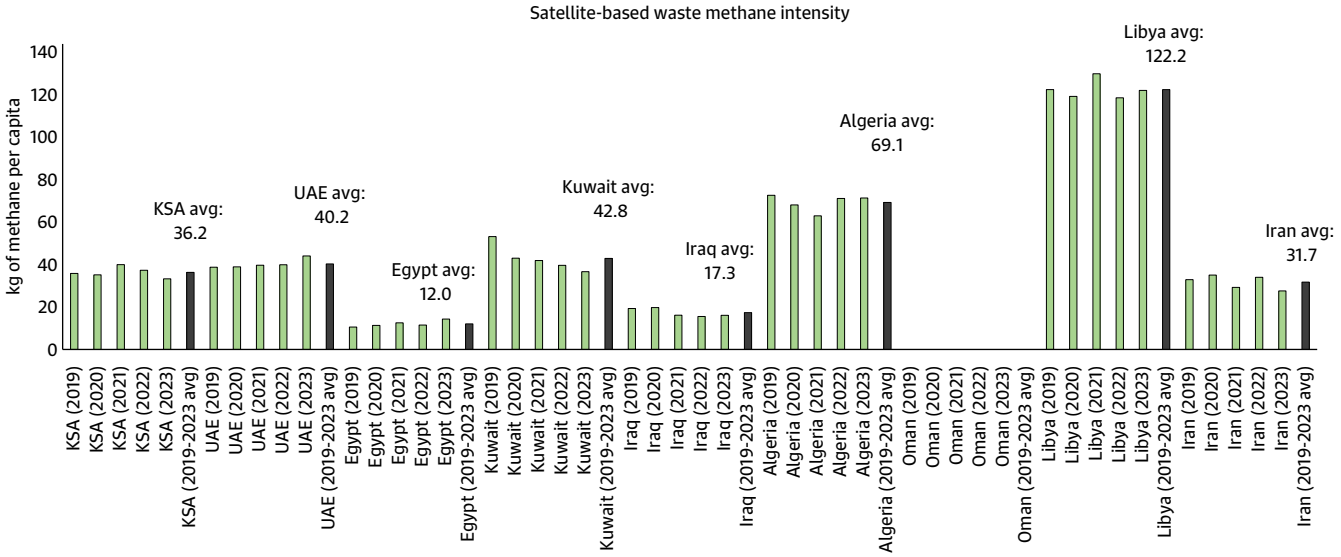
Overall, the large differences in per capita methane intensities observed in Figure 38 underscore the importance of tailored waste management strategies. While oil and gas sector emissions are often the focus of mitigation efforts in the region, our findings show that, in many MENA countries, the waste sector is a significant source of methane emissions that requires targeted interventions to deliver substantial emission reductions.

Figure 37. Comparison of countries' oil and gas sectors using methane intensities derived from the authors' satellite measurements.



Notes: Avg = average; KSA = Kingdom of Saudi Arabia; UAE = United Arab Emirates; year of estimate shown in parentheses.
Source: Authors.

Figure 38. Comparison of countries' waste sectors using methane intensities derived from the authors' satellite measurements.



Notes: Avg = average; KSA = Kingdom of Saudi Arabia; UAE = United Arab Emirates; year of estimate shown in parentheses.
Source: Authors.

Conclusion and Policy Recommendations

05

This paper developed an integrated satellite-based framework to estimate methane emissions for nine MENA countries, combining a wind-rotated plume model and a basin-level atmospheric inversion model with sector-specific assumptions and extrapolations to generate national-level methane emission estimates.

Methodologically, we make two key contributions. First, we demonstrate how the wind-rotated model can be systematically applied to generate national-level estimates by aggregating methane emissions from multiple sources. Second, we introduce a hybrid method that utilizes basin inversions only when methane-emitting assets are densely clustered. Additionally, our basin-inversion model, unlike those in past studies, employs a prior that is independent of public emissions inventories, relying solely on the locations of methane-emitting sources. We also detail how we combine our satellite measurements with assumptions and extrapolations to achieve comprehensive national coverage, addressing challenges posed by topographies that hinder satellite measurements. Our approach illustrates how satellites can be used to estimate national-level inventories in a transparent, reproducible, and progressively improvable manner.

Our satellite measurements of methane emissions help clarify some of the major discrepancies observed in estimates for MENA countries. Across countries and sectors, our results indicate which data sources may be over- or underestimating methane emissions. In the oil and gas sector, official national GHG inventories submitted by governments to the UNFCCC generally fall below our satellite-based estimates, while global activity-based datasets from the IEA and EDGAR are consistently above them. However, exceptions exist, such as Oman, where most sources align closely. In the waste sector, we find that most data sources tend to underestimate waste emissions in the region, which are often a significant source of methane in MENA countries.

Our satellite measurements were also utilized to compare and benchmark MENA countries. In the oil and gas sector, Saudi Arabia and the UAE emerged as the top-performing countries, exhibiting the lowest methane intensities. The significantly higher methane intensities in many other MENA countries highlight the potential for further emission reductions in the region by adopting best practices from low-intensity producers like Saudi Arabia and the UAE.

Our research has several policy implications. First, given the consistently significant discrepancies between data sources for methane emission estimates across countries, including the nine we focus on in this study, the use of satellites can play a pivotal role in improving accuracy and promoting transparency of these measurements (Aganaba-Jeanty and Huggins 2019). Transparency is a foundational element of the Paris Agreement, as articulated in Article 13, and is necessary to foster trust and

ensure that countries are on track to meet climate goals. Both governments and corporations can help improve the accuracy and transparency of methane emissions data by using satellites along with other measurement methods.

The consistent underreporting of methane emissions by countries in the MENA region to the UNFCCC, using the IPCC (2006) guidelines, highlights several potential issues. First, some MENA countries may require capacity building to prepare GHG inventories more effectively. There may also be concerns regarding the quality of the activity data collected for calculations, which can lead to inaccurate estimates. Second, the IPCC (2006) guidelines themselves may need updating. Most countries currently use the default emission factors in the IPCC (2006) guidelines, which may not reflect their actual levels of methane emissions. Future iterations of the IPCC guidelines would benefit from incorporating satellite data into the methodology or to update its default emission factors.

The consistent overreporting of methane emissions by organizations like the IEA for MENA countries also suggests that they need to refine their assumptions around emission factors, especially for countries in the Arabian Gulf region. As discussed by Gasim and Muhsen (2025), the IEA's methane estimates are based on granular measurements made for the U.S. oil and gas industry, with scaling assumptions applied to extrapolate U.S. methane emission factors to other countries. For many MENA countries, these scaling assumptions should be adjusted downward and ideally replaced with actual measurements to obtain country-specific emission factors.

While limitations remain in using satellites to measure emissions, improvements in satellite technology continue to overcome many of these challenges. As the technology continues to improve, producers and users of emissions data will be better equipped to combine different measurement methods, yielding high-quality, trusted information on greenhouse gas emissions. This will unlock effective climate action and help the world meet its climate goals.

Endnotes

[1] Methane and carbon dioxide differ not only in their heat-trapping potency but also in their atmospheric lifetimes. Although a tonne of methane traps more heat than a tonne of carbon dioxide, methane has a relatively shorter lifespan of seven to 12 years in the atmosphere, while carbon dioxide can remain in the atmosphere for over a century. When compared over a shorter 20-year period, methane's global warming potential is roughly 80.

[2] For the second sector, we specifically focus on measuring methane emissions from urban areas. We expect our measurements to mainly capture methane emissions from waste. While there may be minor agricultural activities that occur within urban areas, we expect these agricultural emissions to be minimal. Additionally, any methane emissions from large agricultural areas outside urban areas are excluded from our analysis, as these agricultural emissions are generally diffuse, making them unsuitable for satellite-based measurement.

[3] We expect that the larger discrepancies in oil and gas methane emissions estimates are driven by larger spatial and temporal variations in methane leakage rates. While variations also exist in the ratios of organic waste in landfills and waste practices, we expect these variations to be smaller from country to country.

[4] ERA5 is a global reanalysis dataset produced by the European Centre for Medium-Range Weather Forecasts (ECMWF) under the Copernicus Climate Change Service. It provides hourly, high-resolution estimates of atmospheric variables, including wind, temperature, and pressure.

[5] Following TROPOMI guidelines (Landgraf et al., 2023), a quality assurance threshold of 0.5 was applied under favorable observational conditions (bright and homogeneous backgrounds), while a value of 0.3 was applied in challenging environments (mountains, coastlines, dense vegetation). The lower threshold of 0.3 was used to preserve sufficient coverage, assuming that aggregation compensates for satellite retrieval noise. Images were excluded if the fraction of valid pixels fell below the selected threshold.

[6] In our implementation, for simplicity, we approximate the MAD under a Gaussian assumption (MAD ≈ 1.5 × standard deviation).

[7] Following Schneising et al. (2020), we apply a single representative wind speed uniformly to all cross-sections within a plume. This wind speed is derived from ERA5 data (Hersbach et al. 2024) as the mean of the 10-meter horizontal wind values around the time and location of each TROPOMI observation.

[8] Oil and gas field representing less than 1% of national-level oil and gas production were excluded from the calculation of the average methane intensity that was used for extrapolation.

[9] Specifically, we took an average of three inventories that provided estimates for all nine MENA countries examined in our paper: IEA (2022, 2023, 2024, 2025), EDGAR (2024), and Chen et al. (2023).

[10] We use an L2 regularization in the fitting procedure between HYSPLIT simulations and TROPOMI measurements to retrieve excess methane. The L2 regularization (also known as ridge regression) adds a penalty proportional to the sum of the squared model parameters to the optimization objective. This technique helps prevent overfitting and stabilizes the solution, particularly when variables are correlated or the system is ill-conditioned (Hoerl and Kennard 1970). Although this L2 regularization improves the stability of the inversion, it also tends to limit large variations, potentially leading to a systematic underestimation of the strongest emission hotspots.

[11] As noted in the Methods and Data section, in the case of coastal and mountainous assets, the background removal is done before image aggregation due to the presence of invalid offshore pixels after the rotation of each image. Therefore, a methane-free area near the source was selected for each image, and the background methane concentration was subtracted before image aggregation.

[12] Given the uncertainties and the fluctuations that may be caused from year to year by perturbations in the parameters, we compare countries' methane intensities using an average for the entire period.

References

Aganaba-Jeanty, Timiebi, and Anna Huggins. 2019. "Satellite Measurement of GHG Emissions: Prospects for Enhancing Transparency and Answerability under International Law." *Transnational Environmental Law 8* (2): 303–26. https://doi.org/10.1017/s2047102519000104.

Alvarez, Ramón A., Daniel Zavala-Araiza, David R. Lyon, David T. Allen, Zachary R. Barkley, Adam R. Brandt, Kenneth J. Davis, Scott C. Herndon, Daniel J. Jacob, Anna Karion, Eric A. Kort, Brian K. Lamb, Thomas Lauvaux, Joannes D. Maasakkers, Anthony J. Marchese, Mark Omara, Stephen W. Pacala, Jeff Peischl, Allen L. Robinson, Paul B. Shepson, Colm Sweeney, Amy Townsend-Small, Steven C. Wofsy, and Steven P. Hamburg. 2018. "Assessment of Methane Emissions from the U.S. Oil and Gas Supply Chain." *Science* 361 (6398): 186–188. https://doi.org/10.1126/science.aar7204.

Arab Republic of Egypt Ministry of the Environment. 2025. *Egypt's First Biennial Transparency Report (BTR-1)*. Cairo: Arab Republic of Egypt Ministry of the Environment. https://unfccc.int/sites/default/files/resource/Egypt_BTR1_draft-%20Report_17September2025%20_TC_final.pdf.

Balasus, Nicholas, Daniel J. Jacob, Gabriel Maxemin, Carrie Jenks, Hannah Nesser, Joannes D Maasakkers, Daniel H Cusworth, Tia R Scarpelli, Daniel J Varon, and Xiaolin Wang. "Satellite Monitoring of Annual US Landfill Methane Emissions and Trends." *Environmental Research Letters* 20 (2). https://doi.org/10.1088/1748-9326/ada2b1.

Banja, Manjola, Monica Crippa, Diego Guizzardi, Marilena Muntean, Federico Pagani, and Enrico Pisoni. 2025. "A Comparative Analysis of EDGAR and UNFCCC GHG Emissions Inventories: Insights on Trends, Methodology and Data Discrepancies." *Earth System Science Data* 17 (11): 6461–648: 1–39. https://doi.org/10.5194/essd-2025-385.

Bondarenko Maksym, Rhorom Priyatikanto, Natalia Tejedor-Garavito, Wen Zhang, Thomas McKeen, Alice Cunningham, Timothy Woods, Jonathan Hilton, Deniz Cihan, Bohdan Nosatiuk, Thomas Brinkhoff, Andrew Tatem, and Alessandro Sorichetta. 2025. *Constrained Estimates of 2015–2030 Total Number of People per Grid Square at a Resolution of 3 Arc (Approximately 100 m at the Equator), R2025A Version v1*. Global Demographic Data Project – Funded by the Bill and Melinda Gates Foundation (INV-045237). Southampton: WorldPop, School of Geography and Environmental Science, University of Southampton. https://hub.worldpop.org/geodata/listing?id=135.

Brandt, Adam R., Garvin A. Heath, and Daniel Cooley. 2016. "Methane Leaks from Natural Gas Systems Follow Extreme Distributions." *Environmental Science & Technology* 50 (22). https://doi.org/10.1021/acs.est.6b04303.

Chen, Zichong, Daniel J. Jacob, Ritesh Gautam, Mark Omara, Robert N. Stavins, Robert C. Stowe, Hannah Nesser, Melissa P. Sulprizio, Alba Lorente, Daniel J. Varon, Xiao Lu, Lu Shen, Zhen Qu, Drew C. Pendergrass, and Sarah Hancock. 2023. "Satellite Quantification of Methane Emissions and Oil–Gas Methane Intensities from Individual Countries in the Middle East and North Africa: Implications for Climate Action." *Atmospheric Chemistry and Physics* 23 (10): 5945–5967. https://doi.org/10.5194/acp-23-5945-2023.

Committee on Earth Observation Satellites. 2025. "Greenhouse Gas Satellite Missions Portal." CEOS Database. https://database.eohandbook.com/ghg.

de Jong, Tobias A., Itziar Irribarren, Daniel J. Varon, Christian Frankenberg, and Joannes D. M. de Laat. 2024. *Tracking Methane Super-Emitters with VIIRS Shortwave Infrared Observations*. EarthArXiv. https://doi.org/10.31223/X51M5T.

Designated National Authority (DNA) of the Kingdom of Saudi Arabia. 2024. *Kingdom of Saudi Arabia: The First Biennial Transparency Report – Submitted to the United Nations Framework Convention on Climate Change*. Riyadh: Designated National Authority. https://unfccc.int/sites/default/files/resource/KSA_BTR1_20250320-2.pdf

Emissions Database for Global Atmospheric Research (EDGAR). 2024. *GHG Emissions of All World Countries*. European Union. https://edgar.jrc.ec.europa.eu/report_2024#data_download.

European Commission: Joint Research Centre. 2023. *GHSL Data Package 2023*. Luxembourg: Publications Office of the European Union. https://data.europa.eu/doi/10.2760/098587.

Food and Agricultural Organization of the United Nations (FAO). 2024. "Emissions from Livestock." https://www.fao.org/faostat/en/#data/GLE.

Federal Competitiveness and Statistics Centre (FCSC). 2024. "Statistics by Subject." https://fcsc.gov.ae/en-us/Pages/Statistics/Statistics-by-Subject.aspx#.

Fioletov, V. E., C. A. McLinden, N. Krotkov, and C. Li. 2015. "Lifetimes and Emissions of SO_2 from Point Sources Estimated from OMI." *Geophysical Research Letters* 42 (6): 1–8. https://doi.org/10.1002/2015GL063148.

Gasim, Anwar, and Abdelrahman Muhsen. 2025. "Comparing the Latest 2024 Estimates of Methane Emissions for Saudi Arabia." Riyadh: King Abdullah Petroleum Studies and Research Center (KAPSARC). https://www.kapsarc.org/our-offerings/publications/comparing-the-latest-2024-estimates-of-methane-emissions-for-saudi-arabia.

Gasim, Anwar, Walid Matar, Abdelrahman Muhsen, Srivatsan Anand, and Julian Akani Guery. 2024. "Using Satellite Technology to Measure Methane Emissions in Arabian Gulf Countries." Riyadh: King Abdullah Petroleum Studies and Research Center (KAPSARC). https://www.kapsarc.org/research/publications/using-satellite-technology-to-measure-methane-emissions-in-arabian-gulf-countries.

Gasim, Anwar, Walid Matar, and Abdelrahman Muhsen. 2023. "Using Satellite Technology to Measure Greenhouse Gas Emissions in Saudi Arabia." Riyadh: King Abdullah Petroleum Studies and Research Center (KAPSARC). https://www.kapsarc.org/research/publications/using-satellite-technology-to-measure-greenhouse-gas-emissions-in-saudi-arabia.

Global Energy Monitor. 2025. *Global Oil and Gas Extraction Tracker.* https://globalenergymonitor.org/projects/global-oil-gas-extraction-tracker.

Global Methane Pledge (GMP). 2025. "Global Methane Pledge." https://www.globalmethanepledge.org.

Golhosseini, Zeynab, and Mahdi Jalili Ghazizade. 2024. "Municipal Solid Waste Status in Iran: From Generation to Disposal," *Environmental Protection Research* 4 (1): 16–29. https://doi.org/10.37256/epr.4120243553.

Gorchov Negron, A. M., E. A. Kort, S. A. Conley, and M. L. Smith. 2020. "Airborne Assessment of Methane Emissions from Offshore Platforms in the U.S. Gulf of Mexico." *Environmental Science & Technology* 54 (8): 5112–5120. https://doi.org/10.1021/acs.est.0c00179.

Hersbach, H., B. Bell, P. Berrisford, G. Biavati, A. Horányi, J. Muñoz Sabater, J. Nicolas, C. Peubey, R. Radu, I. Rozum, D. Schepers, A. Simmons, C. Soci, D. Dee, and J.-N. Thépaut. 2023. "ERA5 Hourly Data on Single Levels From 1940 to Present." Copernicus Climate Change Service (C3S) Climate Data Store (CDS). https://doi.org/10.24381/cds.adbb2d47.

Hoerl, Arthur E., and Robert W. Kennard. 1970. "Ridge Regression: Biased Estimation for Nonorthogonal Problems." *Technometrics* 12 (1): 55–67. https://doi.org/10.2307/1267351.

Hybrid Single-Particle Lagrangian Integrated Trajectory (HYSPLIT). 2019. "HYSPLIT Tutorial." https://www.ready.noaa.gov/data/web/workshop/Sep2019.

Intergovernmental Panel on Climate Change (IPCC). 2006. *2006 IPCC Guidelines for National Greenhouse Gas Inventories.* https://www.ipcc-nggip.iges.or.jp/public/2006gl/index.html.

Intergovernmental Panel on Climate Change (IPCC). 2023a. *AR6 Synthesis Report: Climate Change 2023.* https://www.ipcc.ch/report/sixth-assessment-report-cycle.

Intergovernmental Panel on Climate Change (IPCC). 2023b. *Climate Change 2021 – The Physical Science Basis: Working Group I Contribution to the Sixth Assessment Report of the Intergovernmental Panel on Climate Change.* Cambridge: Cambridge University Press. https://doi.org/10.1017/9781009157896.

International Energy Agency (IEA). 2021. "Methane Tracker 2021." https://www.iea.org/reports/methane-tracker-2021.

International Energy Agency (IEA). 2022. "Global Methane Tracker 2022." https://www.iea.org/reports/global-methane-tracker-2022.

International Energy Agency (IEA). 2023. "Global Methane Tracker 2023." https://www.iea.org/reports/global-methane-tracker-2023.

International Energy Agency (IEA). 2024. "Global Methane Tracker 2024." https://www.iea.org/reports/global-methane-tracker-2024.

International Energy Agency (IEA). 2025. "Global Methane Tracker 2025." https://www.iea.org/reports/global-methane-tracker-2025.

Islamic Republic of Iran. 2017. *Third National Communication to the United Nations Framework Convention on Climate Change (UNFCCC).* Tehran: Islamic Republic of Iran. https://unfccc.int/sites/default/files/resource/Third%20National%20communication%20IRAN.pdf.

Jacob, Daniel J., Daniel J. Varon, Daniel H. Cusworth, Philip E. Dennison, Christian Frankenberg, Ritesh Gautam, Luis Guanter, John Kelley, Jason McKeever, Lesley E. Ott, Benjamin Poulter, Zhen Qu, Andrew K. Thorpe, John R. Worden, and Riley M. Duren. 2022. "Quantifying Methane Emissions from the Global Scale Down to Point Sources Using Satellite Observations of Atmospheric Methane." *Atmospheric Chemistry and Physics* 22 (14): 9617–9646. https://doi.org/10.5194/acp-22-9617-2022.

Jacob, Daniel. J., Alexander J. Turner, Joannes D. Maasakkers, Jianxiong Sheng, Kang Sun, Xiong Liu, Kelly Chance, Ilse Aben, Jason McKeever, and Christian Frankenberg. 2016. "Satellite Observations of Atmospheric Methane and Their Value for Quantifying Methane Emissions." *Atmospheric Chemistry and Physics* 16 (22): 14371–14396. https://doi.org/10.5194/acp-16-14371-2016.

Krings, T., K. Gerilowski, M. Buchwitz, M. Reuter, A. Tretner, J. Erzinger, D. Heinze, U. Pflüger, J. P. Burrows, and H. Bovensmann. 2011. "MAMAP – A New Spectrometer System for Column-Averaged Methane and Carbon Dioxide Observations from Aircraft: Retrieval Algorithm and First Inversions for Point Source Emission Rates." *Atmospheric Measurement Techniques* 4 (9): 1735–1758. https://doi.org/10.5194/amt-4-1735-2011.

Kuwait Environment Public Authority. 2019. *Kuwait. Biennial Update Report (BUR) 1.* Submitted 30 September 2019 to the United Nations Framework Convention on Climate Change. https://unfccc.int/documents/200518.

Landgraf, J., A. Lorente, B. Langerock, M. Kumar Sha, J.-C. Lambert, D. Loyola, D. Stein Zweers, A. Dehn, and C. Zehner. 2023. *S5P Mission Performance Centre Methane [L2__CH4___] Readme.* Document No. S5P-MPC-SRON-PRF-CH4, Issue 2.5, Product Version V02.06.00. ESA, November 29, 2023. https://sentinels.copernicus.eu/documents/d/sentinel/s5p-mpc-sron-prf-ch4_v02-06-00_2-5_20231129_signed.

Luomi, Mari, Thamir Al Shehri, and Nicholas Howarth. 2021. "Measuring to Manage: The Case for Improving CO_2 Monitoring and Reporting in Saudi Arabia." Riyadh: King Abdullah Petroleum Studies and Research Center (KAPSARC). https://www.kapsarc.org/our-offerings/publications/measuring-to-manage-the-case-for-improving-co2-monitoring-and-reporting-in-saudi-arabia.

Maasakkers, Joannes D., Daniel J. Varon, Aldís Elfarsdóttir, Jason McKeever, Dylan Jervis, Gourav Mahapatra, Sudhanshu Pandey, Alba Lorente, Tobias Borsdorff, Lodewijck R. Foorthuis, Berend J. Schuit, Paul Tol, Tim A. van Kempen, Richard van Hees, and Ilse Aben. 2022. "Using Satellites to Uncover Large Methane Emissions from Landfills." *Science Advances* 8 (32). https://doi.org/10.1126/sciadv.abn9683.

Ministry of Construction and Housing and Municipalities and Public Works. 2022. *Data Collection Study on Solid Waste Management in Iraq: Final Report.* https://openjicareport.jica.go.jp/pdf/12367256.pdf?utm_source=chatgpt.com

Ministry of Environment and Climate Affairs (Sultanate of Oman). 2019. *Biennial Update Report Submitted to the United Nations Framework Convention on Climate Change.* https://unfccc.int/sites/default/files/resource/BUR%20%2817%20nov%202019%29%20%28Final%29%20%281%29.

National Academies of Sciences, Engineering, and Medicine. 2022. *Greenhouse Gas Emissions Information for Decision Making: A Framework Going Forward.* Washington, DC: The National Academies Press. https://doi.org/10.17226/26641.

Okkacha, Youb, Youb Abderrahmane, and Bouabdessalam Hassiba. 2014. "Municipal Waste Management in the Algerian High Plateaus." *Energy Procedia* 50: 662–669. https://doi.org/10.1016/j.egypro.2014.06.081.

Peng, Shushi, Clément Giron, Gang Liu, Alexandre d'Aspremont, Antoine Benoit, Thomas Lauvaux, Xin Lin, Hugo De Almeidar Rodrigues, Marielle Saunois, and Philippe Ciais. 2023. "High Resolution Assessment of Coal Mining Methane Emissions by Satellite in Shanxi, China." *iScience* 26 (12): 108375. https://doi.org/10.1016/j.isci.2023.108375.

People's Democratic Republic of Algeria, Ministry of Environment and the Quality of Life. 2024. *Premier Rapport Biennal de Transparence (BTR1).* Submission to the United Nations Framework Convention on Climate Change. UNFCCC. https://unfccc.int/first-biennial-transparency-reports.

Republic of Iraq Ministry of Environment. 2025. *Iraq's First Biennial Transparency Report (BTR1).* Baghdad: Republic of Iraq, Ministry of Environment. https://unfccc.int/sites/default/files/resource/Iraq%20BTR%20%209%20September%202025_Final%20English%20Designed.pdf.

Rutherford, Jeffrey S., Evan D. Sherwin, Arvind P. Ravikumar, Garvin A. Heath, Jacob Englander, Daniel Cooley, David Lyon, Mark Omara, Quinn Langfitt, and Adam R. Brandt. 2021. "Closing the Methane Gap in US Oil and Natural Gas Production Emissions Inventories." *Nature Communications* 12: 4715. https://doi.org/10.1038/s41467-021-25017-4.

Rystad Energy. 2025. "Liquids and Gas: Production." Oslo: Rystad Energy.

Schneising, Oliver, Michael Buchwitz, Maximilian Reuter, Steffen Vanselow, Heinrich Bovensmann, and J. P. Burrows. 2020. "Remote Sensing of Methane Leakage from Natural Gas and Petroleum Systems Revisited." *Atmospheric Chemistry and Physics* 20 (15): 9169–9182. https://doi.org/10.5194/acp-20-9169-2020.

Shen, Lu, Daniel J. Jacob, Ritesh Gautam, Mark Omara, Tia R. Scarpelli, Alba Lorente, Daniel Zavala-Araiza, Xiao Lu, Zichong Chen, and Jintai Lin. 2023. "National Quantifications of Methane Emissions from Fuel Exploitation Using High Resolution Inversions of Satellite Observations." *Nature Communications* 14: 4948. https://doi.org/10.1038/s41467-023-40671-6

Statistics Centre. 2018. "Waste Statistics." https://www.scad.ae/Release%20Documents/Waste%20Statistics_2018_Annual_Yearly_en_v1.pdf

Tibrewal, Kushal, Philippe Ciais, Marielle Saunois, Adrien Martinez, Xin Lin, Joel Thanwerdas, Zhu Deng, Frederic Chevallier, Clément Giron, Clément Albergel, Katsumasa Tanaka, Prabir Patra, Aki Tsuruta, Bo Zheng, Dmitry Belikov, Yosuke Niwa, Rajesh Janardanan, Shamil Maksyutov, Arjo Segers, Zitely A. Tzompa-Sosa, Philippe Bousquet, and Jean Sciare. 2024. "Assessment of Methane Emissions from Oil, Gas and Coal Sectors across Inventories and Atmospheric Inversions." *Communications Earth & Environment* 5: 26. https://doi.org/10.1038/s43247-023-01190-w.

TROPOMI. 2024. "TROPOMI." https://www.tropomi.eu.

United Arab Emirates Ministry of Energy and Infrastructure. 2023. *United Arab Emirates. National Communication (NC). NC 5. Biennial Update Report (BUR). BUR 1.* https://unfccc.int/documents/635318.

United Arab Emirates (UAE). 2024. *1st Biennial Update Report (BUR) Addendum. Submission to the United Nations Framework Convention on Climate Change.* https://www4.unfccc.int/sites/SubmissionsStaging/NationalReports/Documents/91846237_United%20Arab%20Emirates%20(UAE)-BUR1-1-1st%20Biennial%20Update%20Report%20(BUR)%20Addendum%20.pdf.

United Nations. 2018. *World Urbanization Prospects 2018.* https://www.un.org/development/desa/pd/news/world-urbanization-prospects-2018.

United Nations Framework Convention on Climate Change (UNFCCC). 2022. *Reference Manual for the Enhanced Transparency Framework under the Paris Agreement.* https://unfccc.int/sites/default/files/resource/v2_ETFreferencemanual.pdf.

White, W. H., J. A. Anderson, D. L. Blumenthal, R. B. Husar, N. V. Gillani, J. D. Husar, and W. E. Wilson, Jr. 1976. "Formation and Transport of Secondary Air Pollutants: Ozone and Aerosols in the St. Louis Urban Plume." *Science* 194 (4261): 187–189. https://doi.org/10.1126/science.959846.

Yu, X., Millet, D. B., Henze, D. K., Turner, A. J., Delgado, A. L., Bloom, A. A., and Sheng, J. 2023. "A High-Resolution Satellite-Based Map of Global Methane Emissions Reveals Missing Wetland, Fossil Fuel, and Monsoon Sources." *Atmospheric Chemistry and Physics* 23 (5): 3325–3346. https://doi.org/10.5194/acp-23-3325-2023.

Appendices

Appendix A: Kayrros Data

Since emissions are not used as priors, we rely instead on infrastructure location data compiled from two sources:

- EDGAR v5.0 (products: PRO_OIL and PRO_GAS): Infrastructure locations are derived using a threshold-based approach, where pixels with values exceeding a defined threshold are classified as infrastructure.
- VIIRS (Suomi-NPP) flaring data, based on the Nightfire algorithm.

This multi-source approach allows us to identify infrastructure relevant to methane emissions more robustly.

Appendix B: Country Notes

Saudi Arabia: The extrapolation methodology faces limitations due to the presence of two small (low production) but high-intensity oil and gas fields, Jaladi and North Arabia. These fields introduce a bias that leads to an overestimation of national emissions. Since there is a higher uncertainty associated with small assets, these fields were excluded from our analysis.

Kuwait: Kuwait is the smallest country by size and population in this study. Due to its limited size and the predominance of onshore production, the basin-inversion model was utilized to quantify total methane emissions across its territory. In this case, no extrapolation was needed, but sectoral splits were estimated using sectoral shares from publicly available inventories.

Iraq: The basin-inversion model for Iraq encompasses most of the upstream oil and gas assets in the southeastern part of the country, including nearby cities such as Basrah, Amarah, and Nasiriyah. A combination of basin-inversion modeling in the southeast and a wind-rotated model for urban areas in the central and northern regions was applied. However, some assets in mountainous areas, such as Sulaymaniyah, could not be quantified.

UAE: A significant portion of production, about half of the country's total, is located offshore, which prevents direct satellite measurement. The average onshore methane intensity is applied to the offshore assets, bringing relatively larger uncertainties in the final estimates. In cases where oil and gas fields or urban areas are located close together, methane emissions were quantified collectively for all nearby assets. These emissions were then apportioned to individual assets based on each asset's share of total sectoral production. Asab, Sahil, and other minor fields such as Haliba, Qusahwira, and Mender could not be quantified, given their location between other major wind-rotation zones, as there was a risk of double-counting emissions, and the wind-filter step would significantly limit the usable images.

Oman: Oman's oil and gas fields have the unique characteristic of being organized in clusters, with major fields surrounded by smaller ones spread across vast areas. This spatial arrangement allowed for the application of a wind-rotation model across eight distinct clusters of fields. Isolated minor fields, which contribute a negligible amount to overall oil and gas production and are located far from the covered clusters, were not included in the analysis. The most densely populated urban areas of Oman are concentrated along the northern coast, nestled between the sea and mountains, which makes direct satellite measurement impossible. Consequently, no wind rotation was applied for urban areas, and thus no satellite-based estimates were generated from Oman's urban areas sector.

Algeria: Similar to Saudi Arabia, we excluded the Ohanet and Touat fields from the extrapolation due to their high methane intensity levels, which result from their small size and low production. Despite this adjustment, oil and gas coverage remains strong in Algeria, largely because all production occurs onshore under favorable topographic conditions, with most fields located in desert areas that are well suited for wind-rotation measurements. On the other hand, waste coverage is relatively low. Most cities are concentrated along the coast, where wind-rotation measurements are less effective. Additionally, Algeria's low level of urbanization presents some limitations in the extrapolation methodology, which not only reduces population and waste generation coverage (Algeria's largest cities account for less than half of the national population) but also introduces bias for emissions at the city level. We extrapolate the urban-area methane emission intensity (based on larger cities) to smaller cities and towns, which may lead to inaccuracies.

Libya: Extrapolation is limited by the lack of data, which is exacerbated by the political context in Libya. No reliable or up-to-date data on waste or population could be found. The most recent census dates back to 2006, failing to capture the rapid urbanization that has taken place in recent years in cities such as Misrata. To address this gap, we relied on alternative population datasets that differ from those used for other countries, as described in Section 4.6.

Egypt: Accurate methane emission measurements in Egypt are challenging due to the concentration of the population along the Nile and its impact on wind-rotation measurements. Consequently, data from Nile-adjacent cities, such as Beni Suef and Asyut, were deemed unreliable and excluded because of unsuitable topographical conditions. Furthermore, the population is sparsely spread across many towns along the Nile, so Egypt's major cities do not account for a large share of the population and waste generation. To improve our coverage, we included minor cities with more than 100,000 inhabitants that were within wind-rotated zones for larger cities. The oil and gas extrapolation also faces limitations, particularly due to Egypt's

significant offshore production, which accounts for nearly 80% of its national output, primarily in the Nile Delta area of the Mediterranean. However, the major onshore oil and gas assets located in the eastern Egyptian desert were successfully quantified.

Iran: Iran is largely characterized by mountainous terrain and a high degree of rurality, which makes agriculture an important source of methane emissions, primarily from rice paddy cultivation and livestock production. For this reason, methane emissions related to agricultural activities were taken into account when splitting emissions in the basin model using sectoral shares from publicly available inventories.

Appendix C: Assumptions

This section lists the assumptions that were made, categorized by data type and model. Some time series were more readily available for some countries than others, leading to variations across countries in the need to apply the assumptions listed below. Table B1 shows which assumptions were applied to which country in the study. Certain overarching assumptions, like the proportionality of methane emissions to oil and gas production and waste generation, were applied across all countries, as shown in Table B1.

Assumptions for oil and gas data:

- **Assumption OG1:** We assume that each oil and gas field has the same production share over time, except if one or more sources prove otherwise. In this case, the production share is calculated based on the additional source(s) for the year the data is sourced, and linear interpolation is applied for the years in between the sourced data.
- **Assumption OG2:** Based on share assumptions, we then assume each field's production follows the trend in total oil and gas production data for the country.
- **Assumption OG3:** We assume that the fields outside of our coverage have negligible production.
- **Assumption OG4:** We assume that there is a proportional relationship between methane emissions from oil and gas fields and oil and gas production.

Assumptions for waste data:

- **Assumption W1:** We assume that there is a proportional relationship between the methane emissions from waste in an urban area and the urban area's waste generation.
- **Assumption W2:** The per capita waste generation rate of an urban area is assumed to remain constant over time. Thus, changes in waste generation are only driven by population growth, without accounting for factors such as income growth or changing consumption patterns.
- **Assumption W3:** The total generated waste of an urban area is the sum of the municipal solid waste (MSW) and rural solid waste (RSW).
- **Assumption W4:** The per capita waste generation rate of an urban area (i.e., city) is assumed to be equal to the regional MSW average, as regional data is generally available in the absence of city-level data.
- **Assumption W5:** Since the MSW is often not available, we calculate it using the ratio between the urban and rural population within a region. Any cities with populations of 100,000 inhabitants or above are classified as urban areas, while smaller towns are classified as rural.
- **Assumption W6:** To better capture differences between urban and rural areas in waste generation, we assume that urban populations generate waste at twice the per capita rate of rural populations. The urbanization rate of each region in a country is assumed to be constant over the study period (2019-2023).
- **Assumption W7:** EDGAR waste data is used as replacement for waste sector methane emissions estimates.
- **Assumption W8:** When the data for total waste at the city level is available, we assume that the share of waste generated by a city is constant over the years.

Assumptions for population data:

- **Assumption P1:** In the absence of data, national and regional population data are estimated using linear regression.
- **Assumption P2:** The share of a city's population relative to the national population is assumed to remain constant over time. Consequently, city-level growth is assumed to be driven solely by national population growth.
- **Assumption P3:** A linear regression was also used to fill in gaps in national population data.

Assumptions for agriculture data:

- **Assumption A1:** We assume that livestock density is a reasonable proxy for the distribution of methane emissions from livestock.
- **Assumption A2:** We assume that the methane intensity of a livestock species is uniform across the country.

Assumptions for wind-rotated model zones:

For the few years when no reliable measurements were possible for an asset, the missing values for its emissions in those years were estimated using averages derived from estimated data for the same wind-rotated zone (when estimation was possible in other years). For assets where no reliable measurements were possible for all years of the study, their emissions were extrapolated using assumptions OG4 and W1.

Table C1. List of assumptions that were applied to each country in the analysis conducted in this study.

Country	Population	Waste	Oil and gas	Agriculture
Iran	Assumption P1 Assumption P2	Assumption W1 Assumption W2 Assumption W3 Assumption W4	Assumption OG1 Assumption OG2 Assumption OG3 Assumption OG4	Assumption A1 Assumption A2
Egypt	Assumption P1 Assumption P2	Assumption W1 Assumption W2 Assumption W4 Assumption W5 Assumption W6	Assumption OG1 Assumption OG2 Assumption OG3 Assumption OG4	–
Saudi Arabia	Assumption P1 Assumption P2	–	Assumption OG1 Assumption OG2 Assumption OG3 Assumption OG4	–
Algeria	Assumption P1 Assumption P2	Assumption W1 Assumption W2 Assumption W4	Assumption OG1 Assumption OG2 Assumption OG3 Assumption OG4	–
Libya	Assumption P1 Assumption P2	–	Assumption OG1 Assumption OG2 Assumption OG3 Assumption OG4	–
Kuwait	Assumption P3	Assumption W1 Assumption W2 Assumption W4	Assumption OG1 Assumption OG2 Assumption OG3 Assumption OG4	
Iraq	Assumption P3	Assumption W1 Assumption W2 Assumption W4	Assumption OG1 Assumption OG2 Assumption OG3 Assumption OG4	
Oman	Assumption P3	Assumption W1 Assumption W2 Assumption W7	Assumption OG1 Assumption OG2 Assumption OG3 Assumption OG4	
UAE	Assumption P3	Assumption W1 Assumption W2 Assumption W8	Assumption OG1 Assumption OG2 Assumption OG3 Assumption OG4	–

Appendix D. Uncertainty Calculations

Six parameters for the wind-rotated model are perturbed to derive the uncertainty ranges. The six parameters, their calibration approach, and the perturbations are summarized in Table D1.

For each parameter that contributes to uncertainty in the methane rate estimate, small perturbations were applied around its central value, which was used to generate the wind-rotated estimates in this paper. The variation in the wind-rotated estimate that resulted from the parameter perturbation was used to compute the parameter-specific standard deviation (σ_i). The magnitude of these perturbations reflects the uncertainty of the parameter, which comes from the parameter calibration.

Table D1. List of parameters for the wind-rotated model and the perturbations that were implemented to derive the uncertainty ranges for the wind-rotated estimates.

Parameter name	Description	Parameter calibration	Parameter perturbations
Methane emission source location	Geographical coordinates of the methane emitting source	Selected from an 8 km grid in the *x* and *y* axes	Sampled on a 4 km grid in *x* and *y*, covering ±8 km around the central value
Plume mask	Mask (boundary) of the plume used to quantify the emissions	The mask is controlled by a threshold, sampled at 0.25 intervals	Sampled at 0.125 intervals within ±0.25 of its central value
AOI area	Dimensions of the monitored AOI	Selected from a 10 km grid	Sampled at 5 km intervals within ±10 km of its central value
Pixel quality	Quality threshold used to consider valid images	Selected from a grid with 10% increments	Sampled at 5 intervals within ±10 of its central value
Background selection	Coordinates of the area where the background is measured; used for coastal and mountainous assets	Selected based on the existence of a methane-free area of a certain size	The background area is adjusted by ±10% of its central size
Wind filtering	Set of bounds defining the wind directions to exclude the influence of nearby sources	Selected from a 5° grid	Each boundary is perturbed by ±5° from its central value

For each data input X_i, the propagated uncertainty contribution is approximated as follows:

$$\sigma_i \approx \left| \frac{\partial f}{\partial x_i} \right| \cdot \Delta X_i$$

The term $\left| \frac{\partial f}{\partial x_i} \right|$ denotes the sensitivity of the output to changes in X_i and ΔX_i denotes the standard deviation of X_i. The two data inputs that were considered for the uncertainty analysis are shown in Table D2.

Table D2.

Input	Description	Standard deviation
TROPOMI methane mixing ratio	Column-averaged dry-air mole fractions of methane (XCH_4) retrieved from TROPOMI. We use the bias-corrected datasets.	We use the product "methane_mixing_ratio_precision" from the TROPOMI images, which capture one standard deviation in this input
ERA5 wind data	Zonal and meridional wind components from the ERA5 global atmospheric reanalysis produced by the European Centre for Medium-Range Weather Forecasts (ECMWF), extracted at 100 m above ground level.	We assume 0.5 m/s uncertainty on both components of the wind, which represent one standard deviation in this input

The total uncertainty σ is then obtained by combining the uncertainty contributions from all the parameters and data inputs as shown below. Assuming Gaussian error distributions, the uncertainty range intervals are defined by $\pm 1.96\sigma$ around each emission estimate, corresponding to a 95% confidence interval:

$$\sigma = \sqrt{\sigma_i^2}$$

Finally, given our use of extrapolations, the uncertainty ranges for country-level total methane emission estimates for each sector are also extrapolated using coverage shares for each sector.

Appendix E. Population Assumptions and Data

When selecting which population data to use for a country, the first decision was whether to use a gridded or non-gridded data source. (Non-gridded data is conventional tabular data, while gridded data is geographical data that shows exactly what the population is in a certain geospatial pixel.) We opted for a gridded population data source because it allows us to define spatial polygons representing urban areas with flexibility, enabling us to extract population figures for specific AOI.

Several open-source gridded datasets are available, as discussed in Section 3.7, which differ in terms of spatial resolution and the range of years they cover. However, they all share a common foundation: integration of satellite imagery and alignment with UN total population estimates. We used WorldPop to calculate the total population at the regional and country levels, since it has good spatial resolution, is available for multiple years, and is consistent with UN estimates. However, the WorldPop dataset is less precise at city level, so it was not directly used to calculate the population at the that level. Instead, we first determined the share of the total population covered by each city, based on the latest census data. Assuming these shares remain constant over the years, we then infer the city population over the years using WorldPop as the reference for national totals.

For Libya, our methodology slightly differs. Since the available census data is from 2006, it does not reflect the rapid urbanization that has occurred in recent years in the country. To address this issue, we used the Global Human Settlement Layer (GHSL) dataset, which provides more accurate estimates at the city level than WorldPop, though it is only available for the years 2015, 2020, and 2025. The missing years were then interpolated using linear regression. For consistency purposes, we also used the GHSL dataset to estimate national and regional populations in Libya only.

About the Authors



Anwar Gasim

Anwar Gasim is a Principal Fellow at KAPSARC in the Climate and Sustainability program. He is an energy and environmental economist with an engineering background and over a decade of research and advisory experience, leading projects in the areas of energy demand, greenhouse gas emission measurement, energy price reform, and carbon pricing. Anwar holds a Ph.D. in Energy Economics from University College London (UCL).



Abdelrahman Muhsen

Abdelrahman Muhsen is the Director of GIS Solutions at KAPSARC. He is certified in GIS (GISP) with over 19 years of experience in GIS, spatial data management, and remote sensing. He has a proven track record of leading and delivering enterprise GIS projects for international corporations in North America and the Middle East. Abdel's work focuses on spatial economic modeling to better understand and forecast the interactions between economic activities, energy demand, land use, and transportation in urban areas. Abdel holds an M.Sc. in Geomatics Engineering from the University of Calgary, Canada.



Srivatsan Anand

Srivatsan Anand is a Project Manager in the Solutions team at Kayrros. Over the last three years, he has been performing in-depth analysis and coordination efforts for more than a dozen projects, leveraging satellite technology to monitor methane emissions, air quality, and renewable energy infrastructure. He currently serves as the Senior Project Manager of World Emission, an applied research project funded by the European Space Agency. Srivatsan holds a master's degree in International Energy from Sciences Po Paris and has previous experience in international research agencies and think tanks focused on energy and the environment.



Maxence Nevoret

Maxence Nevoret is a Junior Data Scientist at Kayrros, specializing in gas detection and quantification from hyperspectral, geostationary, and multispectral satellites. He has contributed to the MEDUSA project, an ESA-funded initiative benchmarking methane detection methods across European teams and also participated in the Stanford controlled release experiments and developed deep neural networks for satellite-based gas detection. Maxence holds a master's degree in Mathematics and Data Science from École CentraleSupélec.



Apolline Pignato

Apolline Pignato is a Data Analyst at Kayrros with experience across the full data lifecycle, from exploration and cleaning to visualization and analysis. She specializes in transforming raw information into meaningful insights, with a focus on methane analysis data that supports clear, decision-oriented outcomes for both internal teams and external stakeholders. Apolline has a background in statistics and programming from École Centrale de Lille, complemented by a master's degree in Sociology and Politics from Sciences Po Lille.



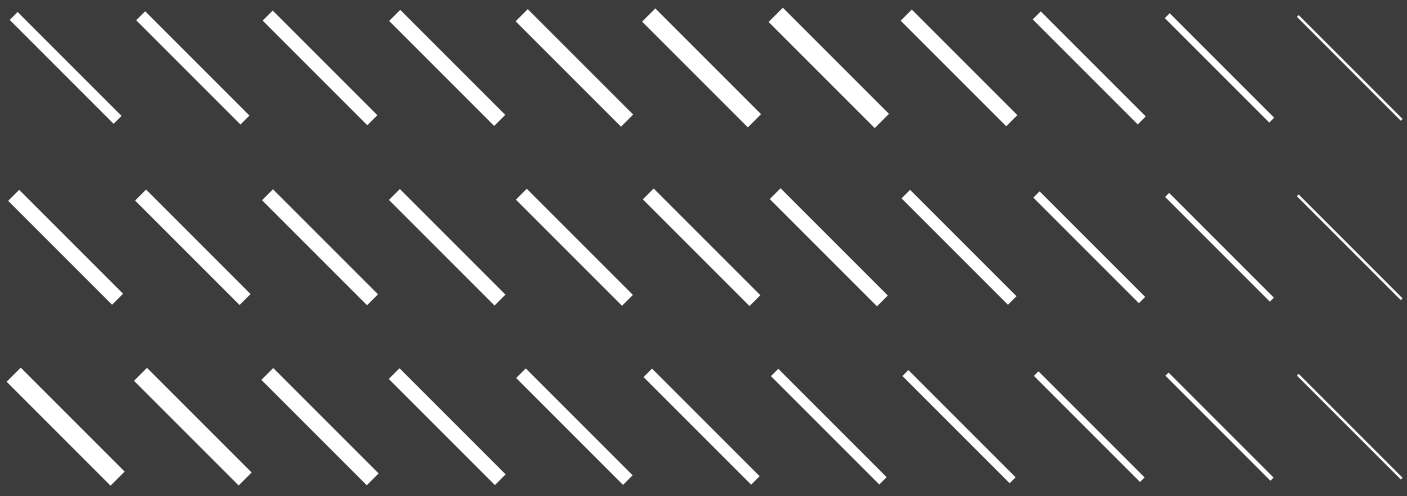
Julian Akani-Guéry

Julian Akani-Guéry is a Lead Data Scientist at Kayrros, specializing in greenhouse gases. He has extensive experience in methane emission estimates based on hyperspectral and multispectral satellite imagery. For nearly four years, he has been developing cutting-edge solutions for clients, including the World Bank and the United Nations Environment Programme. He currently serves as a Scientist on the Methane Emissions Detection Using Satellites Assessment, an applied research project funded by the European Space Agency. His expertise has been recognized in several scientific publications. Julian holds a master's degree in Engineering and Data Analytics from École des Ponts ParisTech.

About the Project

This paper is part of KAPSARC's Knowledge and Analysis project titled "Measuring and Mitigating Methane Emissions." This project contributes to the development and improvement of greenhouse gas emissions measurement, with the goal of obtaining comprehensive, accurate, transparent, and timely information on GHG emissions. It also examines methane mitigation policies, both locally and globally, as well as their effectiveness and implications.





kapsarc.org info@kapsarc.org /kapsarc